GENETIC AND EVOLUTIONARY ANALYSIS OF THE *DROSOPHILA* LARVAL NEUROMUSCULAR JUNCTION

by

Megan Campbell

A dissertation submitted in partial fulfillment of the requirements for the degree of

Doctor of Philosophy

(Neuroscience)

at

University of Wisconsin-Madison

2012

Date of final examination: July 27, 2012

The dissertation was approved by the following members of the Final Oral Committee:

Katherine Kalil, Professor, Neuroscience

Allen Laughon, Professor, Genetics

Gail Robertson, Professor, Neuroscience

Jerry Yin, Professor, Genetics

DEDICATION

I would like to offer my deepest thanks to my advisor, Barry Ganetzky for his mentorship. It has been a true honor and privilege to work with him. His infectious love for biology will continue to inspire me long after I have left the lab. I am indebted to my co-workers in the lab who have offered guidance, intellectual support and friendship. I would also like to thank the faculty and staff at UW, particularly my committee members, Kate Kalil, Al Laughon, Gail Robertson and Jerry Yin, but also Arash Bashirullah, Grace Boekhoff-Faulk, Erik Dent, Donata Oretel, John Pool, Tony Stretton, David Wassarman, Jill Wildonger and the NTP staff for their support.

Additionally, I would like to thank William Anderson, my high school biology teacher. Mr. Anderson introduced me to genetics and molecular biology and I have never looked back. He showed me that science could be exciting, revolutionary and incredibly hard work and for that I am eternally grateful.

Finally, I want to thank my family. Their unwavering support throughout this process has been invaluable. I particularly thank my parents for encouraging and fostering my love of learning.

TABLE OF CONTENTS

ABSTRACT

Although evolution of brains and behaviors is of fundamental biological importance, we lack comprehensive understanding of the general principles governing these processes or the specific mechanisms and molecules through which the evolutionary changes are effected. Because synapses are the basic structural and functional units of nervous systems, one way to address these problems is to dissect the genetic and molecular pathways responsible for morphological evolution of a defined synapse. I have undertaken such an analysis by examining morphology of the larval neuromuscular junction (NMJ) in wild caught *D. melanogaster* as well as in over 20 other species of *Drosophila*. Whereas variation in NMJ morphology within a species is limited, I discovered a surprisingly extensive variation among different species. Compared with evolution of other morphological traits, NMJ morphology appears to be evolving very rapidly. Moreover, my data indicate that natural selection rather than genetic drift is primarily responsible for evolution of NMJ morphology. To dissect underlying molecular mechanisms that may govern NMJ growth and evolutionary divergence, I focused on a naturally occurring variant in *D. melanogaster* that causes NMJ overgrowth. I discovered that the variant mapped to *Mob2*, a gene encoding a kinase adapter protein originally described in yeast as a member of the Mitotic Exit Network (MEN). I have subsequently examined mutations in the *Drosophila* orthologs of all the core components of the yeast MEN and found that all of them function as part of a common pathway that acts presynaptically to negatively regulate NMJ growth. As in the regulation of yeast cytokinesis, these components of the MEN appear to act ultimately by regulating actin dynamics during the process of bouton growth and division. These studies have thus led to the discovery of an entirely new role for the MEN—regulation of

synaptic growth—that is separate from its function in cell division. This work has identified a rich source of material for discovery of novel genes and mechanisms that regulate synaptic growth and development, and has also provided new insights into the mechanisms that underlie morphological evolution of nervous systems.

CHAPTER 1

Introduction

The neural communication that underlies all forms of behavior in complex animals is dependent on assembly and function of neural circuits. Alterations in synaptic connectivity of existing neurons and addition of new neurons are two ways that complex nervous systems can be modified during evolution (Ryan and Grant 2009). These physical changes presumably allow for the acquisition of new adaptive behaviors as species evolve. Establishment of synapses with appropriate size and morphology is therefore essential for proper neural function and behavior. In addition, plastic changes in synaptic size and complexity are important for normal mechanisms of learning and memory and are perturbed by various neurological disorders. Despite the importance of the mechanisms that regulate synaptic development and growth, we still lack detailed understanding of such questions as: How do synapses determine when and where to form branches? How do they determine how long these branches should be? How do synapses decide when and where to elaborate new boutons? How do synapses know when to stop growing? Do the genes and proteins involved in synaptic growth during development, overlap with those that are required later for plastic changes in synaptic morphology in the mature organism?

Evolution of Morphological Traits

Evolutionary processes are commonly studied through variation in morphological traits either among different species or within divergent populations of the same species. Through the study of these traits we can gain a better understanding of how an organism adapts to its environment. By identifying the genetic aberrations that are responsible for that variation we are able to gain insights into the evolutionary process

while also contributing to a better understanding of the genetic regulation of that trait. For example, multiple polymorphisms in cis-regulatory elements of the gene *yellow* have independently evolved and are responsible for extensive variation in both body pigmentation and wing color patterning in different species of *Drosophila* (Wittkopp et al. 2002, Gompel et al. 2005, Prud'homme et al. 2006, Jeong et al. 2008). This discovery not only provided insights into the evolutionary mechanism of pigmentation patterns, but also provided a better understanding of the genetic regulation of pigmentation mechanisms. Likewise, similar studies have been conducted using variant populations of a single species. For example, mutations in *ocular-albinism 2* were associated with albinism that evolved in multiple independent populations of the Mexican cave tetra (Protas et al. 2006). In this case natural populations of a single species were utilized to identify a key genetic difference that was responsible for trait evolution. In both examples insights were gained into both the evolutionary mechanism of the morphological trait as well as the genetic regulation of that trait. I utilized *Drosophila* larval neuromuscular junction (NMJ) formation as a morphological trait to address questions about how nervous systems evolve while also hoping to gain a better understanding of the mechanisms that regulate synapse morphology.

Drosophila **NMJ as a model for neural development**

The larval neuromuscular junction is very well suited for morphological analysis because the larval body wall muscles are large single cells arranged in an invariant, segmentally repeating pattern and innervated by individual motor neurons that form stereotypic synapses on the muscle surface (Gramates and Budnik 1999). Thus reliable

comparisons between animals as well as analysis of multiple iterations of the same developmental event within a single larva can be made easily. Morphological features of the synapse, such as number of synaptic boutons and branch points can be readily observed and quantified. As a synapse grows, new boutons are added either de novo or by budding from an existing bouton in a process that has been described to resemble budding in yeast (Zito et al. 1999). Branching occurs when two or more boutons emerge from an existing bouton. The larval NMJ also shares numerous characteristics of vertebrate central synapses, including being glutamatergic. Additionally, many of the proteins involved in regulating synaptic growth and function are conserved between flies and mammals including humans (Keshishian et al. 1996). Thus, it is likely that insights derived from studies of *Drosophila* will be of general biological and medical significance.

One of the most important aspects of using the *Drosophila* larval NMJ as an experimental model is the availability of powerful genetic tools. In particular, molecular analysis of mutations that alter synaptic growth and morphology of the larval NMJ have provided essential information about some of the key proteins involved in regulating synaptic growth and the pathways they affect. Examples of regulators of NMJ growth include cell BMP signaling molecules (Aberle et al. 2002, Marques et al. 2002, McCabe et al. 2003), cell adhesion molecules (Schuster et al. 1996a, Schuster et al. 1996b), ubiquitin ligase pathway (Wan et al. 2000, Wu et al. 2005) and wnt signaling (Packard et al. 2002, Speese and Budnik 2007). Taken together, these studies reveal the genetic and molecular complexity of synaptic growth regulation and highlight how much more remains to be learned.

The same features that make the larval NMJ well suited for developmental studies using mutation analysis also makes it an ideal system for studying the evolution of synaptic morphology by analyzing the NMJ phenotype among different species of *Drosophila* as well as natural isolates of *D. melanogaster*. The overall body plan, musculature and motor neuron innervation pattern are precisely conserved among all *Drosophila* species and are even shared with many more distantly related *Dipteran* species (Lachaise and Tsacas 1986). With the overall body plan so precisely conserved, numerous questions can be raised. Is synaptic morphology also highly conserved among these different species? Is there variation among populations of *D. melanogaster*? Do natural wild-type NMJs have the same structure as those that have been maintained in the lab for almost 100 year and bred to be slow, sluggish and stupid? Given the presumptive links between synaptic morphology and behavior and between behavior and fitness, answers to these questions have broad biological ramifications for studies of synaptic development, neurobiology, behavior, and evolutionary mechanisms.

Mob Proteins

Through a screen of natural populations of *D. melanogaster* a polymorphism causing NMJ overgrowth was identified within the gene *Mob2*. Mob (Monopolar spindle one binding) proteins were originally identified in yeast as Nuclear Dbf2-related (NDR) kinase adaptor proteins. In *Saccharomyces cerevisiae* there are 2 Mob proteins which both regulate cell division processes such as polarized cell growth, bud site selection and cell morphology (Luca and Winey 1998). Mob1 is a member of the Mitotic Exit Network (MEN), a pathway that initiates cytokinesis during the cell cycle (Luca and

Winey 1998). Mob2 is a member of the RAM (Regulation of Ace2 activity and cellular morphogenesis) signaling network which is involved in regulating cell polarity and daughter cell specific transcription (Weiss et al. 2002, Nelson et al. 2003).

In *Drosophila melanogaster*, *Caenorhabditis elegans* and *Danio rerio* there are four Mob proteins, while in mammals such as *Homo sapiens* there are seven (Li et al 2006, Mrkobrada et al. 2006). Compared with yeast, less is known about the role of Mob proteins in *Drosophila*, however they are thought to have conserved roles in cell cycle regulation (Lai et al. 2005, He et al. 2005, Shimizu et al. 2008, Trammell et al. 2008). A few additional roles for Mob proteins have also been identified. For example Mob2 regulates photoreceptor and wing hair morphogenesis (He et al. 2005, Liu et al. 2009). Additionally, Mob4 (pheocin) is a negative regulator of NMJ growth affecting axonal transport and microtubule dynamics (Schulte et al. 2010). Additionally, mammalian Mob proteins have been localized to neuronal dendrites where NDR kinases are regulating branching and tiling (Zallen et al. 2000, Baillat et al. 2001). Therefore, Mob proteins can regulate developmental processes in post-mitotic cells.

The Mitotic Exit Network

Mitosis is a highly complex, genetically regulated process culminating in cytokinesis. The Mitotic Exit Network (MEN) is the pathway responsible for turning off cell proliferation mechanisms and for promoting septum formation and cell division. While MEN was originally identified in *Saccharomyces cerevisiae*, it is a highly conserved pathway with orthologous pathway members being found in other fungi to mammals, including *Drosophila*. The precise regulation of the genes in this pathway has been

determined through genetic and biochemical studies of cytokinesis in *S. cerecisiae*. In this pathway, Mps1 (Monopolar spindle 1) phosphorylates Mob1 (Mps one binder 1) to activate it. Once phosphorylated Mob1 binds and enhances the function of the serine/threonine kinase Dbf2 (Dumbbell forming 2). The Dbf2-Mob1 complex then activates, through phosphorylation, Cdc14 (Cell division cycle 14). This phosphatase, Cdc14, has numerous functions including initiating a negative feedback loop on the MEN and critically dephosphorylating Cdk1 (Cyclin-dependent kinase 1). Once dephosphorylated, Cdk1 is targeted for degradation which causes a sharp decline in Cdk1 levels that were elevated earlier in the cell cycle. The drop in Cdk1 levels inhibits cell proliferation machinery and promotes cytokinesis by allowing for localization of Mob1, Dbf2, Cdc14 and other proteins to the bud neck. Localization of the Mob1-Dbf2 complex to the bud neck is required for localization of a complex of proteins, Hof1 (Homolog of cdc fifteen 1), Cyk3 (Cytokinesis 1) and Inn1 (required for ingression 1). The Hof1-Cyk3-Inn1 complex associates with the actomyosin ring and septin proteins allowing for the coordinated contraction of the septum and completion of cytokinesis (McCollum and Gould 2001, de Bettignies and Johnston 2003, Meitinger et al. 2012).

While all of the core members of the MEN pathway in *Drosophila* have known roles in cell cycle regulation, many are pleiotropic suggesting a role for these pathway members outside of the cell cycle. For example, a *Drosophila* ortholog of Dbf2 kinase, *tricornered* (*trc*) is involved in dendritic tiling (Emoto et al. 2004, Emoto et al. 2006, Grueber et al. 2007, Koike-Kumagai et al. 2009, Han et al. 2012) and hair cell development (Dickinson and Thatcher 1997, He et al. 2005a, He et al. 2005b, Fang and Adler 2010). Therefore,

it is likely that many members of the MEN may be co-opted for other functions during development.

References

Aberle H, Haghighi AP, Fetter RD, McCabe BD, Magalhaes TR and CS Goodman. 2002. Wishful thinking encodes a BMP type II receptor that regulates synaptic growth in *Drosophila*. *Neuron* 33:545-558.

Baillat G, Moqrich A, Castets F, Baude A, Bailly Y, Benmerah A and A Monneron. 2001. Molecular cloning and characterization of phocein, a protein found from the Golgi complex to dendritic spines. *Mol Biol Cell 12:663-73.*

de Bettignies G and LH Johnston. 2003. The Mitotic Exit Network. *Curr Biol* 13:R301.

Dickinson WJ and JW Thatcher. 1997. Morphogenesis of dentricles and hairs in *Drosophila* embryos: involvement of actin-associated proteins that also affect adult structures. *Cell Motility Cytoskel* 38:9-21.

Emoto K, He Y, Ye B, Grueber WB, Adler PN, Jan LY and YN Jan. 2004. Control of dendritic branching and tiling by the Tricornered-kinase/Furry signaling pathway in *Drosophila* sensory neurons. *Cell* 119:245-56.

Emoto K, Parrish JZ, Jan LY and YN Jan. 2006. The tumor suppressor Hippo acts with the NDR kinases in dendritic tiling and maintenance. *Nature* 443:210-3.

Fang X and PN Adler. 2010. Regulation of cell shape, wing hair initiation and the actin cytoskeleton by Trc/Fry and Wts/Mats complexes. *Dev Biol* 341:360-74.

Gompel N, Prud'homme B, Wittkopp PJ, Kassner VA and SB Carroll. 2005. Change caught on the wing: cis-regulatory evolution and the origin of pigment patterns in *Drosophila*. *Nature* 433:481-7.

Gramates LS and V Budnik. 1999. Assembly and maturation of the *Drosophila* larval neuromuscular junction. *Int Rev Neurobiol* 43:93-117.

Grueber WB, Ye B, Yang CH, Younger S, Borden K, Jan LY and YN Jan. 2007. Projections of *Drosophila* multidendritic neurons in the central nervous system: links with peripheral dendrite morphology. *Development* 134:55-64.

Han C, Wang D, Soba P, Zhu S, Lin X, Jan LY and YN Jan. 2012. Integrins regulate repulsion-mediated dendritic patterning of *Drosophila* sensory neurons by restricting dendrites in a 2D space. *Neuron* 73:64-78.

He Y, Fang X, Emoto K, Jan YN and PN Adler. 2005a. The tricornered Ser/Thr protein kinase is regulated by phosphorylation and interacts with furry during *Drosophila* wing hair development. *Mol Biol Cell* 16:689-700.

He Y, Emoto K, Fang X, Ren N, Tian X, Jan YN and PN Adler. 2005b. *Drosophila* mob family proteins interacts with the related tricornered (trc) and warts (wts) kinases. *Mol Biol Cell* 16:4139-52.

Jeong S, Rebeiz M, Andolfatto P, Werner T, True J and SB Carroll. 2008. The evolution of gene regulation underlies a morphological difference between two *Drosophila* sister species. *Cell* 132:783-93.

Keshishian H, Broadie K, Chiba A and M Bate. 1996. The D*rosophila* neuromuscular junction: a model system for studying synaptic development and function. *Annu Rev Neurosci* 19:545-75.

Koike-Kumagai M, Yasunaga KI, Morikawa R, Kanamori T and K Emoto. 2009. The target of rapamycin complex 2 controls dendritic tiling of *Drosophila* sensory neurons through the Tricornered kinase signaling pathway. *EMBO J* 28:3879-92.

Lachaise D and L Tsacas. 1986. *The Genetics and Biology of Drosophila*, eds Ashburner M, Carson HL, Thompon JN (Norton, New York), Vol 3D, pp 221-332.

Lai ZC, Wei X, Shimizu T, Ramos E, Rohrbaugh M, Nikolaidis N, Ho LL and Y Li. 2005. Control of cell proliferation and apoptosis by mob as tumor suppressor, mats. *Cell* 120:675-85.

Li H, Coghlan A, Ruan J, Coin LJ, Heriche JK, Osmotherly L, Li R, Liu T, Zhang Z, Bolund L, Wong GK, Zheng W, Dehal P, Wang J and R Durbin. 2006. TreeFam: a curated database of phylogenetic trees of animal gene families. *Nucleic Acid Res* 34:D572-80.

Liu L-Y, Lin C-H and S-S Fan. 2009. Function of *Drosophila* mob2 in photoreceptor morphogenesis. *Cell Tissue Res* 338:377-89.

Luca FC and M Winey. 1998. MOB1, an essential yeast gene required for completion of mitosis and maintenance of ploidy. *Mol Biol Cell* 9:29-46.

Marques G, Bao H, Haerry TE, Shimell MJ, Duchek P, Zhang B and MB O'Connor. 2002. The *Drosophila* BMP type II receptor Wishful Thinking regulates neuromuscular synapse morphology and function. *Neuron* 33:529-543.

McCabe BD, Marques G, Haghighi AP, Fetter RD, Crotty ML, Haerry TE, Goodman CS and MB O'Connor. 2003. The BMP homolog Gbb provides a retrograde signal that regulates synaptic growth at the *Drosophila* neuromuscular junction. *Neuron* 39:241-54.

McMollum D and KL Gould. 2001. Timing is everything: regulation of mitotic exit and cytokinesis by the MEN and SIN. *Trends Cell Biol* 11:89-95.

Meitinger F, Palani S and G Pereira. 2012. The power of MEN in cytokinesis. *Cell Cycle* 11:219-28.

Mrkobrada S, Boucher L, Ceccarelli DF, Tyers M and F Sicheri. 2006. Structural and functional analysis of Saccaromyces cerevisiae Mob1. *J Mol Biol* 362:430-40.

Nelson B, Kurischko C, Horecka J, Mody M, Nair P, Pratt L, Zougman A, McBroom LD, Hughes TR, Boone C and FC Luca. 2003. RAM: a conserved signaling network that regulates Ace2p transcriptional activity and polarized morphogenesis. *Mol Biol Cell* 14:3782-803.

Packard M, Koo ES, Gorczya M, Sharpe J, Cumberledge S and V Budnik. 2002. The *Drosophila* Wnt, wingless, provides an essential signal for pre- and postsynaptic differentiation. *Cell* 111:319-30.

Protas ME, Hersey C, Kochanek D, Zhou Y, Wilkens H, Jeffery WR, Zon LI, Borowsky R and CJ Tabin. 2006. Genetic analysis of cavefish revels molecular convergence in the evolution of albinism. *Nat Genet* 38:107-11.

Prud'homme B, Gompel N, Rokas A, Kassner VA, Williams TM, Yeh SD, True JR and SB Carroll. 2006. Repeated morphological evolution through cis-regulatory changes in a pleiotropic gene. *Nature* 440:1050-3.

Ryan TJ, Grant SGN (2009) The origin and evolution of synapses. Nat Rev Neuro 10:701-712.

Schulte J, Sepp KJ, Jorquera RA, Wu C, Song Y, Hong P and JT Littleton. 2010. DMob4/Phocein Regulates Synapse Formation, Axonal Transport, and Microtubule Organization. *J Neurosci* 30:5189-203.

Schuster CM, Davis GW, Fetter RD and CS Goodman. 1996a. Genetic dissection of structural and functional components of synaptic plasticity. I. Fasciclin II controls synaptic stabilization and growth. *Neuron* 17:641-54.

Schuster CM, Davis GW, Fetter RD and CS Goodman. 1996b. Genetic dissection of structural and functional components of synaptic plasticity. II. Fasciclin II controls presynaptic structural plasticity. *Neuron* 17:655-67.

Shimizu T, Ho LL and ZC Lai. 2008. The mob as tumor suppressor gene is essential for early development and regulates tissue growth in *Drosophila*. *Genetics* 178”957-65.

Speese SD and V Budnik. 2007. Wnts: up-and-coming at the synapse. *TRENDS Neurosci* 30:268-75.

Trammell MA, Mahoney NM, Agard DA and RD Vale. 2008. Mob4 plays a role in spindle focusing in *Drosophila* S2 cells. *J Cell Sci* 121:1284-92.

Wan HI, DiAntonio A, Fetter RD, Bergstrom K, Strauss R and CS Goodman. 2000. Highwire regulates synaptic growth in *Drosophila*. *Neuron* 26:313-329.

Weiss EL, Kurischko C, Zhang C, Shokat K, Drubin DG and FC Luca. 2002. Saccharomyces cerevisiae Mob2p-Cbk1p kinase complex promotes polarized growth and acts with the mitotic exit network to facilitate daughter cell-specific localization of Ace2 transcription factor. *J Cell Biol* 158:558-900.

Wittkopp PJ, True JR and SB Carroll. 2002. Reciprocal functions of the *Drosophila* yellow and ebony proteins in the development of pigment patterns. *Development* 129:1849-58.

Wittkopp PJ, Vaccaro K and SB Carroll. 2002. Evolution of yellow gene regulation and pigmentation in *Drosophila*. *Curr Biol* 12:1547-56.

Wu C, Wairkar YP, Collins CA and A DiAntonio. 2005. Highwire functions at the *Drosophila* neuromuscular junction: spatial, structural and temporal requirements. *J Neurosci* 25:9557-66.

Zallen JA, Peckol EL, Tobin DM and CI Bargmann. 2000. Neuronal cell shape and neurite initiation are regulated by the Ndr kinase SAX-1, a member of the Orb6/COT-1/warts serine/threonine kinase family. *Mol Biol Cell* 11:3177-90.

CHAPTER 2

Extensive morphological divergence and rapid evolution of the larval neuromuscular junction in *Drosophila*

This paper was published by Megan Campbell and Barry Ganetzky in

PNAS (2012) 109:E648-55.

ABSTRACT

Although the complexity and circuitry of nervous systems undergoes evolutionary change, we lack understanding of the general principles and specific mechanisms through which it occurs. The *Drosophila* larval neuromuscular junction (NMJ), which has been widely used for studies of synaptic development and function, is also an excellent system for studies of synaptic evolution because the genus spans over 40 million years of evolution and the same identified synapse can be examined across the entire phylogeny. We have now characterized morphology of the NMJ on muscle 4 (NMJ4) in more than 20 species of *Drosophila*. Although there is little variation within a species, NMJ morphology and complexity varies extensively between species. We find no significant correlation between NMJ phenotypes and phylogeny for the species examined suggesting that drift alone cannot explain the phenotypic variation and that selection likely plays an important role. However, the nature of the selective pressure is still unclear since basic parameters of synaptic function remain uniform. Whatever the mechanism, NMJ morphology is evolving rapidly in comparison with other morphological features because NMJ phenotypes differ even between several sibling species pairs. The discovery of this unexpectedly extensive divergence in NMJ morphology among *Drosophila* species provides unique opportunities to investigate mechanisms that regulate synaptic growth, the interrelationships between synaptic morphology, neural function and behavior, and the evolution of nervous systems and behavior in natural populations.

INTRODUCTION

Over the course of evolution, the complex circuitry of nervous systems are modified both by the addition of new types of neurons and by alterations in the synaptic connectivity of preexisting neurons (1). These changes presumably provide the physical basis for acquisition of new behaviors that serve adaptive functions as new species evolve. Although the evolution of brains and behaviors is of fundamental biological importance, we lack comprehensive understanding of the general principles governing these processes or the specific mechanisms and molecules through which evolutionary changes are effected. Because synapses are the basic structural and functional units of nervous systems, one way to begin to address these problems is to investigate a defined synapse across evolutionary time, which will allow us to correlate morphological variation with genetic differences.

The *Drosophila* larval neuromuscular junction (NMJ) is a powerful system for investigating molecular mechanisms of synaptic growth and development. The muscles are large, arranged in an invariant, segmentally repeating pattern, and each muscle is innervated by the same identified motor neurons and form NMJs with stereotypic morphology in each animal. These NMJs are large, easily accessible for microscopic and electrophysiological analyses, and their morphological features, such as the number of synaptic boutons and branch points, can be readily observed and quantified. A number of investigators have taken advantage of these features to identify genes encoding positive and negative regulators of NMJ growth that have revealed the signaling pathways regulating NMJ development (2).

The same features of the larval NMJ that make it well suited for developmental studies also make it an ideal system for studying the evolution of synaptic morphology by analyzing NMJ phenotypes in different species of *Drosophila*. The overall body plan, musculature, and motor innervation pattern are precisely conserved among all species of *Drosophila*, and are even shared with more distantly related groups of *Diptera* (3), despite enormous differences in size, habitat, food source, predation, and other aspects of their natural history and concomitant differences in behavior. Moreover, the subgenus *Drosophila* by itself encompasses at least 40 million years of evolutionary history (4). The conservation of body plan and muscle innervation over the evolutionary history of *Drosophila* immediately raises the question of whether NMJ morphology is also conserved or has undergone modification in different species. Because the body plan is conserved, it is possible to compare exactly the same genetically determined synapse among all species of *Drosophila*, which is particularly advantageous for this type of analysis.

Drosophila has featured prominently in the molecular analysis of regulatory changes in gene expression and developmental mechanisms that underlie evolutionary changes in morphological features among different species such as wing spots, body coloration and denticle pattern (5-8). Surprisingly, however, synaptic morphology, with its implications for evolution of brains and behavior, has not previously been examined as an evolutionary trait among different species of *Drosophila*. Thus, an investigation of variation in NMJ morphology among different species of *Drosophila* should provide a

wealth of important new information with implications for the evolution of nervous systems.

Here, we describe the results of such an investigation. We examined NMJ morphology in wild-caught *Drosophila melanogaster* for comparison with laboratory-bred wild-type stocks. We also examined NMJ morphology in over 20 different species of *Drosophila*. Whereas variation in NMJ morphology within a species is limited, we discovered a surprisingly extensive degree of variation among different species. No phylogenetic structure is apparent among the NMJ phenotypes, suggesting that genetic drift alone cannot explain the observed phenotypic variation and that selection is likely to play a predominant role in sculpting the NMJ. Compared with evolution of other morphological traits, NMJ morphology appears to be evolving rapidly as revealed by the striking differences in phenotype we find even among sibling species. Despite the vast differences in NMJ structure, the basic electrophysiological features of synaptic function are relatively constant. Understanding why NMJ morphology should have undergone such dramatic divergence, the adaptive and behavioral consequences of the different phenotypes, and the genetic and molecular mechanisms that generate them are important challenges for the future.

RESULTS

NMJ morphology shows extensive phenotypic variation among different species of *Drosophila*

Despite differences in size, habitat, food preference, and natural history, all species of *Drosophila* share a common larval body plan with identical body wall musculature and motor neuron innervations. Figure 1 shows the musculature of three *Drosophila* species: *D. melanogaster*, *D. punjabiensis* (the smallest species examined) and *D. virilis* (the largest and most distant from *D. melanogaster* of the species examined). However, the details of the morphological features of larval NMJs in these species have not previously been described. Is synaptic morphology also conserved or does it vary among species? If the phenotype is variable does it show any predictable pattern of variation among different *Drosophila* species?

As a basis for comparison, we first examined a number of isolates from natural populations of *Drosophila melanogaster* to determine the extent of variation in synaptic morphology within a species. To describe the phenotype quantitatively, we counted the number of synaptic boutons and branch points, commonly used metrics for this type of analysis, focusing on NMJ4 because of its relative simplicity. At least twenty isolates were examined both from local populations in Madison, Wisconsin as well as from more distant populations including African isolates. Although we did find an occasional variant, NMJ morphology in natural populations of *D. melanogaster* is generally uniform and comparable to the phenotype described for wild type laboratory stocks (average

number of boutons per NMJ4 ranged from 17 to 28 with a standard error of 1.0 between groups which is comparable to the error observed within a single population).

We performed a similar quantitative analysis of NMJ4 morphology on 20 additional species of *Drosophila*. Although we again found little variation within each species for the parameters we measured, we discovered surprisingly extensive variation in NMJ size and complexity between species (Figure 2, Table 1). Indeed, the range of phenotypes we observed in these species from *D. punjabiensis* to *D. funebris* is comparable to the phenotypic differences observed in *D. melanogaster* between mutants with the most severe NMJ undergrowth (~10 boutons/NMJ4) (9) to those with the most elaborate overgrowth (~50 boutons/NMJ4) (10). A substantial fraction of this variation in bouton number can be attributed to differences in larval body size (as estimated by average surface area of muscle 4) (Table 1, Figure 3). This result is in accord with the correlation between bouton number and muscle size observed in *D. melanogaster* throughout larval development and reflects the fact that as muscles increase in size they require more neurotransmitter release from presynaptic motor terminals to drive their contraction (11). Nonetheless, the value of r^2 for the correlation between bouton number and muscle size for NMJ4 among the different species (Figure 3) indicates that only about 50% of the variation in bouton number can be attributed to variation in muscle size, with the remaining 50% dependent on other factors. Moreover, variation in synaptic complexity and architecture are not strongly dependent on muscle size. For example, r^2 for the correlation between NMJ branch points and muscle area for NMJ4 is only 0.16 (Table 1, Figure 3). We also note that the parameters we have

measured capture only a portion of the observed variation in NMJ phenotypes as some species also exhibit novel morphological features that are difficult to quantify such as the unusual arrangement or appearance of boutons observed in *D. vulcana*, with boutons growing off the main stem rather than the typical 'beads-on-a-string' morphology, and *D. willistoni*, with boutons appearing diffuse and not readily resolved from the rest of the axon terminal. These differences in NMJ morphology that we observe are not limited to NMJ4 as we observe similar phenotypic differences for NMJ6/7 and NMJ 12/13. Thus, in contrast with the overall larval body plan, which is invariant among *Drosophila* species, NMJ morphology shows remarkably extensive evolutionary divergence.

NMJ phenotypes do not correlate with phylogenetic relationships

The discovery of this striking and extensive variation in NMJ morphology among *Drosophila* species immediately raises the question of what biological significance this variation has. One way to begin to address this question is to determine whether any consistent patterns emerge when we compare morphological phenotypes with the phylogenetic relationships among the various species. Are the NMJ phenotypes for two closely related species more similar than for two distantly related species? To minimize uncertainty about the phylogeny, we focused on eleven species of *Drosophila* whose genomes have been sequenced and whose evolutionary relationships are therefore known with a high degree of accuracy (12).

The phylogenetic tree for these eleven species is shown in Figure 4. The number of boutons, which is the parameter of NMJ morphology we used for this analysis, is presented for each species on the same tree. Examination of these data reveals no discernible pattern between phenotypic similarity and phylogenetic distance. Some closely related species such as *D. melanogaster* and *D. simulans* do share similar NMJ phenotypes but other pairs of sibling species such as *D. simulans* and *D. sechellia* have very distinct NMJ phenotypes. Conversely, some distantly related species have morphologically similar NMJs. For example, the NMJ morphology of *D. virilis* is quite distinct from that of the related *D. mojavensis* but the overall morphology is very similar to that of *D. melanogaster* from which it has been diverging for over 40 million years (4) (Figures 2 and 4). We see a similar absence of a correlation between NMJ morphologies and phylogenetic relationships among the larger sample of 21 species even though the exact phylogenetic tree for all these species has not been determined from genome sequences. The lack of any apparent correlation between phylogeny and phenotype means that the NMJ phenotype of any given species of *Drosophila* can only be determined by direct examination; it cannot be predicted based on NMJ phenotypes of any related species. Furthermore, as explored in more detail below, these results constrain the possible explanations for the evolutionary basis of the variation in NMJ phenotypes among different *Drosophila* species.

NMJ morphology can evolve rapidly

Regardless of mechanism driving the evolution of NMJ morphology in nature, it is apparent that it can occur over a rapid time scale. Even pairs of sibling species such as

D. simulans and *D. sechellia*, which diverged about 0.5 mya (4) or *D. yakuba* and *D. erecta*, which diverged about 2 mya (4) exhibit striking phenotypic differences in NMJ morphology (Figures 2 and 4). The contrast between the conserved external morphological appearance of the adults and the extensive phenotypic variation in NMJ morphology in these species is especially striking. Adult females in the *melanogaster* clade are almost indistinguishable and adult males can be distinguished only by differences in their genitalia (13). In fact, we are unaware of any morphological trait other than NMJ morphology that varies as extensively among these closely related species or that distinguishes them so readily. Thus, NMJ morphology appears to be evolving rapidly in comparison with other morphological traits.

Genetic drift is unlikely to explain evolution of NMJ morphology

Is NMJ morphology for each species being shaped primarily by natural selection or is it mainly due to genetic drift with random accumulation of adaptively neutral mutations? If genetic drift is the major force affecting the evolution of a trait (as it is for a non-coding DNA sequence), the similarity in phenotype between two species will generally be primarily dependent on their time of divergence; closely related species should be more similar in phenotype than more distantly related species. Similar reasoning has been used to develop computational models that statistically evaluate the evolution of more complex quantitative traits (14). The models partition the phenotypic value, z, for a quantitative trait (such as bouton number) into three components: $z_i = u + a_i + e_i$ where u is the underlying phenotypic component shared by all members of a phylogeny, a_i is the heritable additive effect for a particular species, and e_i is the residual error, which

includes measurement error, phylogenetic uncertainty, fluctuating selection, etc. Phylogenetic heritability, H_P^2, is then defined as $H_P^2 = \sigma_a^2 / \left(\sigma_a^2 + \sigma_e^2\right)$ where σ_a^2 is the variance associated with the heritable additive effect and σ_e^2 is the variance associated with the residual error. Because σ_a^2 is dependent primarily on phylogenetic relatedness, H_P^2 estimates the proportion of the phenotypic variation that is attributable to the underlying phylogeny. Thus, H_P^2 provides some measure of genetic drift.

An underlying assumption of this model is that the phenotypic values are normally distributed. We confirmed this assumption for our data by using a Q-Q plot and did not observe any deviation from normality within our dataset (p=0.03). Furthermore, a log-transformation of the data to force normality yielded a similar H_P^2 value (4.63×10^{-3}, p=0.24). This model also assumes that the error associated with phenotypic measurement is randomly distributed across the phylogenetic tree. In this case, all measurements were conducted in the same manner and the error associated with these measurements is quite small. Regardless, there is no discernable pattern of error across the phylogeny (r^2=0.1). A third assumption of the model is that the phylogeny is known without error. We used a phylogeny based on complete sequenced genomes, therefore the error associated with the phylogeny is minimal. Thus, it appears that the necessary conditions have been met to apply this model to our data.

Using average bouton number as the quantitative measure of NMJ morphology, we can compute the value of H_P^2 for the data presented in Figure 4. We apply this analysis to

the eleven species whose genomes have been completely sequenced thereby minimizing any sources of residual error due to inaccuracies in presumed phylogenetic relationships. Under this model, if a trait is evolving primarily under the influence of genetic drift, most of the phenotypic variation should be attributable to the underlying phylogeny and the value of H_P^2 should approach 1. Conversely, if the trait is under selective pressure, phylogeny alone is relatively less important in determining the phenotypic values and H_P^2 should approach 0. To increase statistical power in determining whether the computed value for H_P^2 is consistent with genetic drift, the topology of the phylogenetic tree is held constant and the phenotypic values are randomly shuffled and reassigned to the tree. The resulting value of H_P^2 for this reassignment is then recomputed and the process repeated 10,000 times. Since the random reassignment of phenotypic values is independent of actual phylogenic relationship, the value of H_P^2 is expected to be low for most permutations. Genetic drift is presumed to be acting when the actual observed value of H_P^2 is significantly greater than the value of H_P^2 calculated from the random permutations. The value of H_P^2 calculated from our data, 5.01×10^{-4}, is not significantly different from the values of H_P^2 generated by random shuffling of phenotypic values ($p = 0.27$) (Figure 5). Note that although we used bouton number for this analysis, equivalent conclusions are reached if we use other parameters such as branch number ($H_P^2 = 7.04 \times 10^{-4}$, $p=0.39$) as a quantitative metric of NMJ phenotypes. The data for these parameters are more consistent with the hypothesis that genetic drift alone is insufficient to account for the observed variation and that selection is likely to be a significant factor in shaping NMJ

morphology. Although we favor this interpretation, it is appropriate to emphasize that our analysis does not enable us to exclude other more complicated scenarios or to conclude that NMJ morphology is being shaped exclusively by selection.

Synaptic function is conserved among species

If selection is playing an important role to determine the differences in NMJ morphology among different *Drosophila* species, what are the targets of selection? The most obvious possibility is that differences in morphology would be associated with differences in synaptic function and that selection would act on synaptic function to meet the adaptive requirements of each particular species. We investigated this possibility by performing intracellular recording from muscle 4 in several different *Drosophila* species to assay various parameters of synaptic function including both spontaneous and evoked transmitter release. Spontaneous fusion of single synaptic vesicles with the presynaptic terminal elicits quantal depolarization events in the muscle called miniature excitatory junctional potentials (mEJP's). The amplitude of mEJP's is a measure of the size of synaptic vesicles and the amount of neurotransmitter packaged into each vesicle. The frequency of spontaneous fusion events provides an indication of the baseline properties of the synaptic release machinery. Electrical stimulation of the motor nerve, generates an action potential that triggers the coordinated and simultaneous release of many synaptic vesicles that produce an excitatory junctional potential (EJP) in the muscle, whose amplitude is a measure of the total number of synaptic vesicles released in response to an action potential. We measured each of these parameters in D. *melanogaster, D. punjabiensis, D. funebris* and *D. virilis* (Figure

6). We chose these species because they span the range of NMJ phenotypes as well as the breadth of the phylogenetic tree for the collection of *Drosophila* species we have examined. We performed the recordings in a low Ca^{2+} (0.4mM) Ringer's solution to avoid saturating muscle depolarization thereby enabling better resolution of any subtle differences in neurotransmitter release.

Despite the variation in NMJ morphology and time since divergence among these species, we did not observe substantial differences in any of the electrophysiological parameters we measured (Figure 6). Although there are some minor differences in mEJP frequency and EJP amplitude, such as a higher frequency of mEJPs in *D. funebris* and smaller EJP amplitude in *D. melanogaster*, there is no apparent correlation between the number and arrangement of boutons or muscle size in the various species and the measured parameters of synaptic function. One caveat is that the ionic concentrations of the hemolymph of species other than *D. melanogaster* are not known. Therefore, it is possible that our electrophysiological analyses on dissected preparations bathed in a standard Ringer's solution fails to detect some differences in synaptic function that may occur *in vivo* if there are significant differences in the normal concentrations of ions in the hemolymph of these species. However, any such differences are not expected to be large. Thus, to a first approximation, the functional output of the NMJs of different species is comparable despite their very different morphologies. This result is consistent with previous studies of mutants affect NMJ growth in *D. melanogaster* where EJP amplitudes do not correlate with NMJ size or complexity. Consequently, if selection is acting on synaptic function it must be operating

on parameters more subtle than those we have measured here, such as synaptic fatigue, following frequency etc., which could be of major significance under natural conditions.

DISCUSSION

The *Drosophila* larval NMJ has been used extensively as an experimental system for studies of synaptic function, development, and plasticity utilizing the wide array of genetic, molecular, histological, and electrophysiological tools available in this organism. Here, we add a new dimension to previous studies by taking an evolutionary perspective to examine phenotypic diversity of NMJ morphology among different species of *Drosophila*. The surprisingly high degree of morphological variation that we have discovered has the potential to lead to important insights concerning the molecular mechanisms that regulate synaptic development and growth, the relationship between synaptic structure and synaptic function, and the evolution of nervous systems and behavior.

Given the complete conservation of the larval body plan, musculature, and pattern of innervation among all species of *Drosophila* and even among other very distantly related families of *Diptera*, the great diversity of NMJ morphologies we have found was wholly unexpected. Although we have attempted to represent this diversity by quantifying parameters such as number of boutons and number of branch points, these measures alone do not fully capture the extent of the diverse phenotypes we observe, which include differences in bouton size, morphology, and distribution as well as

differences in the overall topography and geometry of the NMJs. The NMJ phenotypes span the range from the most undergrown to the most overgrown mutants characterized in *D. melanogaster* and include several novel phenotypes that have not yet been found in mutant screens. In this case however, these phenotypes have not been generated as a result of deliberate mutagenesis and screening but rather represent the typical appearance of NMJs for each species.

For most species we were limited to the single stocks that were available, therefore there is some question of whether the lines are truly representative of that particular species. To resolve this question with certainty, it will be necessary to collect and characterize multiple additional representatives of each of these species from nature. However, for several reasons, we believe that a more exhaustive analysis is unlikely to alter our results in any substantive way. First, for at least six of the species examined, more than one isolate was available and in each case, we observed no significant difference in phenotypes among the isolates. Second, for *D. melanogaster* we have characterized over twenty natural isolates from diverse climates and geographic locations and again found only limited variation in synaptic morphology. Third, although it is possible to imagine that for a few of the species the established isolates happen to carry a random mutation that conferrs an unusual NMJ phenotype, it seems highly unlikely that this would be true for the majority of species examined. Fourth, even large-scale screens in *D. melanogaster* have only rarely resulted in the identification of mutants with extreme or unusual NMJ phenotypes so the probability that such variants would by chance be incorporated into the isolates established for most *Drosophila*

species should be extremely small. Consequently, we believe that the phenotypes we describe are likely to be representative for each species.

We have used a phylogenetic quantitative model (14) to ask whether random accumulation of neutral mutations is sufficient to explain the observed phenotypic diversity in NMJ morphology. The underlying premise of the model is that if adaptively neutral mutations are the primary force driving the evolution of the quantitative trait under analysis, the similarity in phenotypes between two different species should reflect their phylogenetic distance: species that are more closely related should be more comparable in phenotype than more distantly related species. That is, the phenotypes should be structured in a way that reflects phylogeny. This model has been used previously to examine other quantitative traits that vary between species such as rates of meiotic recombination in different species of mice (14). In that case, the phenotypes are phylogenetically structured suggesting that neutral mutations are largely responsible for the evolutionary divergence of this phenotype. We applied this analysis to eleven species of *Drosophila* whose genomes have been completely sequenced and whose phylogenetic relationships are very well defined. We found that the key parameter, phenotypic heritability, calculated from our data set did not differ significantly from the values obtained by computer simulations where the phenotypic values were randomly shuffled along the phylogenetic tree. These results indicate that there is no apparent phylogenetic structure for the NMJ morphological phenotypes we examined and suggest that neutral mutations are unlikely to account for all of the observed phylogenetic diversity in NMJ morphology. Instead, it seems likely that the phenotypic

appearance of NMJs in different *Drosophila* species is under selection. However, the source of selective pressure remains unclear. For example, we do not know whether selection might be acting directly on NMJ morphology or whether changes in this phenotype merely reflect a pleiotropic byproduct of selection acting elsewhere. Previous mutational analysis has revealed that NMJ development is dependent upon many regulatory pathways and signal transduction mechanisms including BMP (9, 15) and Wg signaling (16), protein turnover via proteasomal- and autophagy-dependent mechanisms (17), and neuronal activity (18), all of which affect many aspects of fly development and physiology aside from the NMJ. One of these other developmental processes could be the actual target of selection with changes in NMJ morphology occurring as a secondary consequence. If this were the case, we would expect to see some other phenotype that shows an equally extensive range of phylogenetic variation but we are aware of no other phenotype for which this is true. This is particularly notable in comparisons of NMJ morphology in sibling species such as *D. simulans* and *D. sechellia*, which are not yet completely sexually isolated. These species are almost indistinguishable on the basis of external morphology, but their NMJs are highly divergent with NMJs in *D. sechellia* containing twice as many boutons arranged in a much more elaborate branching pattern compared with *D. melanogaster*. Although we cannot rule out selection with pleiotropic effects, our results can be explained more readily if selection is acting on NMJ morphology more directly rather than on some other developmental process.

Given the substantial differences in natural history among the various *Drosophila* species, it would seem likely that selection is acting upon synaptic function modifying it as required to provide each species with a selective advantage in its respective environment. Form would then follow function. However, contrary to this expectation, we have not observed any obvious differences among the various species in synaptic function as measured by the amplitude or frequency of mEJPs or by the amplitude of evoked potentials that correlate with the size or shape of the NMJ. The lack of any simple relationship between NMJ morphology and synaptic function has been previously encountered in studies of mutants affecting NMJ growth in *D. melanogaster* where EJP amplitudes do not correlate in any predictable way with NMJ size or complexity. In addition, homeostatic regulatory systems can potentially compensate for some differences in synaptic size and complexity by modulating other aspects of synaptic function to maintain stable synaptic output (19).

We have not observed any obvious differences in simple behaviors such as crawling ability. One possibility is that the precise size and layout of the NMJ has no physiological significance and a functional NMJ of any type is all that matters. However, this interpretation seems unlikely based on several different observations: the NMJ phenotype is relatively uniform within a species; NMJ morphology varies for different muscles within a body segment but is stereotypic for any given muscle; and our phylogenetic analysis suggests that random genetic drift is an insufficient explanation for the observed phenotypic variation. Thus, we suspect that a more likely explanation is that the key differences in synaptic function and behavior are more subtle than those we

have examined here. Under natural conditions where fitness would depend strongly on appropriate responses to changes in temperature and humidity, ability to forage for food, and successfully avoiding predation even small differences in parameters such as speed of transmission or synaptic fatigue could have profound effects on fitness but easily missed in our initial basic examination of synaptic function and behavior. Consequently, more extensive and systematic behavioral studies, particularly under conditions that approximate the natural environment, will be very desirable to seek behavioral correlates for the different NMJ phenotypes.

In screening the literature for possible ecological or behavioral parameters that correlate with NMJ morphology, we have identified one intriguing connection that may be relevant. Among the species we examined, three are feeding specialists: *D. sechellia* (20)*, D. erecta* (21), and *D. mojavensis* (22). In fact, both *D. sechellia* and *D. erecta* feed exclusively on plants that are toxic to their sibling species (20-21). All three of these species have large and complex NMJs by comparison with their close relatives, which are generalists. This trait cannot fully account for the diversity of NMJ phenotypes because some generalists also have large, complex NMJs. Nonetheless, these results suggest that it may be worthwhile to identify other parameters that may correlate with NMJ morphology.

NMJ morphology appears to evolve rapidly relative to the evolution of other morphological traits. This is again best illustrated by the differences between sibling species, such as *D. melanogaster* and *D. sechellia*, which have very distinct NMJ

morphologies. Although this rapid evolution is consistent with strong selection, further studies are necessary to understand the basis for it. One appealing speculation is that synaptic structure is not only a target on which selection acts but is also itself an evolutionary driving force. For example, one could imagine that a genetic variant altering the structure of NMJs (and presumably some central synapses as well) confers some behavioral changes that affect selection of mates or preferred microenvironment. These behavioral changes could restrict gene flow with other members of the population by creating an artificial mating barrier leading to the accumulation of additional genetic variants that further modify synapses and behavior. The net result would be a positive feedback loop in which changes in synaptic morphology would lead increasingly to reproductive isolation and incipient speciation even in the absence of geographic barriers. Whether any mechanism of this type actually operates in natural populations awaits future studies.

Ultimately, it will be important to identify the genes and molecular pathways responsible for the remarkable variation in NMJ phenotypes among *Drosophila* species. One possibility is that the same genes that have been identified via mutational analyses in the laboratory mediate these phenotypes in nature. Alternatively, the naturally occurring phenotypes may lead to the discovery of new mechanisms that regulate synaptic growth and development. Either of these outcomes will be of substantial interest.

The extraordinary phenotypic variation in NMJ morphology that we have discovered among species of *Drosophila* is a remarkable and unexpected feature of the biology of these organisms that challenges our understanding and poses many more questions

than we have been able to answer. At the same time, the existence of this phenomenon affords unique opportunities for further investigation that can provide novel insights into mechanisms that regulate synaptic growth, the interrelationships between synaptic morphology, neural function and behavior, and the evolution of nervous systems and behavior in natural populations. We believe that concerted efforts by investigators from the various disciplines touched upon by this work will be required to address the challenges and to extract all the information that the discovery of extensive evolutionary divergence in NMJ morphology has the potential to provide.

MATERIALS AND METHODS

Fly Stocks

Canton-S was used as the laboratory wild-type stock of *D. melanogaster*. Other stocks of *D. melanogaster* were established from wild isolates trapped in Madison, WI. Stocks of various *Drosophila* species were obtained Dr. Sean Carroll, University of Wisconsin-Madison, or from the San Diego stock center.

Imaging

All larvae were obtained from crosses of ten females and ten males incubated at 25˚C. Wandering third-instar larvae were dissected in ice-cold Ca^{2+}-free saline and fixed for 15 minutes in 4% formaldehyde in PBS. Larvae were incubated in FITC-conjugated anti-HRP (Jackson ImmunoResearch) at 1:100 overnight at 4˚C. NMJs were imaged using a Ziess 510 confocal microscope. Body wall images were obtained with bright field optics on a compound microscope.

Quantification of boutons and branch points were performed at NMJ4 in segments A2-A4 as described (23). Branch points were determined for each bouton with branch points defined as the number of projections from that bouton minus one (excluding terminal boutons). Branchpoints for each bouton were then added to determine the total number of branch points per NMJ. Muscle 4 surface area was measured using IMAGEJ software.

Computational Modeling

The phylogenetic tree was obtained from (12). The computational model used was adapted from (14) which uses Lynch's mixed model approach (24) to partition the phenotypic value, z, for a quantitative trait into three components: $z_i = u + a_i + e_i$ where u is the underlying phenotypic component shared by all members of a phylogeny, a_i is the heritable additive effect for a particular species, and e_i is the residual error, which includes measurement error, phylogenetic uncertainty, fluctuating selection, etc. Phylogenetic heritability, H_P^2, is then defined as $H_P^2 = \sigma_a^2 / \left(\sigma_a^2 + \sigma_e^2\right)$ where σ_a^2 is the variance associated with the heritable additive effect and σ_e^2 is the variance associated with the residual error. In our analysis H_P^2 estimates the proportion of variation in synaptic morphology that can be attributed to the phylogenetic relationship. Quantitative measures of synaptic morphology (primarily bouton number) were randomly shuffled along the tips of the phylogenetic tree and H_P^2 was recalculated. A total of 10,000 permutations were performed to calculate p-values and assess significance of the estimated H_P^2. When using branch number as the quantitative parameter, only 1000 permuations were calculated owing to computational limitations. All computational

analyses were performed in the R environment using base package functions and function calls within the APE contributed package (25-26).

Electrophysiology

Electrophysiology was performed on muscle 4 (segments 3 and 4) of wandering third-instar larvae. Standard HL-3 saline with 0.4mM external calcium was used for recording. Preparations were visualized on an inverted Nikon DIAPHOT200 using Normarski optics. Microelectrodes with R of ~25MΩ were filled with 3M KCl and nerve stimulation electrodes were filled with bath saline. Average muscle input resistances were D. melanogster: 14.4MΩ, D. punjabiensis: 16.7, D. funebris: 13.9 and D. virilis: 12.5. Evoked EJPs were recorded in current-clamp using the Axoclamp 2B amplifier (Axon Instruments, Union City, CA). Mean EJP amplitudes were determined from 100 consecutive evoked EJPs at 2Hz stimulation. Traces were analyzed using AxonClamp software. mEJP amplitude and frequency were analyzed using Mini Analysis software 5.6.4 (Synaptosoft, Deactur, GA).

ACKNOWLEDGEMENTS

We are particularly grateful to Sean Carroll and his laboratory for providing stocks of many of the *Drosophila* species used in these analyses. We also thank Bret Payseur and Beth Dumont for their assistance with the computational model; all members of the Ganetzky laboratory for helpful discussion and critical comments on the manuscript; and the San Diego Stock Center at the University of California-San Diego for supplying

stocks of several species examined here. This research was supported by the National Institutes of Health through a predoctoral training grant (T32 GM007507) to the Neuroscience Training Program and a research grant (RO1NS15390) to B. Ganetzky.

REFERENCES

1. Ryan TJ, Grant SGN (2009) The origin and evolution of synapses. Nat Rev Neuro 10:701-712.

2. Collins CA, DiAntonio A (2007) Synaptic development: insights from *Drosophila*. Curr Opin Neurobiol 17:35-42.

3. Lachaise D, Tsacas L (1964) in *The Genetics and Biology of Drosophila*. eds Ashburner M, Carson HL, Thompson JN (Norton, New York), pp 221-332.

4. Russo CAM, Takezaki N, Nei M (1995) Molecular Phylogeny and Divergence Times of *Drosophilid* Species. Mol Biol Evol 12:391-404.

5. Gompel N, Prud'homme B, Wittkopp PJ, Kassner VA, Carroll SB (2005) Chance caught on the wing: cis-regulatory evolution and the origin of pigment patterns in *Drosophila*. Nature 433:481-487.

6. Jeong S, Rokas A, Carroll SB (2006) Regulation of body pigmentation by the Abdominal-B Hox protein and its gain and loss in *Drosophila* evolution. Cell 125:1387-1399.

7. Jeong S, et al. (2008) The evolution of gene regulation underlies a morphological difference between two *Drosophila* sister species. Cell 132:783-793.

8. McGregor AP, et al. (2007) Morphological evolution through multiple cis-regulatory mutations at a single gene. Nature 488:587-590.

9. Marqués G, et al. (2002) The *Drosophila* BMP type II receptor Whishful Thinking regulates neuromuscular synapse morphology and function. Neuron 33:529-543.

10. Wan HI et al. (2000) Highwire regulates synaptic growth in *Drosophila*. Neuron 26:313-329.

11. Schuster CM, Davis GW, Fetter RD, Goodman CS (1996) Genetic dissection of structural and functional components of synaptic plasiticity. I. Fasciclin II controls synaptic stabilization and growth. Neuron 17:641-654.

12. Stark A, et al. (2007) Discovery of functional elements in 12 *Drosophila* genomes using evolutionary signatures. Nature 450:219-232.

13. Liu J, et al. (1996) Genetic Analysis of a Morphological Shape Difference in the Male Genitalia of *Drosophila simulans* and *D. mauritiana*. Genetics 142:1129-1145.

14. Dumont B, Payseur B (2008) Evolution of the Genomic Rate of Recombination in Mammals. Evolution 62:276-294.

15. O'Connor-Giles KM, Ho LL, Ganetzky B (2008) Nervous wreck interacts with thickveins and the endocytic machinery to attenuate retrograde BMP signaling during synaptic growth. Neuron 58:507-518.

16. Budnick V, Salinas PC (2011) Wnt signaling during synaptic development and plasticity. Curr Opin Neurobiol 21:151-159.

17. Shen W, Ganetzky B (2010) Autophagy promotes synapse development. JCB 187:71-79.

18. de Bivort BL, Guo HF, Zhong Y (2009) Notch signaling is required for activity-dependent synaptic plasticity at the *Drosophila* neuromuscular junction. J Neurogenet 23:395-404.

19. Davis GW (2006) Homeostatic control of neural activity: from phenomenology to molecular design. Annu Rev Neurosci 29:307-323.

20. R'Kha S, Capy P, David JR (1991) Host-plant specialization in the *Drosophila melanogaster* species complex: a physiological, behavioral, and genetic analysis. Proc Natl Acad Sci USA 88:1835-1839.

21. Lachaise and Tsacas (1974) Les *Drosophilidae* fruits de *Pandanus candelabrum* (*Pandancíes*). Ann Univ Abidjan 7:153-192.

22. Fogleman JC, Starmer WT, Heed WB (1981) Larval selectivity for yeast species by *Drosophila mojavensis* in natural substrates. Proc Natl Acad Sci USA 78:4435-4439.

23. Coyle IP, et al. (2004) *Nervous wreck*, an SH3 adaptor protein that interacts with *Wsp*, regulates synaptic growth in *Drosophila*. Neuron 41:521-534.

24. Lynch M (1991) Methods for the analysis of comparative data in evolutionary biology. Evolution 5:1065-1080.

25. Pardis E, Claude J, Dtrimmer K (2004) APE: analyses of phylogenetics and evolution in R language. Bioinformatics 20:289-290.

26. R Development Core Team (2006) T:a language and environment for statistical computing. R Foundation for Statistical Computing, Vienna, Austria.

Table 1

	n	Boutons	Branch Points	Muscle Surface Area ($\mu m^2 \times 10^4$)
ananassae	25	22.7 ± 0.8	3.7 ± 0.3	5.41 ± 0.23
erecta	25	29.5 ± 1.4	9.4 ± 0.6	3.95 ± 0.19
funebris	30	42.2 ± 1.4	8.1 ± 0.5	5.87 ± 0.22
greeni	25	33.1 ± 1.1	8.7 ± 0.7	4.79 ± 0.39
jambulina	25	19.5 ± 1.2	3.3 ± 0.4	2.95 ± 0.07
malerkotliana	30	18.3 ± 0.8	2.9 ± 0.3	2.93 ± 0.10
mauritiana	25	30.8 ± 0.7	7.3 ± 0.4	4.84 ± 0.18
melanogaster	45	19.3 ± 0.8	1.8 ± 0.2	4.94 ± 0.11
mojavensis	30	34.8 ± 1.3	11.4 ± 0.7	4.13 ± 0.23
pallidosa	25	21.8 ± 0.7	2.1 ± 0.4	3.11 ± 0.06
persimilis	25	39.1 ± 1.6	9.0 ± 0.8	5.53 ± 0.08
pseudoobscura	30	50.3 ± 2.2	9.9 ± 0.8	5.37 ± 0.20
punjabiensis	25	11.7 ± 0.5	2.6 ± 0.3	3.70 ± 0.11
sechellia	45	45.9 ± 1.2	11.5 ± 0.7	4.65 ± 0.16
seguyi	30	23.2 ± 1.1	4.2 ± 0.3	3.23 ± 0.17
serrata	25	20.0 ± 0.9	3.7 ± 0.4	2.90 ± 0.11
simulans	30	21.2 ± 0.7	5.8 ± 0.4	4.35 ± 0.10
virilis	30	39.4 ± 1.2	4.7 ± 0.3	7.15 ± 0.19
vulcana	25	16.0 ± 0.7	4.4 ± 0.4	2.92 ± 0.07
willistoni	30	20.0 ± 0.5	2.2 ± 0.2	3.37 ± 0.14
yakuba	25	16.4 ± 1.0	3.7 ± 0.4	3.71 ± 0.14

TABLE 1: Quantification of bouton number, branch points and muscle 4 surface area in various species of *Drosophila*.

Mean ± SEM. All analyses were performed on NMJ4 in abdominal segments 2-4 of each species.

Figure 1

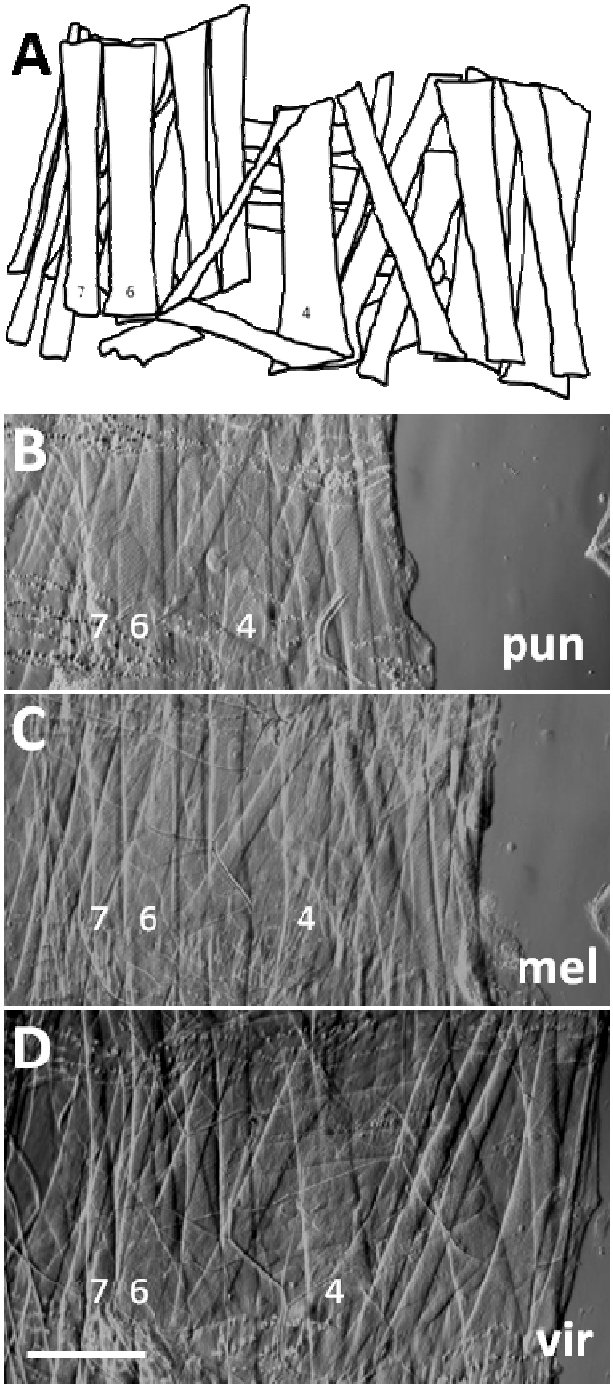

FIGURE 1. Larval body wall musculature is precisely conserved among *Drosophila* species. Brightfield images of dissected third-instar larvae from *D. punjabiensis* (pun), *D. melanogaster* (mel), and *D. virilis* (vir) showing musculature in right hemisegment 2. Diagram at the top illustrates the complete pattern of musculature in each of these species. All of these muscles cannot be seen in the microscopic images, which were focused on the most superficial muscle layers. For orientation, muscles 4, 6, and 7 are labeled. This analysis focused on the NMJs that form on muscle 4.

Scale bar, 200 µm.

Figure 2

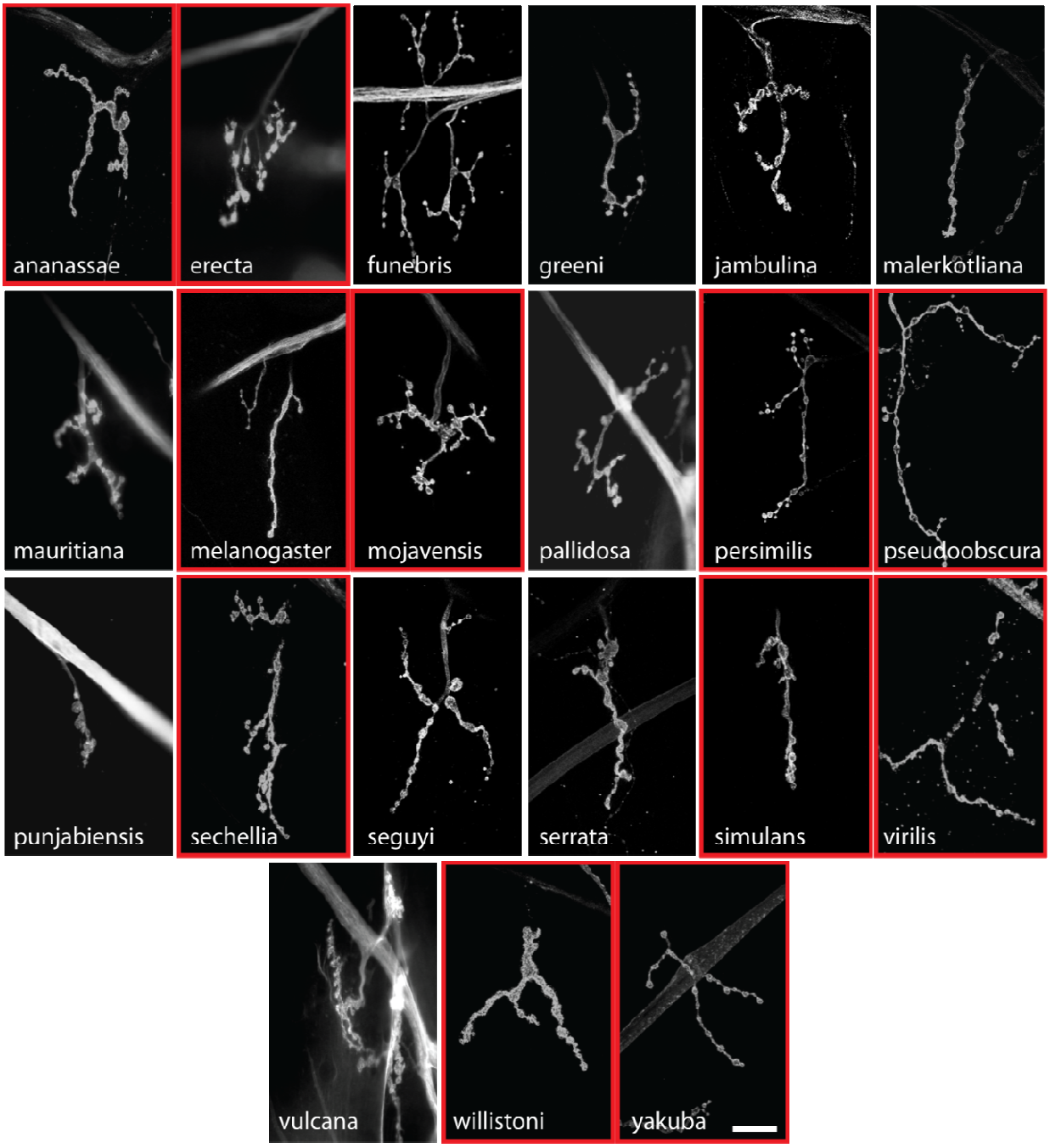
ananassae
erecta
funebris
greeni
jambulina
malerkotliana
mauritiana
melanogaster
mojavensis
pallidosa
persimilis
pseudoobscura
punjabiensis
sechellia
seguyi
serrata
simulans
virilis
vulcana
willistoni
yakuba

FIGURE 2. Larval NMJs show extensive morphological variation in different species of *Drosophila*. Third-instar larvae of each species were dissected and stained with FITC-conjugated anti-HRP. Representative confocal images of NMJ4 in abdominal segment 2 are shown. There is substantial variation in NMJ morphology among these species with respect to overall geometry, number of boutons and number of branch points. The eleven species enclosed by red boxes are those whose genome has been completely sequenced and whose precise phylogenetic relationships have been ascertained.

Scale bar, 20 μm.

Figure 3

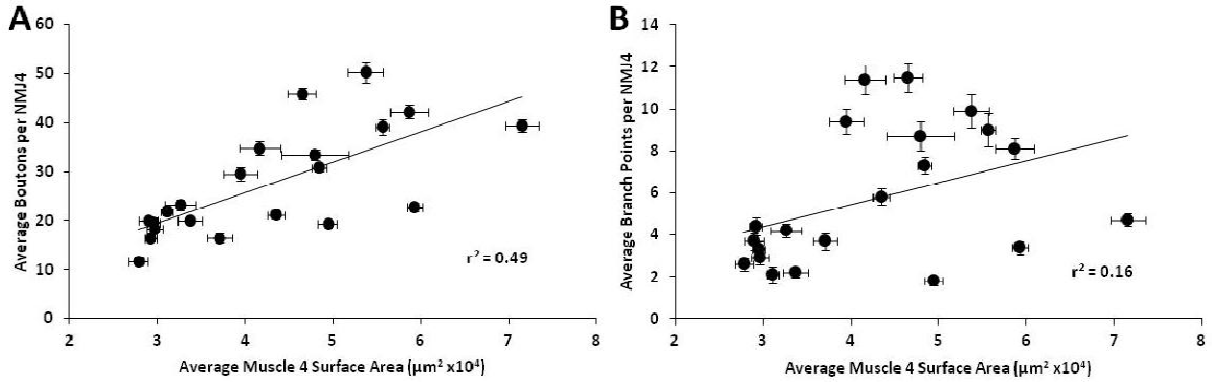
A
Average Boutons per NMJ4
Average Muscle 4 Surface Area (µm² x10⁴)
r² = 0.49
B
Average Branch Points per NMJ4
Average Muscle 4 Surface Area (µm² x10⁴)
r² = 0.16

FIGURE 3. Differences in muscle size cannot fully explain all the variation observed in NMJ size. For each species the average numbers of boutons (A) or branch points (B) per NMJ4 are plotted against the average muscle 4 surface area with the linear regression line superimposed. Scale bars represent SEM for each parameter.

Figure 4

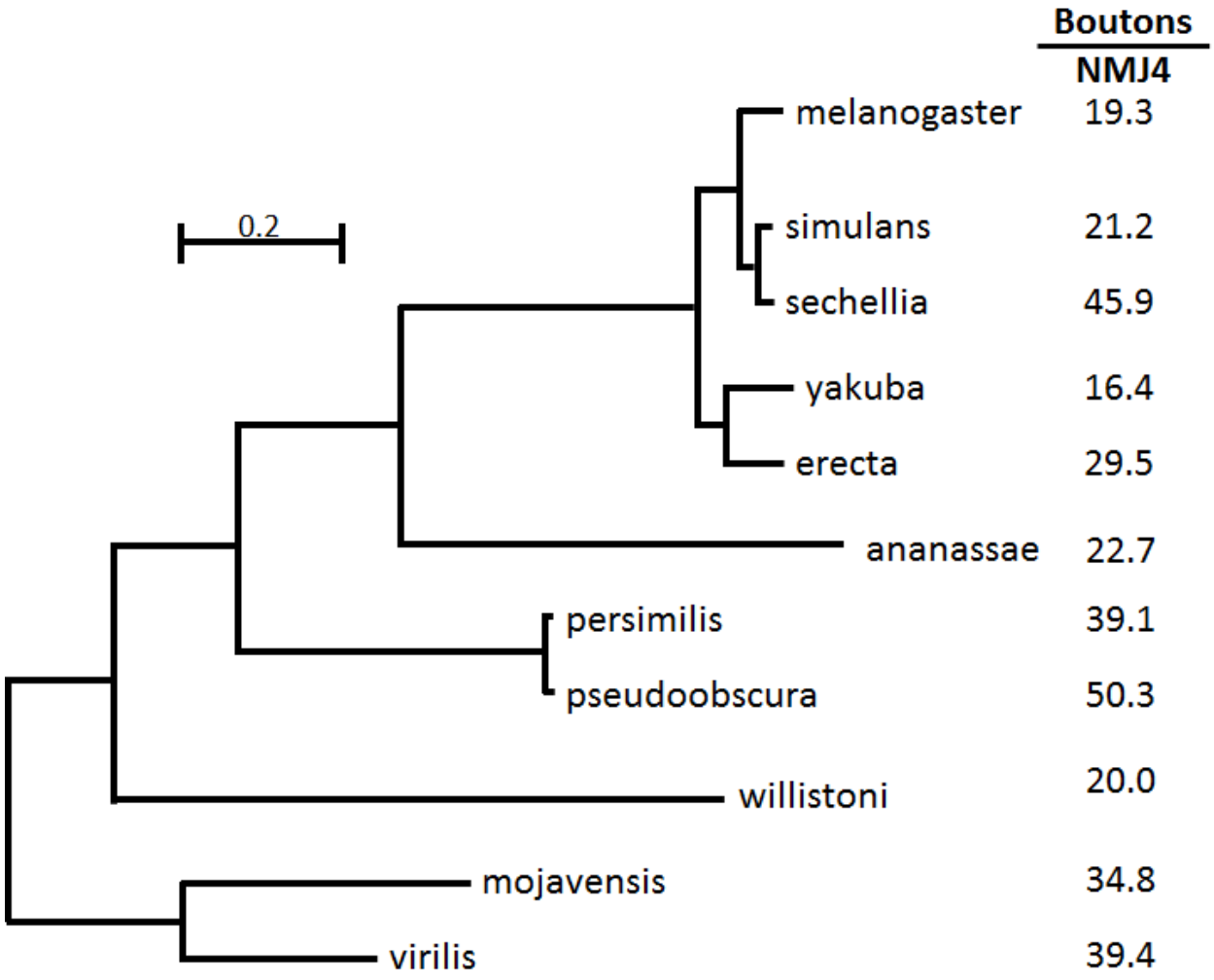
Boutons
NMJ4
melanogaster
19.3
0.2
simulans
21.2
sechellia
45.9
yakuba
16.4
erecta
29.5
ananassae
22.7
persimilis
39.1
pseudoobscura
50.3
willistoni
20.0
mojavensis
34.8
virilis
39.4

FIGURE 4. NMJ phenotypes among different species of *Drosophila* lack phylogenetic structure. The phylogenetic tree is derived from the complete genomic sequences of the species shown based on rates of neutral substitutions at 12,000 sites (Stark et al. 2007). Scale bar, number of substitutions per site. The total evolutionary distance spanned by this phylogeny is more than 40 million years with the distance from *D. melanogaster* to *D. mojavensis* being estimated at 40mya (Russo et al. 1995). Shown to the right of each species is the average number of boutons per NMJ4 as a representative quantitative measure of NMJ phenotype for that species (see Table 1). Examination of the data reveals no obvious relationship between phylogenetic distance between the various species and their phenotypic similarity. The same is true if NMJ phenotypes are represented instead by number of synaptic branches.

Figure 5

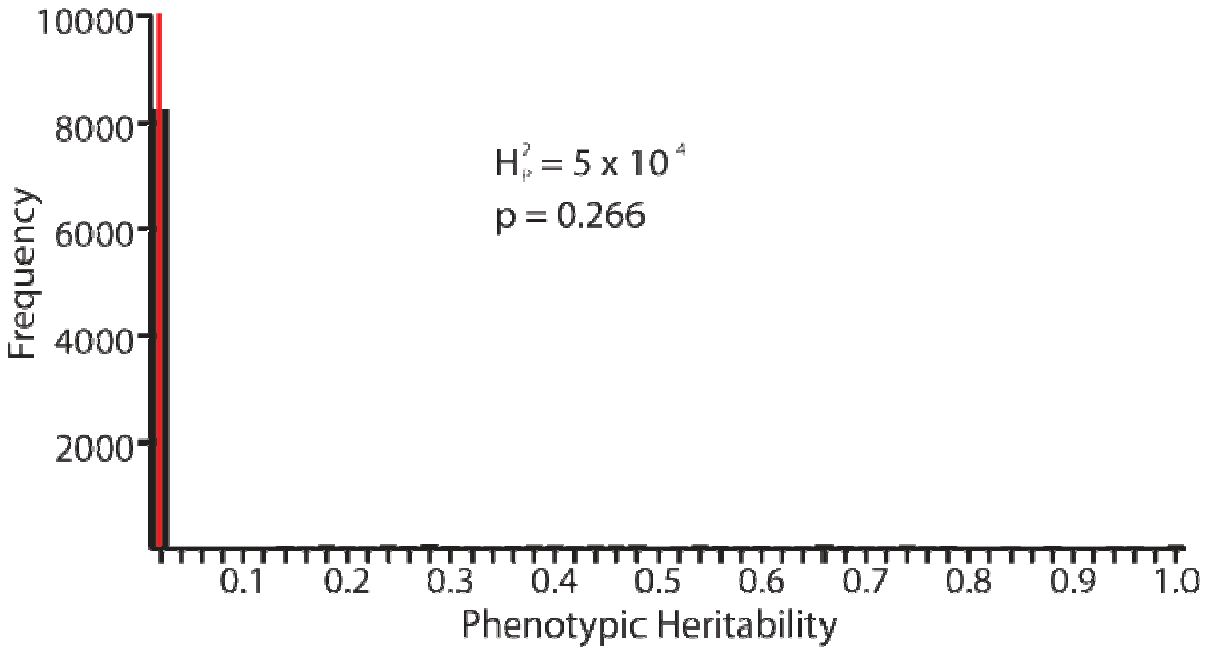
10000
8000
6000
4000
2000
Frequency
$H_p^2 = 5 \times 10^{-4}$
p = 0.266
0.1
0.2
0.3
0.4
0.5
0.6
0.7
0.8
0.9
1.0
Phenotypic Heritability

FIGURE 5. Genetic drift does not seem to account for variation in NMJ phenotypes among different species of *Drosophila*. Computational analysis was performed for the eleven species shown in Figure 2 whose genomes have been sequenced and whose phylogenetic tree has been precisely established. The average number of boutons per NMJ4 for each species was used as the quantitative character analyzed. Comparable results were obtained using number of branch points (H_P^2 = 7.04 x 10^{-4}, p=0.39) instead of number of boutons. The value of H_P^2 for bouton number was calculated as described in the text and Materials and Methods. According to the model, if the variation in bouton number among the different species is primarily determined by their phylogenetic relatedness, the value of H_P^2 will approach 1. A high value of H_P^2 is therefore consistent with genetic drift playing a major role in the evolution of NMJ morphology. The computed value for H_P^2 for our data set is 5.01 x 10^{-4} (thin red line). To determine whether this outcome is consistent with a strong phylogenetic effect on NMJ morphology, bouton numbers shown in Figure 2 were randomly shuffled among species on the phylogenetic tree and the value of H_P^2 for that arrangement was calculated. This procedure was repeated 10,000 times to generate the distribution of H_P^2 values shown in the histogram. As expected, random shuffling of bouton numbers among species, irrespective of phylogeny, results in mostly very low values for H_P^2. However, 61% of the H_P^2 values from the random shuffling fall above the observed H_P^2 value calculated from our data set. Therefore, the results are consistent with the absence of a strong phylogenetic contribution to NMJ phenotype and suggest that the observed variation in NMJ morphology cannot be explained by genetic drift alone.

Figure 6

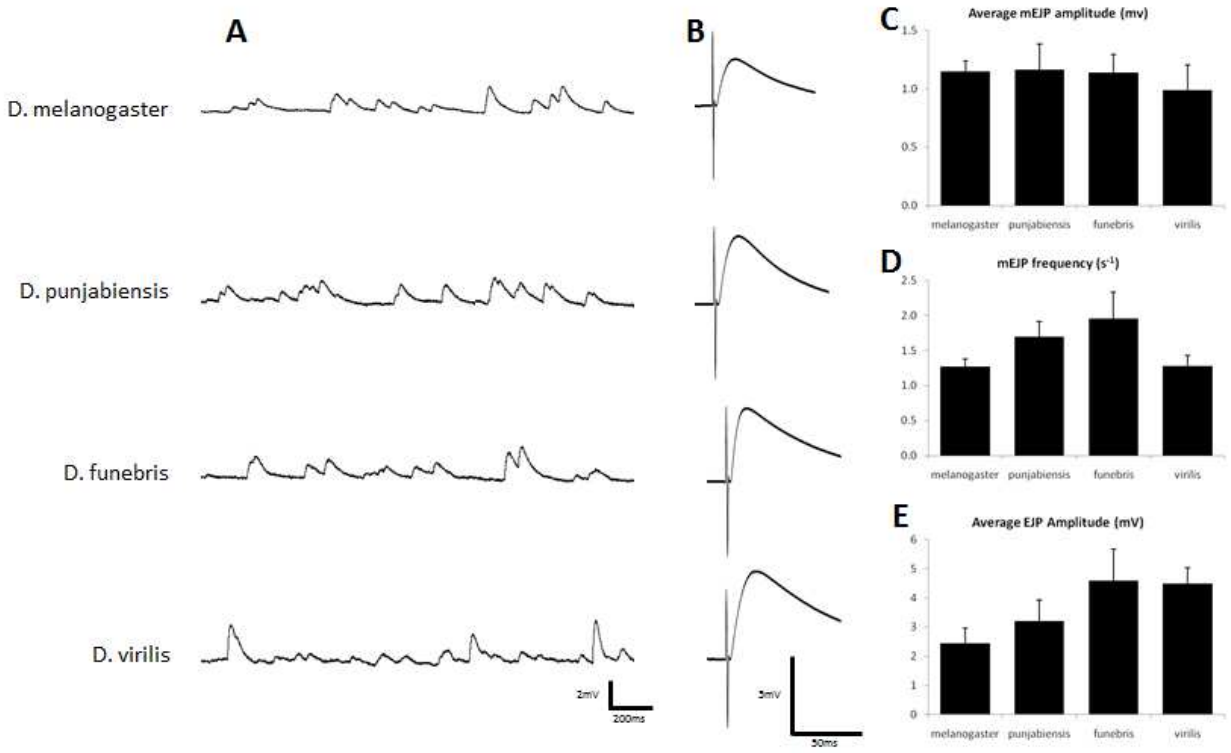
A
B
C
D
E
D. melanogaster
D. punjabiensis
D. funebris
D. virilis
2mV
200ms
5mV
50ms
Average mEJP amplitude (mv)
mEJP frequency (s-1)
Average EJP Amplitude (mV)
melanogaster
punjabiensis
funebris
virilis

FIGURE 6. Synaptic function of NMJ4 does not correlate with morphology. Intracellular recordings of mEJP amplitude and frequency and evoked excitatory junction potentials (EJP) are from muscle 4 in 0.4mM external calcium. A. Representative mEJP recordings, quantified in C. and D. B. Representative EJPs evoked by electrical stimulation of the appropriate segmental nerve bundle. E. Average EJP amplitude, a measure of the number of vesicles released in response to an evoked action potential, is quantified for each species. Error bars indicate SEM (minimum n of 12).

CHAPTER 3

Identification of Mob2, a novel regulator of larval neuromuscular junction morphology, from natural populations of *Drosophila melanogaster*

This chapter is in preparation for publication by Megan Campbell and Barry Ganetzky

ABSTRACT

Nervous systems undergo evolutionary adaption to modify behaviors enabling organisms to meet challenges and survive in nature; however we lack understanding of the general principles and specific mechanisms that regulate this adaptation. While morphology of the larval neuromuscular junctions (NMJs) varies extensively among different species of *Drosophila*, it is largely conserved among natural populations of *D. melanogaster* despite widely varied environments and climates (e.g. temperate climates, deserts, tropical rainforests). However, mild overgrowth is observed in two natural isolates among twenty populations screened. Both of these variants are isofemale lines collected in Madison, WI. Through further characterization by isolating single chromosomes of one of these variant lines, H4, we determined that mutations in multiple genes encoding both positive and negative regulators of NMJ morphology are segregating within this line. Focusing on a single overgrown subisolate, H4-5, we mapped the relevant polymorphism to *Mob2* (*Mps1 binding 2*), a Nuclear Dbf2-related (NDR) kinase adaptor, originally identified in yeast for its role in cytokinesis. Presynaptic expression of Mob2 is necessary and sufficient for regulating NMJ growth. Furthermore, Mob2 genetically interacts with one of the two NDR kinases in *Drosophila tricornered* (*trc*), but not *warts* (*wts*) to dominantly enhance the NMJ overgrowth phenotype. This work has identified a rich source of material for discovery of novel genes that regulate synaptic growth and development, and has also provided new insights into the mechanisms that underlie morphological evolution of nervous systems.

INTRODUCTION

The study of evolution utilizes morphological traits in order to better understand how an organism adapts to its environment. Variation in that morphological trait can then be used to identify the genes and pathways that are responsible for generating phenotypic diversity. Studying morphological variation within natural populations of a single species can provide insights into the genes upon which evolution can act can to drive variation within populations and potentially contribute to speciation.

The *Drosophila* larval neuromuscular junction (NMJ) is a powerful model for studying the genetic and molecular mechanisms of synaptic growth and development. Numerous investigators have taken advantage of the larval NMJ to identify positive and negative regulators of NMJ growth which have revealed signaling pathways that regulate NMJ development (Collins and DiAntonio 2007). Previous work demonstrated that NMJ morphology varies extensively among different *Drosophila* species (Campbell and Ganetzky 2012). Significantly, the sibling species *D. simulans* and *D. sechellia*, both within the melanogaster clade, have different NMJ morphologies. *D. sechellia* is overgrown with additional boutons and branch points compared with *D. simulans*. Because these species can be interbred, we attempted to identify the genes responsible for the difference in morphology by interspecific crosses and quantitative trait loci (QTL) mapping. While we were able to determine that approximately five loci contribute to the phenotypic variation, the genetic limitations of these interspecies hybrid crosses prevented us from identifying specific genetic aberrations. In order to identify genes

and pathways responsible for variation in NMJ morphology in nature, we focused on natural populations of *D. melanogaster*, which is more genetically accessible while still providing insights into the regulation of synaptic morphology in an evolutionary context. It is reasonable to believe that polymorphisms within a species are the foundation from which evolution can act leading to the variation observed among species

Through isolating single chromosomes from an isofemale line of *D. melanogaster* with a variant NMJ morphology collected in Madison, WI, we were able to identify a polymorphism in the gene *Monopolar spindle One Binding 2*, *Mob2.* Mob proteins were originally identified in yeast as Nuclear Dbf2-related (NDR) kinase adaptor proteins involved in cytokinesis (Luca and Winey 1998). Less is known about the role of Mob proteins in *Drosophila*, of which there are four, however they are thought to have conserved roles in cell cycle (Lai et al. 2005, He et al. 2005, Shimizu et al. 2008, Trammell et al. 2008). Mob2, specifically, has been shown to regulate photoreceptor and wing hair morphogenesis (He et al. 2005, Liu et al. 2009). While Mob2 has not been studied at the NMJ, Mob4 (pheocin) has been shown to be a negative regulator of NMJ growth affecting axonal transport and microtubule dynamics (Schulte et al. 2010). Additionally, mammalian Mob proteins have been localized to neuronal dendrites where NDR kinases are regulating branching and tiling (Zallen et al. 2000, Baillat et al. 2001). Therefore, Mob proteins can also regulate developmental processes in post-mitotic neurons.

Here we describe a screen for variation in NMJ morphology of natural populations of *D. melanogaster*. While morphologies are mostly conserved, two examples of mild overgrowth were observed from the twenty lines examined. Isolating single chromosomes from one of these variant lines isolated six non-complementing negative growth regulators and one positive growth regulator. Through further investigation of one of these semi-isogenic lines, we identified a polymorphism in the regulatory region of *Mob2.* Mob2 functions presynaptically with the NDR kinase Tricornered (Trc) to negatively regulate NMJ growth.

RESULTS AND DISCUSSION

NMJ morphology is conserved in natural populations of *D. melanogaster*

What is the "wild-type" phenotype for larval NMJ morphology? Many laboratory stocks have been maintained for over one hundred years, during which time they have been inadvertently artificially selected for those animals that thrive under laboratory conditions (non-escapers, etc.). These laboratory animals are living in their food, with regulated temperature and humidity, availability of mates, and absence of predators. In contrast, natural populations of *D. melanogaster* inhabit a wide variety of climates and habitats (e.g. temperate climates, deserts, tropical rainforests) that present numerous different ecological and behavioral challenges absent in the laboratory. Successful adaptation to meet these challenges and survive in nature likely entails genetic changes to synaptic structure and function that modify behavior. Therefore, it is reasonable to ask whether the standard NMJ morphology observed in laboratory wild-type stocks is an accurate

depiction of the phenotype of wild-type flies in nature. We have previously discovered that there is extensive variation in NMJ morphology between different species of *Drosophila* but how much variation in NMJ morphology is there within natural populations of one species—in particular, *D. melanogaster*?

To address these questions, we examined larval NMJ morphology in three laboratory wild-type stocks (Canton-S, Oregon-R, Urbana) as well as isolates from 20 natural populations (12 inbred lines from diverse locations and 8 isofemale lines from Madison, WI). To describe the phenotypes quantitatively, we counted the number of synaptic boutons (an estimate of NMJ size) and branch points (an estimate of NMJ complexity), focusing on the NMJ on muscle 4 (NMJ4) because of its relative simplicity. Despite the differences in environments from which these lines were obtained, NMJ morphology is relatively uniform among these lines (Figure 1). The three laboratory wild-type stocks show no significant differences in NMJ morphology either for bouton number or branch points. Furthermore, we also found no significant variation among the inbred natural isolates. The average number of boutons per NMJ4 across these lines was 20.5 with a standard error of 0.7 between groups, which is comparable to error observed within a single population. The average number of branch points per NMJ4 across populations was 2.6±0.5. This uniformity in phenotype was largely true for the 8 isofemale lines from Madison, WI, with two exceptions. These two lines, H4 and H5 (Figure 1) exhibit a mild overgrowth phenotype with increased branching. H4 has an average of 25.9±1.0 boutons and 6.9±0.7 branch points per NMJ4. H5 has an average of 23.8±0.8 boutons and 5.7±0.4 branch points per NMJ4.

Thus, overall it appears that in contrast with the extensive variation in NMJ morphology that exists among different species of *Drosophila* (Campbell and Ganetzky 2012), there is little variation in NMJ morphology among different populations of *D. melanogaster*. Nonetheless, the recovery of two isofemale lines from the Madison population with distinct NMJ morphologies indicates that at least some genetic variation for this phenotype is present in natural populations of *D. melanogaster*. The existence of these variants raises questions about which genes and pathways are responsible and whether they could identify novel mechanisms that regulate NMJ growth and morphology.

Both positive and negative regulators of NMJ morphology are segregating in the H4 isofemale line

We focused on a single isofemale variant line, H4 (Figure 1) to try to identify individual genes that were responsible for the variation in NMJ morphology. Because this line, derived from a single mated female was not isogenic, we observed phenotypic variation among her larval progeny and over the next several generations of maintaining this line by mass transfer. This suggests that multiple different genes affecting NMJ morphology are segregating within this line. To reduce this complexity in order to identify individual genes, we crossed flies from the H4 line with laboratory balancer stocks to isolate single chromosomes from H4 and breed them to homozygosity (Supp. Fig. 1). From these crosses, we generated a number of individual sublines homozygous for a single H4 chromosome in an otherwise laboratory wild-type background. Most of the 45 semi-

isogenic sublines examined exhibited normal NMJ morphology. However, seven of these lines had distinctive NMJ phenotypes (Figure 2). Six of the sublines (H4-1 to H4-6) displayed an overgrowth phenotype characterized by an increased number of satellite boutons and hyperbudded boutons that was even more robust than the original H4 line (Figure 2). The remaining subline (H4-7) had a strong NMJ undergrowth phenotype. Complementation analysis indicated that the similar phenotypes of the six sublines with NMJ overgrowth were caused by different genes. These results, together with the isolation of a subline exhibiting NMJ undergrowth indicate that multiple variants in both positive and negative regulators of NMJ growth were originally present in the H4 female isolated from nature.

Identification of Mob2 as a negative regulator of NMJ growth

We focused on subline H4-5, homozygous for a third chromosome from nature, for subsequent analysis to identify a specific gene(s) responsible for its NMJ phenotype. The overgrowth phenotype in this line was of interest because it differs in several ways from other hyperbudded mutants that have been described. The main axonal stalk of the NMJ is broader than normal and discrete individual boutons along that axis are not as apparent as in lab wild-type strains where they appear as beads on a string. Boutons along the main trunk in H4-5 are larger than normal and appear almost to merge with neighboring boutons. In addition, numerous small satellite boutons branch off the main axis and hyperbudded boutons appear along the length of the NMJ and hyperbudding of terminal boutons is especially prominent. These features suggested

that H4-5 harbored a genetic variant that did not correspond with any previously described NMJ mutant, making it an interesting candidate to pursue.

To determine whether the H4-5 phenotype was caused by mutation of a single gene and, if so, to map the location of this gene we carried out deficiency mapping of the third chromosomes using the *Drosophila* deficiency collection. Although *H4-5/+* heterozygotes have a mild semi-dominant phenotype (Figure 3), this phenotype was readily distinguishable from *H4-5/H4-5* homozygotes and *H4-5/Df* hemizygotes so failure of complementation could be scored (Figure 3). After testing deficiencies spanning the third chromosome, we were able to map the *H4-5* phenotype to a single small region on 3L, at cytological location 68C13. Any deletion that removed this chromosome segment uncovered the mutant phenotype when heterozygous with *H4-5* but produced NMJs of normal appearance in *Df/+* larvae. The phenotype of *H4-5/Df* is even stronger than that of *H4-5* homozygotes suggesting that *H4-5* is a hypomorphic allele.

Of the thirteen candidate genes within the chromosome region that uncovers *H4-5*, *Mob2* (*Monopolar spindle one binding protein*), which encodes a kinase adaptor protein, is the largest (Figure 4). An insertion allele of *Mob2* (*Mob2*^{DG30103}), containing a P-element in the first intron (Figure 4), conferred a mild overgrowth phenotype with increased branching when homozygous and failed to complement H4-5 (Figure 3) suggesting that *H4-5* might contain a mutation of *Mob2*. To test this possibility further,

we generated precise and imprecise excisions of the P-element insertion in *Mob2*^{DG30103} (Figure 4). As expected, the imprecise excision, *Mob2*$^{\Delta 18}$, still exhibits an NMJ overgrowth phenotype and fails to complement H4-5 (Figure 3). However, the precise excision, *Mob2* $^{\Delta 17}$, is reverted to a standard NMJ morphology and it fully complements H4-5. These results support the conclusion that *H4-5* is an allele of *Mob2*. This conclusion is fully confirmed by results presented in the following sections and we will subsequently refer to the *H4-5* mutation as *Mob2*$^{H4-5}$*.*

We subsequently sequenced the entire *Mob2* coding region in *Mob2*$^{H4-5}$ but did not find any lesions suggesting that the relevant polymorphism resides within a non-coding region and affects expression of the gene. *Mob2* is a large and complex gene that contains over 30kb of intronic sequence and encodes four distinct mRNAs each with its own transcriptional start site (Figure 4) making the identification of a non-coding lesion extremely difficult. To help narrow the search, we first identified regions of conserved sequence within introns by sequence alignment with other *Drosophila* species (*D. simulans, D. sechellia, D. yakuba* and *D. erecta*). We sequenced the regions with at least 40% identity across species in *H4-5*. Within one of these regions, just upstream of the start site for the A isoform mRNA, we discovered a 49bp deletion in Mob2^{H4-5}, but absent in laboratory wild-type and in another third chromosome isolated from H4 with normal NMJ morphology (Figure 4). Several additional lines of evidence support the conclusion that the 49bp deletion is responsible for the mutant phenotype: First, transposon insertions within this region are associated with a mild NMJ overgrowth phenotype and fail to complement *Mob2*$^{H4-5}$. Curiously, this region also appears to be a

hotspot for transposon insertions with over 30 of the 60 annotated insertions in the gene tightly clustered in a region of several hundred nucleotides. Second, one of the deletions originally used to map *Mob2*$^{H4-5}$ has an endpoint within this intron a short distance beyond the *Mob2*$^{H4-5}$ lesion and extends to the right leaving most of the *Mob2* gene intact (Figure 4). Third, as described below, consistent with the hypothesis that the 49bp deletion in *Mob2*$^{H4-5}$ alters expression of the gene, we found that transcript levels are reduced in *Mob2*$^{H4-5}$.

To test whether expression of Mob2 RNA is impaired in Mob2^{H4-5}, we performed quantitative PCR on cDNA generated from larval brains. Primers were designed for the conserved portion of the gene to target all isoforms of Mob2. Compared with either laboratory wild-type (*CS*) or a different third chromosome isolate from *H4* (*H4-3*), *Mob2* RNA levels are significantly decreased in larval brains in *Mob2*$^{H4-5}$ homozygotes compared with expression level of ribosomal protein L17 as an internal control (Figure 5). Taken together with the sequence data and complementation analysis, these results support the conclusion that the NMJ overgrowth phenotype in H4-5 is due to a mutation in the *Mob2* gene that deletes 49bp within the first large intron and causes a reduction in expression of this gene.

Mob2 functions presynaptically to regulate NMJ growth

To obtain definitive evidence that *H4-5* is an allele of *Mob2*, we carried out transgenic rescue experiments using the full length A isoform cDNA of Mob2. Presynaptic

expression of *UAS-Mob2* using the pan-neuronal driver *C155-Gal4* fully rescues the *Mob2*$^{H4-5}$ mutant phenotype both for the number of boutons and the number of branch points (Figure 6). In addition, neural-specific expression of RNAi directed against *Mob2* using C155-Gal4 results in NMJ overgrowth similar to that of *Mob2*$^{H4-5}$. In contrast, we observe no NMJ phenotype with muscle-specific expression of *Mob2* RNAi using 24B-Gal4 (Figure 6). These results provide conclusive confirmation that *H4-5* is an allele of *Mob2* and further indicate that *Mob2* functions presynaptically to regulate NMJ development.

trc interacts with Mob2 to regulate NMJ growth

Thus far we have demonstrated that a naturally occurring genetic variant affecting NMJ growth is defective in the *Drosophila Mob2* gene. The overgrowth phenotype exhibited by hypomorphic alleles of *Mob2* indicates that it is a negative regulator of NMJ growth. But what is the cellular pathway by which Mob2 exerts its effect on NMJ growth? In *S. cerevisiae* where Mob proteins were originally characterized, there are two Mob proteins encoded by different genes. Both Mob1 and Mob2 activate NDR (Nuclear Dbf2-related) kinases to regulate polarized cell growth, bud site selection, and cell morphology (Luca and Winey 1998). The two Mob proteins in yeast regulate two different NDR kinases: Dbf2 is activated by Mob1 as part of the Mitotic Exit Network (MEN) (Luca and Winey 1998), whereas Cbk1 is activated by Mob2 in the RAM (regulation of Ace2 activity and cellular morphogenesis) pathway (Weiss et al. 2002, Nelson et al. 2003). It is unclear which of the two yeast Mob proteins is the counterpart of *Drosophila* Mob2, because the

Drosophila protein shares the same degree of identify with either yeast protein. Moreover, it has been shown that *Drosophila* Mob2 can physically interact with both Trc (Tricornered) and Wts (Warts) the two NDR kinases in flies (He et al. 2005). Thus, Mob2 could normally regulate NMJ growth via activation of Trc, Wts or both.

To investigate these possibilities further we examined the NMJ phenotype of loss-of-function alleles of both *trc* (trc^{1}) and *wts* ($wts^{3\text{-}17}$). Both of these mutations are lethal, when homozygous, so we were not able to examine the NMJ phenotype in larvae homozygous for either mutation. However, we did observe a strong dominant genetic interaction between *trc* and *Mob2*. $trc^{1}/Mob2^{H4\text{-}5}$ larvae exhibit an NMJ overgrowth phenotype comparable to that of $Mob2^{H4\text{-}5}$ homozygotes (Figure 7). We found the same dominant interaction in heterozygotes between $Mob2^{H4\text{-}5}$ and a deficiency that uncovers *trc*. In contrast, we did not find any interaction between *wts* and *Mob2* as NMJs in $wts^{3\text{-}17}/Mob2^{H4\text{-}5}$ larvae appear phenotypically normal (Figure 7). Thus, *Mob2* appears to regulate NMJ morphology via an interaction with *trc* and not the related kinase *wts*.

Through a screen of natural populations of *D. melanogaster* we have been able to demonstrate that while NMJ morphology is largely conserved across these populations, some variation in this phenotype does exist. Through further characterization of one of these variant lines we were able to identify a novel regulator of NMJ morphology, *Mob2*. These results suggest that by examining natural populations we may uncover new and

interesting mechanisms that regulate NMJ morphology while also gaining the potential for a better understanding of the evolution of nervous systems.

MATERIALS AND METHODS

Fly Stocks

Natural isolates of *D. melanogaster* from Madison, WI were collected by Helen Hartman and Josh Gnerer. African isolates were obtained from Sean Carroll (University of Wisconsin-Madison) and Chung-I Wu (University of Chicago). C155-Gal4 UAS-Dcr2 was provided by Kate O'Connor-Giles (University of Wisconsin-Madison). UAS-Mob2 was provided by Paul Adler (University of Virginia). UAS-Mob2-RNAi was obtained from the Vienna *Drosophila* RNAi Center. All other stocks were obtained from the Bloomington Stock Center.

Imaging

All larvae were obtained from low density crosses incubated at 25ºC. Wandering third-instar larvae were dissected in ice-cold Ca^{2+}-free saline and fixed for 15 minutes in 4% formaldehyde in PBS. Larvae were incubated in FITC-conjugated anti-HRP (Jackson ImmunoResearch) at 1:100 overnight at 4 ºC. NMJs were imaged using a Zeiss 510 confocal microscope. Brightness and contrast were adjusted using Photoshop (Adobe).

Quantification of boutons and branch points was performed at NMJ4 in segments A2-A4 as described in (Coyle et al. 2004). Branch points were determined for each bouton with branch points defined as the number of projections from that bouton minus one (excluding terminal boutons). Branch points for each bouton were then added to determine the total number of branch points per NMJ. At least 25 NMJs were quantified for each genotype. Statistical analyses were performed via Student's t tests for pairwise comparisons. Significance levels of <0.05, <0.01, <0.001 are indicated by one, two and three asterisks respectively. Error bars denote standard error of the mean.

Quantitative RT-PCR

Approximately 15 larval brains were dissected from wandering third instar larvae of each genotype. RNA was isolated using the RNeasy Plus Mini Kit (Qiagen). cDNA was generated with an iScript cDNA Kit (Bio-Rad). Real-time qPCR was carried out as described by Katzenberger et al. 2006. Three independent biological isolations were each analyzed three times. All primer sets produced a single product of expected size. Primer sets (oriented 5' to 3') for qPCR were as follows: total *Mob2*, GTGGATCTTCCAGCTGGTTT and GTCTTCTTGCCCTTCTCGTC; RpL17, CCAATCTACGTGTGCACTTCA and ACTCCTTCTGGTCGATGACG.

ACKNOWLEDGEMENTS

We would like to thank Helen Hartman and Josh Gnerer for collecting natural *D. melanogaster*. We also thank all members of the B.G. laboratory for helpful discussion and critical comments on the manuscript and the Bloomington Stock Center for supplying numerous stocks. This research was supported by the National Institutes of Health through a predoctoral training grant (T32 GM007507) to the Neuroscience Training Program and a research grant (RO1NS015390) (to B.G.).

REFERENCES

Baillat G, Moqrich A, Castets F, Baude A, Bailly Y, Benmerah A and A Monneron. 2001. Molecular cloning and characterization of phocein, a protein found from the Golgi complex to dendritic spines. *Mol Biol Cell 12:663-73.*

Campbell M and B Ganetzky. 2012. Extensive morphological divergence and rapid evolution of the larval neuromuscular junction in *Drosophila*. *Proc Natl Acad Sci USA* 109:E645-55.

Collins CA and A DiAntonio. 2007. Synaptic development: insights from *Drosophila*. *Curr Opin Neurobiol* 17:35-42.

Coyle IP, Koh Y-H, Mimi Lee W-C, Slind J, Fergestad T, Littleton JT and B Ganetzyk. 2004. Nervous Wreck, an SH3 Adaptor Protein that Interacts with Wsp, Regulates Synaptic Growth in *Drosophila*. *Neuron* 41:521-34.

Gregory SL, Shandala T, O'Keefe L, Jones L, Myrray MJ and R Saint. 2007. A *Drosophila* overexpression screen for modifiers of Rho signaling in cytokinesis. *Fly* 1:13-22.

He Y, Emoto K, Fang C, Ren N, Tian X, Jan Y-N and PN Adler. 2005. *Drosophila* Mob Family Proteins Interact with the Related Tricornered (Trc) and Warts (Wts) Kinases. 16:4139-52.

Ji Y, Rath U, Girton J, Johansen KM and J Johansen. 2005. D-Hilarin, a novel W180-domain protein, affects cytokinesis through interaction with the spetin family member Pnut. *J Neurobiol* 64:157-69.

Katzenberger R, Marengo MA and DA Wassarman. 2006. ATM and ATR Pathways Signal Alternative Splicing of *Drosophila* TAF1 Pre-mRNA in Response to DNA Damage. *Mol Cell Biol* 26:9256-67.

Lai ZC, Wei X, Shimizu T, Ramos E, Rohrbaugh M, Nikolaidis N, Ho LL and Y Li. 2005. Control of cell proliferation and apoptosis by mob as tumor suppressor, mats. *Cell* 120:675-85.

Liu L-Y, Lin C-H and S-S Fan. 2009. Function of *Drosophila* mob2 in photoreceptor morphogenesis. *Cell Tissue Res* 338:377-89.

Luca FC and M Winey. 1998. MOB1, an essential yeast gene required for completion of mitosis and maintenance of ploidy. *Mol Biol Cell* 9:29-46.

Nelson B, Kurischko C, Horecka J, Mody M, Nair P, Pratt L, Zougman A, McBroom LD, Hughes TR, Boone C and FC Luca. 2003. RAM: a conserved signaling network that regulates Ace2p transcriptional activity and polarized morphogenesis. *Mol Biol Cell* 14:3782-803.

O'Tousa J. 1982. Meiotic chromosome behavior influenced by mutation-altered disjunction in *Drosophila* melanogaster females. *Genetics* 102:503-24.

Protas ME, Hersey C, Kochanek D, Zhou Y, Wilkens H, Jeffery WR, Zon LI, Borowsky R and CJ Tabin. 2006. Genetic analysis of cavefish revels molecular convergence in the evolution of albinism. *Nat Genet* 38:107-11.

Scharloo W, Hoogmoed S and A Ter Kuile. 1967. Stabalizing and disruptive selection on a mutant character in *Drosophila*. I. The phenotypic variance and its components. *Genetics* 56:709-26.

Schulte J, Sepp KJ, Jorquera RA, Wu C, Song Y, Hong P and JT Littleton. 2010. DMob4/Phocein Regulates Synapse Formation, Axonal Transport, and Microtubule Organization. *J Neurosci* 30:5189-203.

Shimizu T, Ho LL and ZC Lai. 2008. The mob as tumor suppressor gene is essential for early development and regulates tissue growth in *Drosophila*. *Genetics* 178"957-65.

Sigrist S, Jacobs H, Stratmann R and CF Lehner. 1995. Exit from mitosis is regulated by *Drosophila* frizzy and the sequential destruction of cyclins A, B and B3. *EMBO J* 14:4827-38.

Trammell MA, Mahoney NM, Agard DA and RD Vale. 2008. Mob4 plays a role in spindle focusing in *Drosophila* S2 cells. *J Cell Sci* 121:1284-92.

Weiss EL, Kurischko C, Zhang C, Shokat K, Drubin DG and FC Luca. 2002. Saccharomyces cerevisiae Mob2p-Cbk1p kinase complex promotes polarized growth and acts with the mitotic exit network to facilitate daughter cell-specific localization of Ace2 transcription factor. *J Cell Biol* 158:558-900.

Zallen JA, Peckol EL, Tobin DM and CI Bargmann. 2000. Neuronal cell shape and neurite initiation are regulated by the Ndr kinase SAX-1, a member of the Orb6/COT-1/warts serine/threonine kinase family. *Mol Biol Cell* 11:3177-90.

Figure 1

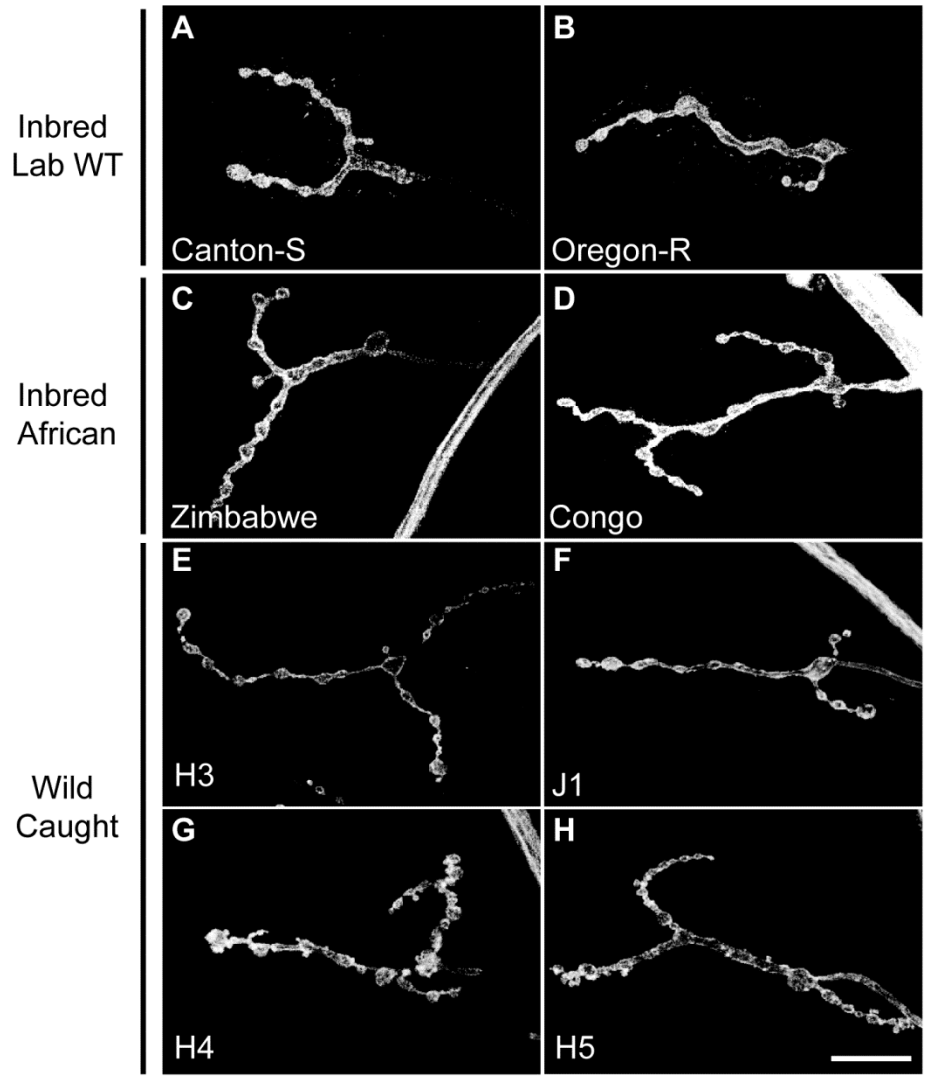
Inbred
Lab WT
Inbred
African
Wild
Caught
A
Canton-S
B
Oregon-R
C
Zimbabwe
D
Congo
E
H3
F
J1
G
H4
H
H5

Figure 1: Larval NMJ morphology is conserved in natural populations of *D. melanogaster*

Confocal images of NMJ4 labeled with FITC-anti-HRP. (A, B) Laboratory wild-type strains and inbred lines derived from natural populations in Africa(C, D) all share similar phenotypes. Six of eight isofemale lines derived from wild populations in Madison, WI also exhibited the standard NMJ phenotype (E-F). However, two of these isofemale lines had variant NMJ morphology (G-H). Scale bar, 20µm

Figure 2

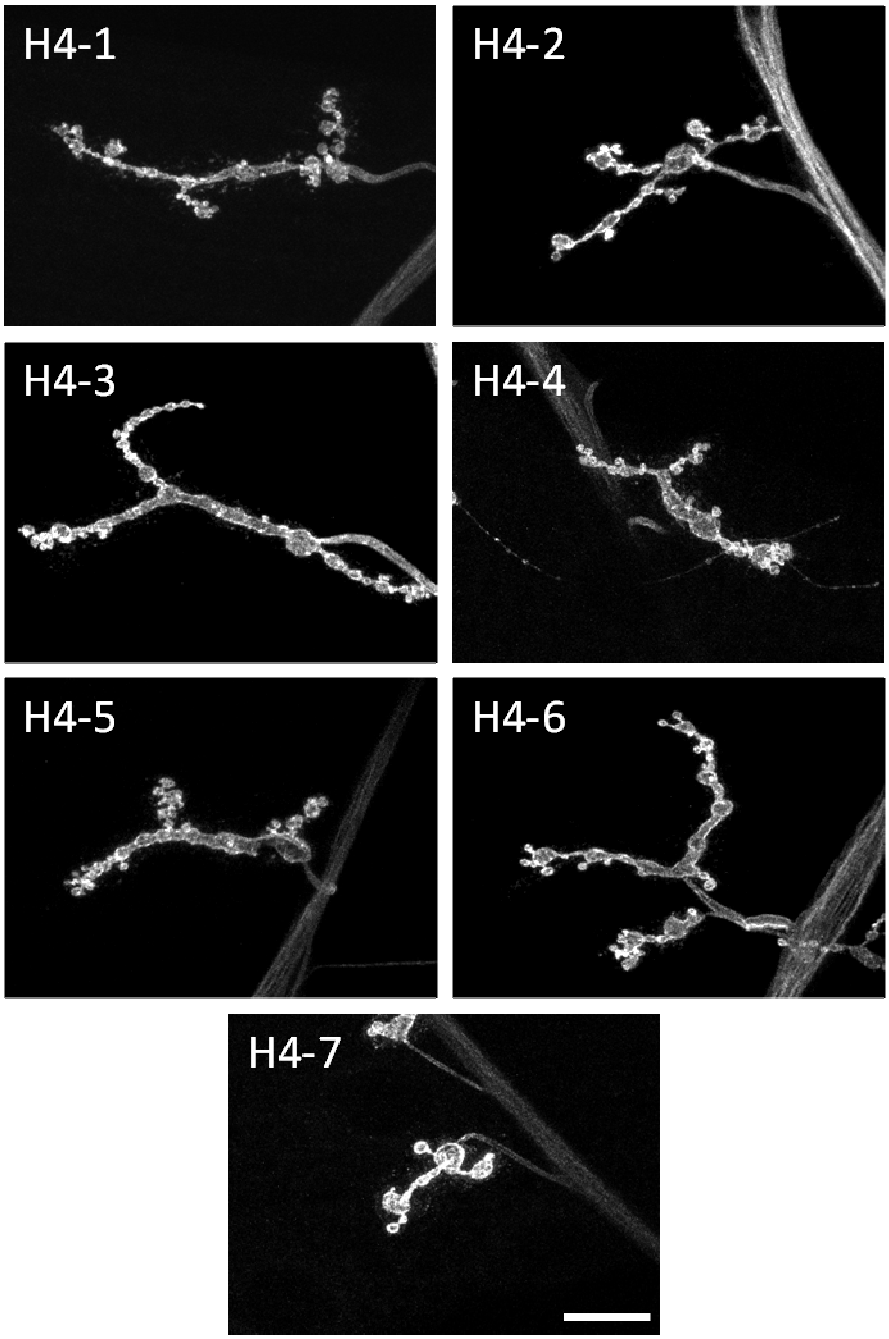

Figure 2: Segregation of positive and negative regulators of NMJ growth in sublines derived from Madison *H4* isofemale line.

Sublines from the *H4* isofemale line were derived by outcrossing single *H4* flies to laboratory balancer strains to recover individual chromosome that were bred to homozygosity in each subline. Confocal images of NMJ4 labeled with FITC-anti-HRP from these sublines (A-G). Six of these sublines (A-F) display an NMJ overgrowth phenotype indicating loss of a negative regulator whereas one line has an NMJ undergrowth phenotype (G) indicating loss of a positive regulator. Scale bar, 20µm

Figure 3

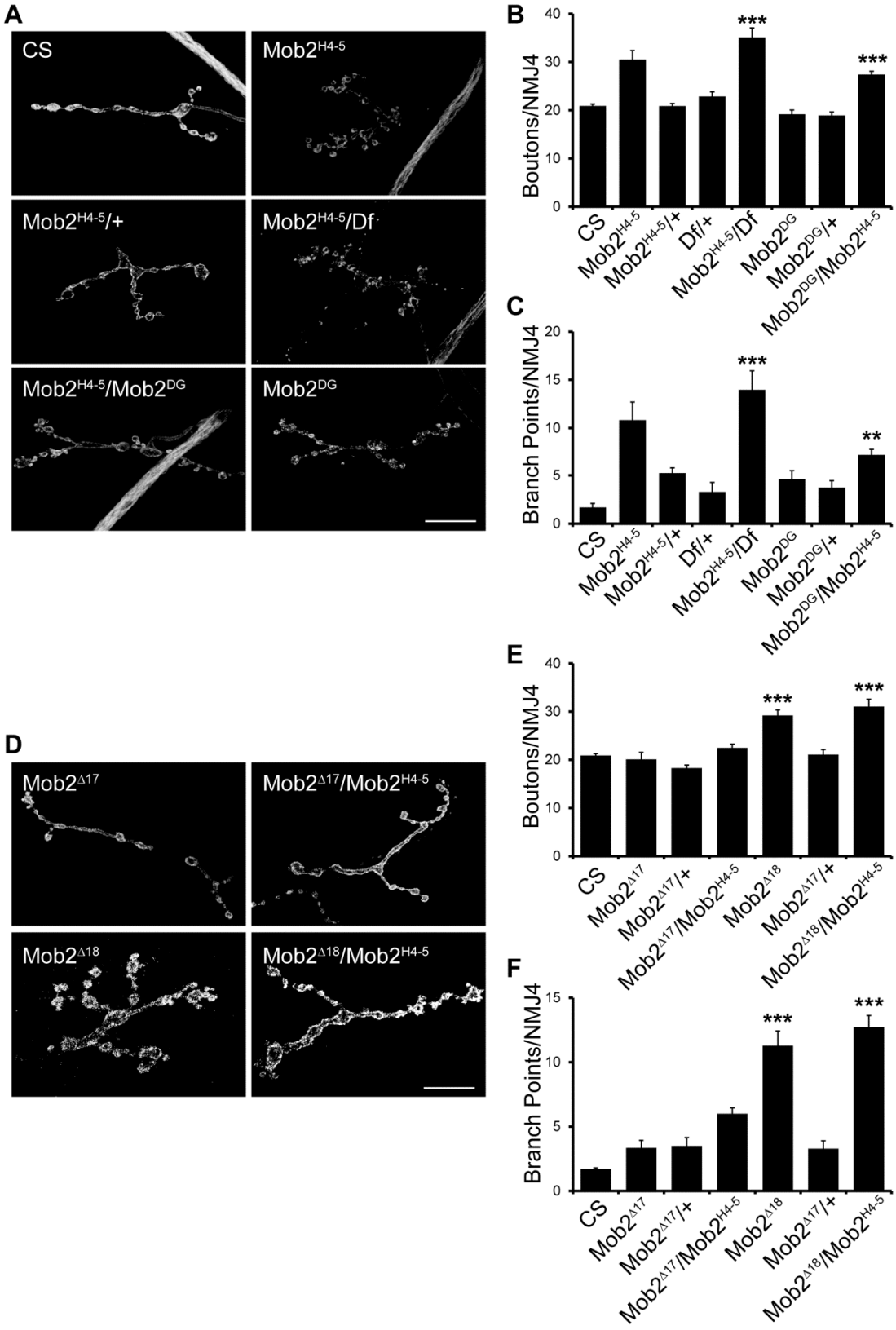
A
CS
Mob2H4-5
Mob2H4-5/+
Mob2H4-5/Df
Mob2H4-5/Mob2DG
Mob2DG
B
Boutons/NMJ4
***
***
CS
Mob2H4-5
Mob2H4-5/+
Df/+
Mob2H4-5/Df
Mob2DG
Mob2DG/+
Mob2DG/Mob2H4-5
C
Branch Points/NMJ4
***
**
D
Mob2Δ17
Mob2Δ17/Mob2H4-5
Mob2Δ18
Mob2Δ18/Mob2H4-5
E
Boutons/NMJ4
***
***
CS
Mob2Δ17
Mob2Δ17/+
Mob2Δ17/Mob2H4-5
Mob2Δ18
Mob2Δ17/+
Mob2Δ18/Mob2H4-5
F
Branch Points/NMJ4
***
***

Figure 3: Genetic variant affecting NMJ growth in *H4-5* subline is an allele of *Mob2*

(A,D) Confocal images of NMJ4 labeled with FITC-anti-HRP. (A) *H4-5* homozygotes, *H4-5/Df(3L)BSC577* and *H4-5/Mob2^{DG}* larvae exhibit similar NMJ overgrowth phenotypes compared with *CS* (*Canton-S*) or *H4-5/+* controls. (D) Precise excision (*Mob2$^{\Delta 17}$*) of a P-element insertion allele (*Mob2^{DG}*) results in reversion back to standard NMJ phenotype that complements *H4-5* (*Mob2$^{\Delta 17}$/H4-5)*. Imprecise excision of the same element (*Mob2$^{\Delta 18}$*) still exhibits an overgrowth phenotype similar to that of *H4-5* and fails to complement. (B-C and E-F) Quantification of the number of boutons (B,E) and branch points (C,F) at NMJ4 in larvae of the genotypes shown. Error bars denote SEM. **, P<0.01; ***, P<0.001. Scale bars, 20µm.

Figure 4

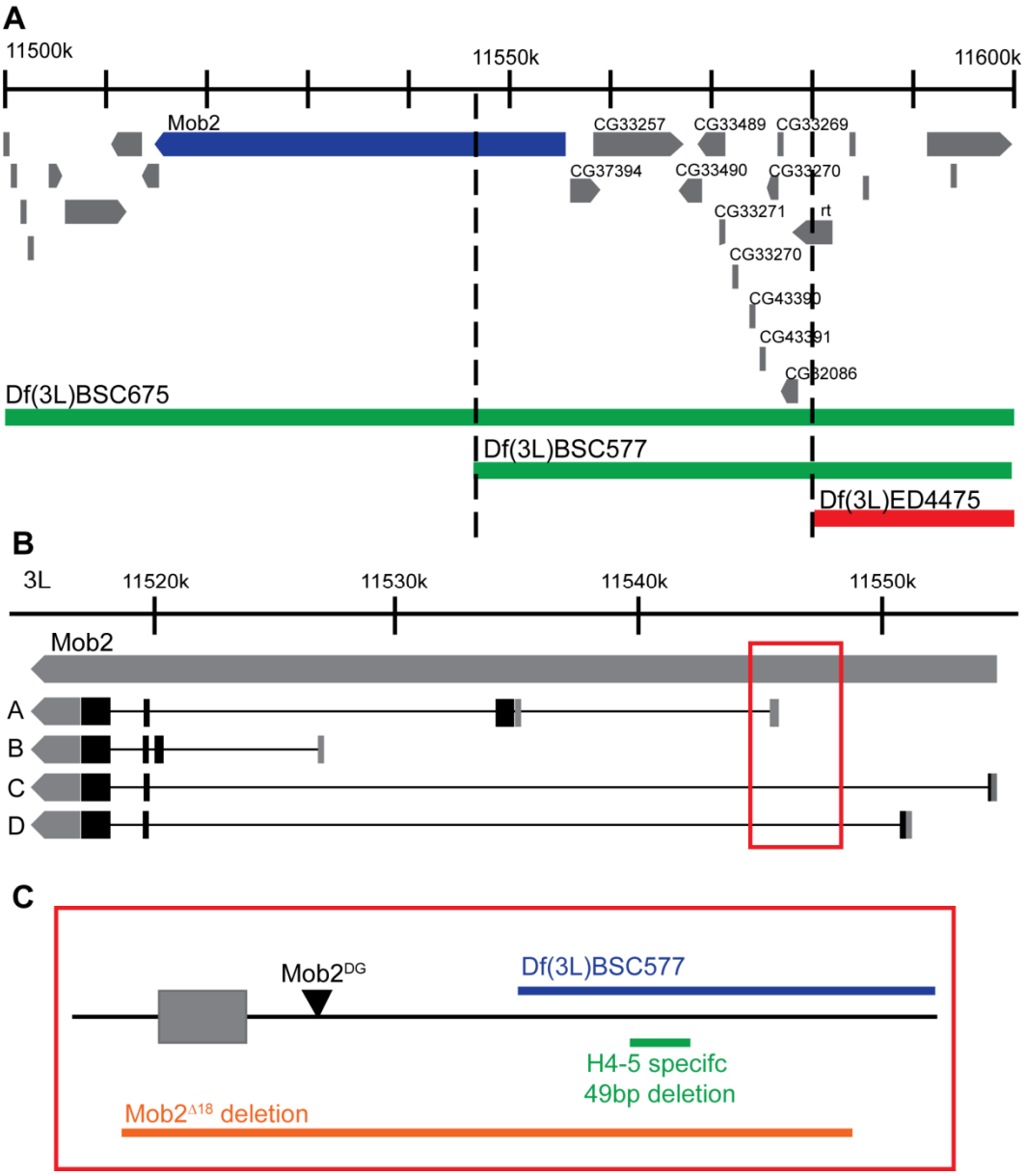
A
11500k
11550k
11600k
Mob2
CG33257
CG33489
CG33269
CG37394
CG33490
CG33270
CG33271
rt
CG33270
CG43390
CG43391
CG32086
Df(3L)BSC675
Df(3L)BSC577
Df(3L)ED4475
B
3L
11520k
11530k
11540k
11550k
Mob2
A
B
C
D
C
Mob2DG
Df(3L)BSC577
H4-5 specifc
49bp deletion
Mob2Δ18 deletion

Figure 4: Diagram of genomic region containing *Mob2* showing location of various lesions in this gene.

(A) A representation of the genomic region containing *Mob2*. Each gene is represented by a thick gray bar below the genomic scale. *Mob2* is the thick blue bar. Below the genes are three deficiencies used to map *H4-5*. Both *Df(3L)BSC675* and *Df(3L)BSC577* (green) failed to complement the *H4-5* NMJ phenotype, while *Df(3L)ED4475* (red) complemented *H4-5.* The genomic region that *H4-5* was mapped to is defined by the dashed black lines. (B) The genomic segment spanned by the *Mob2* gene is shown as the solid thick bar below the genomic scale. Below this bar, the four different mRNAs encoded by *Mob2* are shown. Each of these alternatively spliced mRNAs initiates transcription from a different start site. Thick gray bars represent untranslated exon sequence; thick black bars correspond to translated regions. Thick black lines are introns. (C) Enlarged close up view of the boxed region in (A). This region contains the 49bp deletion present in *H4-5* (green), the left endpoint of a deficiency coming in from the right that fails to complement *H4-5* (blue), the site of P-element insertion in $Mob2^{DG}$, and the breakpoints of $Mob2^{\Delta 18}$ (orange), an imprecise excision derived from $Mob2^{DG}$.

Figure 5

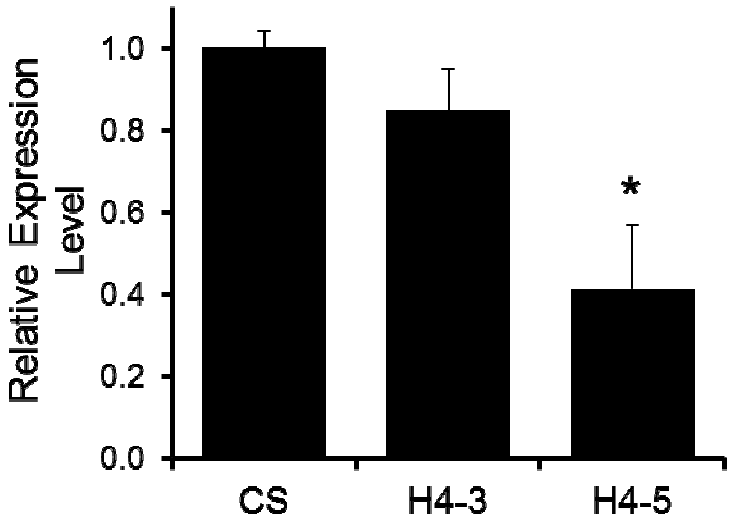

Figure 5: Expression of Mob2 RNA is decreased in *H4-5* larval brain

Quantitative RT-PCR was used to quantify levels of *Mob2* RNA in samples isolated from larval brains of *H4-5*, *Canton-S* (*CS*), and *H4-3*, another introgressed subline derived from H4 with an NMJ overgrowth phenotype. The level of Mob2 RNA is significantly reduced compared with either of the controls. Error bars are standard deviation.

Figure 6

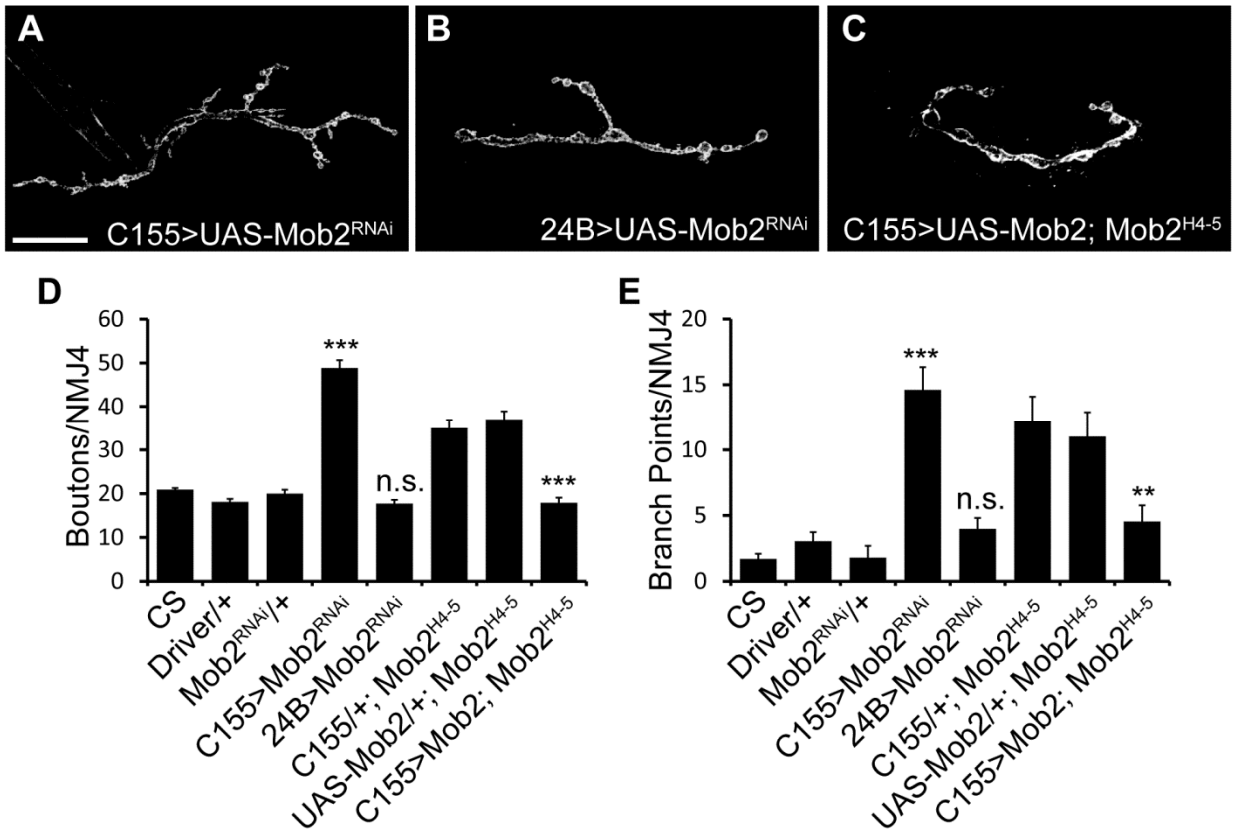
A
B
C
C155>UAS-Mob2RNAi
24B>UAS-Mob2RNAi
C155>UAS-Mob2; Mob2H4-5
D
Boutons/NMJ4
60
50
40
30
20
10
0
***
n.s.
***
CS
Driver/+
Mob2RNAi/+
C155>Mob2RNAi
24B>Mob2RNAi
C155/+; Mob2H4-5
UAS-Mob2/+; Mob2H4-5
C155>Mob2; Mob2H4-5
E
Branch Points/NMJ4
20
15
10
5
0
***
n.s.
**
CS
Driver/+
Mob2RNAi/+
C155>Mob2RNAi
24B>Mob2RNAi
C155/+; Mob2H4-5
UAS-Mob2/+; Mob2H4-5
C155>Mob2; Mob2H4-5

Figure 6: Mob2 acts presynaptically to regulate NMJ morphology

(A-C) Confocal images of NMJ4 labeled with FITC-anti-HRP. (A) RNAi knockdown of *Mob2* with the neuron-specific driver *C155-Gal4* causes an NMJ overgrowth phenotype similar to that of $Mob2^{H4-5}$. (B) This phenotype is not seen with RNAi knockdown of *Mob2* in muscles with the driver *24B-Gal4*. (C) Neural expression of *UAS-Mob2* by *C155-Gal4* in a $Mob2^{H4-5}$ background produces significant rescue of the NMJ overgrowth phenotype. Quantification of the number of boutons (D) and branch points (E) at NMJ4 in larvae of the genotypes shown. Error bars denote SEM. **, $P<0.01$; ***, $P<0.001$, n.s., not significant ($P>0.05$).

Figure 7

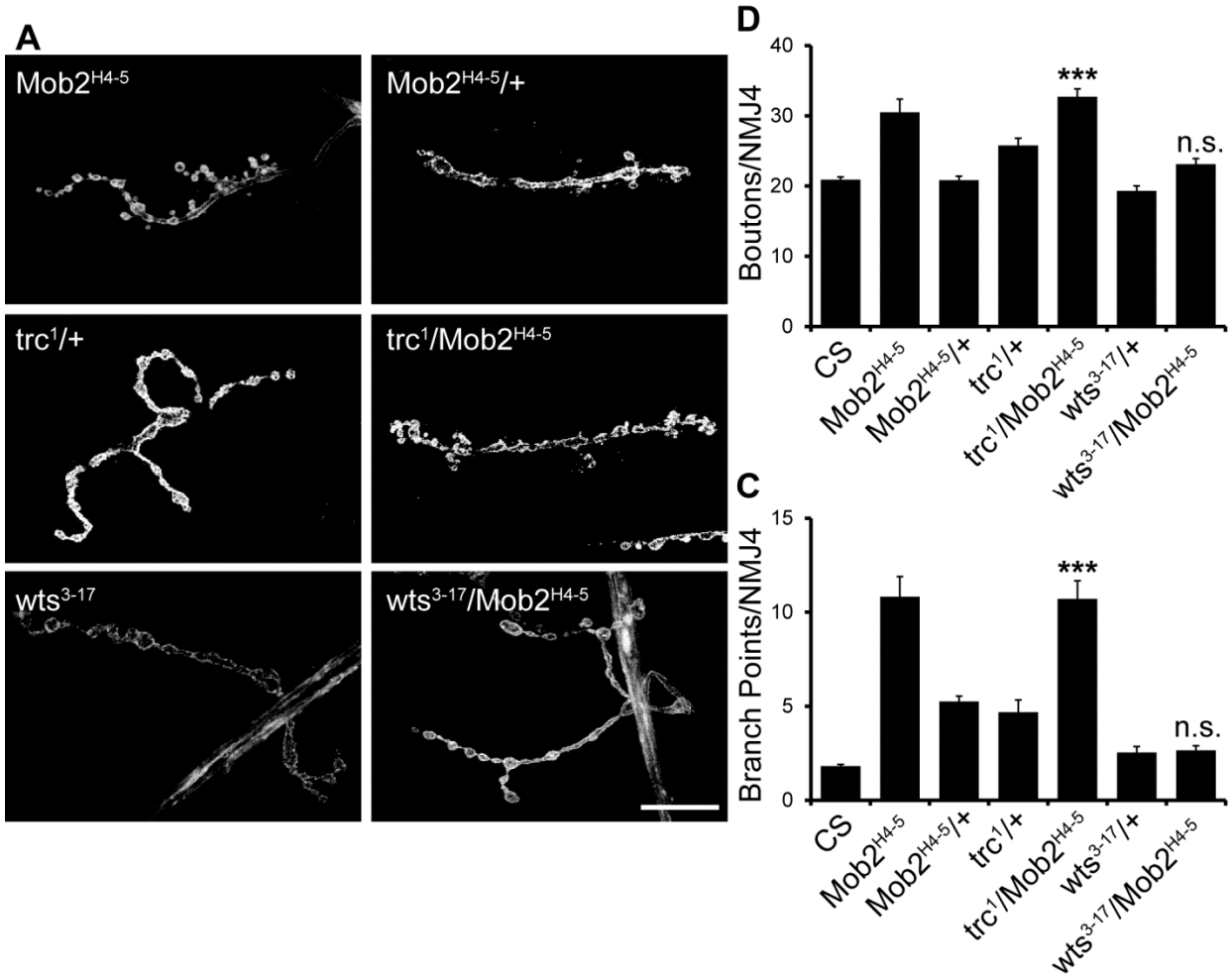
A
Mob2H4-5
Mob2H4-5/+
trc1/+
trc1/Mob2H4-5
wts3-17
wts3-17/Mob2H4-5
D
Boutons/NMJ4
40
30
20
10
0
***
n.s.
CS
Mob2H4-5
Mob2H4-5/+
trc1/+
trc1/Mob2H4-5
wts3-17/+
wts3-17/Mob2H4-5
C
Branch Points/NMJ4
15
10
5
0
***
n.s.
CS
Mob2H4-5
Mob2H4-5/+
trc1/+
trc1/Mob2H4-5
wts3-17/+
wts3-17/Mob2H4-5

Figure 7: Mob2 genetically interacts with *trc* but not wts to regulate NMJ growth

(A) Confocal images of NMJ4 labeled with FITC-anti-HRP. *trc*^{1}/*Mob2*$^{H4-5}$ double heterozygotes exhibit significantly enhanced NMJ overgrowth compared with either single heterozygote alone, whereas NMJs of *wts*$^{3-17}$/*Mob2*$^{H4-5}$ double heterozygotes do not differ from single heterozygote controls. Quantification of the number of boutons(B) and branch points (C) at NMJ4 in larvae of the genotypes shown. Error bars denote SEM. ***, P<0.001; n.s., not significant (P>0.05).

Supplemental Figure 1

Creating semi-isogenic lines by isolating natural X and 3rd chromosomes:

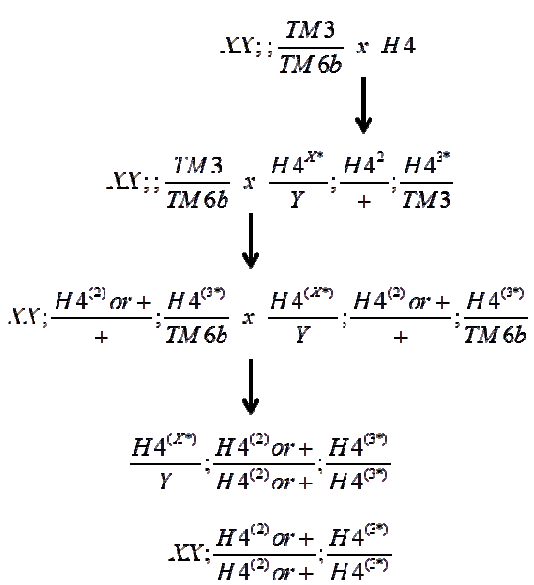

Isogenizing line with isolated natural 3rd chromosome:

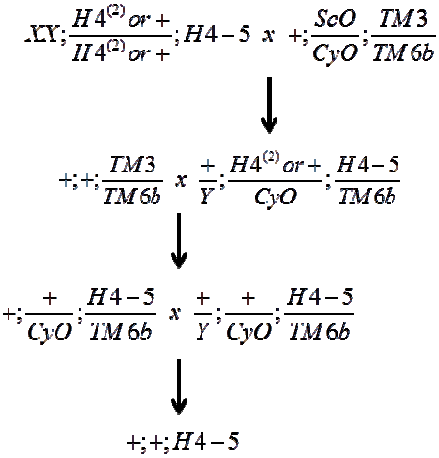

Supplemental Figure 1: Crossing scheme used to isolate single chromosomes from natural populations

The original isofemale line, H4, was crossed to a third chromosome balancer line with an attached X. F1 males were crossed back to the original balancer stock, whose selected progeny were used to generate a stock with a single natural third and first chromosome and a variable second chromosome. To specifically isolate only the natural third chromosome, attached X females from the generated stock were crossed to a line with second and third chromosome balancers. F1 males were then crossed to a third chromosome balancer stock and progeny were crossed to generate a line with a single isolated third chromosome in a lab wild-type background.

CHAPTER 4

The Mitotic Exit Network (MEN) regulates growth of the *Drosophila* larval neuromuscular junction

This chapter is in preparation for publication by Megan Campbell and Barry Ganetzky

ABSTRACT

The Mitotic Exit Network (MEN) is the pathway that drives cytokinesis by targeting specific proteins to the bud neck of dividing cells. While many individual members of this pathway are pleiotropic with functional roles in post-mitotic cells, the pathway as a whole had not been shown to function outside the cell cycle. Here, we demonstrate that each core member of the MEN functions as part of a common pathway that acts presynaptically to negatively regulate larval neuromuscular junction (NMJ) growth in *Drosophila*. Mutations in each member exhibit overgrowth at the NMJ and dominantly enhance the *Mob2* (*Mps1 binding 2*) overgrowth phenotype. As in cytokinesis, Tricornered (Trc) localizes to the 'bud neck' in developing NMJs suggesting that subcellular localization is important for its function in regulating bouton division. Additional members of the contractile ring, Hilarin (Hil) and Cyclase-associated protein (CAP) also negatively regulate bouton division and functionally interact with Mob2. These components of the MEN appear to act by regulating actin dynamics. Mutations in the genes that encode actin binding proteins *multiple wing hairs* (*mwh*) and *chickadee* (*chic*) dominantly enhance the *Mob2* mutant overgrowth phenotype. Therefore, the MEN ultimately regulates actin dynamics during the process of bouton growth and division. These studies have thus led to the discovery of an entirely new role for the MEN—regulation of synaptic growth—that is separate from its function in cell division.

INTRODUCTION

Proper synaptic growth is critical for normal nervous system development. The *Drosophila* larval neuromuscular junction (NMJ) is a powerful genetic model for studying the genetic and molecular mechanisms of synaptic growth and development. Numerous investigators have taken advantage of the larval NMJ to identify many positive and negative regulators of NMJ growth which have revealed signaling pathways that regulate NMJ development (Collins and DiAntonio 2007).

Through a screen of natural populations of *D. melagnoaster*, we identified a polymorphism in the regulatory region of a novel negative regulator of NMJ growth, *Mob2* (Mps One Binder 2). Mob proteins were originally described in yeast as Nuclear Dbf2-related (NDR) kinase adaptor proteins involved in the cell cycle. In *Saccharomyces cerevisiae* there are 2 Mob proteins. Mob1 is a member of the Mitotic Exit Network (MEN), a pathway that initiates cytokinesis during the cell cycle (Luca and Winey 1998). Mob2 is a member of the RAM (Regulation of *AceII* activity and cellular morphogenesis) signaling network which is involved in regulating cell polarity and daughter cell specific transcription (Weiss et al. 2002, Nelson et al. 2003). Less is known about the role of Mob proteins in *Drosophila*, of which there are four, however they are thought to have conserved roles in cell cycle (Lai et al. 2005, He et al. 2005, Shimizu et al. 2008, Trammell et al. 2008). Mob2, specifically, has also been shown to regulate photoreceptor and wing hair morphogenesis (He et al. 2005, Liu et al. 2009). Additionally, Mob4 (pheocin) has been shown to be a negative regulator of NMJ growth

affecting axonal transport and microtubule dynamics (Schulte et al. 2010). Additionally, mammalian Mob proteins have been localized to neuronal dendrites where NDR kinases are regulating branching and tiling (Zallen et al. 2000, Baillat et al. 2001). Therefore, Mob proteins can regulate developmental processes in post-mitotic neurons.

At the NMJ, Mob2 functions through an interaction with Tricornered (Trc), a NDR kinase to regulate growth. While none of the members of the RAM signaling network affect NMJ growth (data not shown), we discovered that each core member of the MEN is a negative regulator of NMJ growth and functions in a common pathway with Mob2. In *S.cerevisiae*, the Mitotic Exit Network (MEN) transitions a dividing cell into the early stages of cytokinesis. In this highly conserved pathway, Mps1 (Monopolar spindle 1) phosphorylates Mob1 (Mps one binder 1) to activate it. Once phosphorylated Mob1 binds and enhances the function of the serine/threonine kinase Dbf2 (Dumbbell forming 2). The Dbf2-Mob1 complex then activates Cdc14 (Cell division cycle 14) through phosphorylation, releasing it from the nucleus. The phosphatase, cdc14 then dephosphorylates Cdk1 (Cyclin-dependent kinase 1) leading to its degradation and causing a sharp decline in Cdk1 levels, which were elevated earlier in the cell cycle. The drop in Cdk1 levels is required for localization of Mob1, Dbf2, Cdc14 and other proteins to the bud neck where they interact with a complex of proteins, Hof1 (Homolog of cdc fifteen 1), Cyk3 (Cytokinesis 1) and Inn1 (required for ingression 1). This complex associates with the actomyosin ring and septin proteins allowing for contraction of the ring and completion of cytokinesis (Figure 1) (McCollum and Gould 2001, de Bettignies and Johnston 2003, Meitinger et al. 2012).

In this paper, we demonstrate that each orthologous member of the MEN is a negative regulator of NMJ growth and function in a common pathway to regulate synaptic morphology. Additionally, Trc, as in cytokinesis, localizes to the' bud neck' of developing boutons further suggesting that subcellular localization is important for its function in regulating bouton division. Dominant enhancement of the Mob2 NMJ overgrowth phenotype with mutations in genes that encode additional components of the contractile ring and actin binding proteins suggest that MEN ultimately regulates actin dynamics at the NMJ.

RESULTS/DISCUSSION

Members of the Mitotic Exit Network negatively regulate NMJ growth and interact with *Mob2*

We previously identified a mutation of *Mob2* (*Mob2*$^{H4\text{-}5}$) in screens of wild populations of *D. melanogaster* for naturally occurring variants affecting NMJ morphology. We also found that *Mob2*$^{H4\text{-}5}$ showed a strong dominant phenotypic interaction in heterozygous combination with mutations of *trc*, which encodes one of the two NDR kinases in *Drosophila*. These genes are counterparts of the *S.cerevisae* genes *Mob1* and *Dbf2*, which are components of the Mitotic Exit Network in yeast (Luca and Winey 1998). These results raise the question of whether other known MEN components also affect NMJ growth regulation. The possible role of the MEN pathway in NMJ growth is particular intriguing because the growth of boutons and their division to form new boutons as the NMJ expands during larval development has been described as

resembling budding in yeast. Moreover, the NMJ overgrowth phenotype of *Mob2* and *trc* mutants involves excessive and ectopic bouton division resulting in hyperbudded boutons and satellite bouton formation. The MEN pathway is involved in regulating bud-site selection and cytokinesis in yeast. Thus, growth and division of boutons could share previously uncharacterized mechanistic links with budding in yeast. Therefore, we asked whether we could obtain additional evidence for regulation of NMJ growth by the MEN by examining other known components of this network for their effect on NMJ morphology.

In yeast, before Mob1 can bind to and activate Dbf2 kinase, it must first be phosphorylated via the Mps1 kinase (Figure 1). The homolog of *Mps1* is *altered disjunction* (*ald*), which was originally identified as a meiotic mutant (O'Tousa 1982, Dernburg et al. 1996). We examined *ald* null larvae and discovered that they exhibit overgrown NMJs with significant increases in number of both boutons and branch points compared with controls (Figure 2, F-H). This NMJ phenotype is similar to that of $Mob2^{H4\text{-}5}$. Moreover, although loss of one copy of *ald* in a wild-type background (*ald/+*) does not affect NMJ growth, it significantly enhances NMJ overgrowth when heterozygous with $Mob2^{H4\text{-}5}$ ($Mob2^{H4\text{-}5}$/*ald*) as measured by number of boutons and branch points (Figure 2, D, G-H). The dominant phenotypic interaction between *ald* and $Mob2^{H4\text{-}5}$ suggests that they are components of a common regulatory pathway.

Mps1, and its *Drosophila* counterpart Ald, act upstream of the Mob1-Dbf2 (yeast) and Mob2-Trc (fly) complexes. In the yeast MEN, the downstream target of this activated kinase complex is Cdc14. In *Drosophila cdc14* has been shown to affect cytokinesis consistent with a role in the *Drosophila* MEN (Gregory et al. 2007). We tested whether a mutation of *cdc14*, also affects NMJ morphology and interacts with $Mob2^{H4\text{-}5}$. An insertion allele of *cdc14* containing a transposon in the 5' UTR results in a mild, but significant overgrowth phenotype when homozygous (Figure 3 E, G-H). When this allele is heterozygous in an otherwise wild-type background, it appears to be almost fully recessive with only a mild increase in branch number and no effect on bouton number. However, heterozygosity for this mutation in a $Mob2^{H4\text{-}5}$/+ background results in significant NMJ overgrowth with a phenotype comparable to that of $Mob2^{H4\text{-}5}$ homozygotes (Figure 3 C-D, G-H). RNAi knockdown of *cdc14* using the pan-neuronal *C155-Gal4* driver also causes signficant NMJ overgrowth (Figure 2, F-H). Taken together, these results support the idea that *cdc14* and $Mob2^{H4\text{-}5}$ are components of a common regulatory pathway acting presynaptically to negatively regulate NMJ growth.

A critical role of Cdc14 in the MEN in yeast is to dephosphorylate Cdk1, which targets it for degradation. In *Drosophila*, the counterpart of Cdk1 is encoded by the *cdc2* gene. Numerous studies have confirmed that cdc2, in *Drosophila*, functions in several aspects of the cell cycle including, spindle checkpoint, DNA damage response and mitotic exit (Sigrist et al. 1995, Hayashi 1996, Su et al. 2000). Cdk1 protein is highly conserved across organisms. Expression of *Drosophila cdc2* in yeast rescues cell cycle arrest in scCdk1 mutants (Lehner and O'Farrell 1990, Leopold and O'Farrell 1991). To

determine whether MEN components that are not immediately upstream or downstream of Mob2-Trc also affect synaptic growth, we examined the NMJ phenotype of larvae homozygous for a null allele of *cdc2*. Once again we observed NMJ overgrowth with a phenotype comparable to $Mob2^{H4-5}$ homozygotes (Figure 4 F-H). As in the case of other known MEN components, loss of one copy of *cdc2* significantly enhances NMJ overgrowth in a $Mob2^{H4-5}$/+ background (Figure 4, D, E, G-H). Taken together, our results demonstrate that the *Drosophila* orthologs of the central players of the MEN in yeast, each function in a previously uncharacterized pathway to negatively regulate NMJ growth, particularly the regulation of bouton division.

Levels of Cdc2 in presynaptic terminals varies with NMJ development

We have found that mutations of both Cdc14 and Cdc2 cause a similar NMJ overgrowth phenotype indicating that both proteins act as negative regulators. This result appears to depart from the standard MEN pathway in yeast, where Cdc14 is a negative regulator of Cdk1(Cdc2) and should thus have opposite mutant phenotypes. It is likely that this apparent discrepancy is due to differences in the details of the mechanisms regulating cytokinesis versus bouton growth and division and exactly how the NMJ overgrowth phenotype we observe is generated. In cytokinesis, high levels of Cdk1 prevent completion of cell division thereby blocking exit from mitosis. In NMJ growth, loss of Cdc2 results in an excess number of boutons, most noticeably due to proliferation of hyperbudded boutons in which the state of active division apparently fails to turn off. The presence or absence of various checkpoints that prevent entry into a new round of

division before the previous round is completed could be a key difference between cytokinesis and bouton division.

Differences in developmental timing may also be an important consideration. In yeast, every mitotic cell cycle is essentially the same. For NMJ growth, boutons are being added both de novo and by division of existing boutons throughout larval development and the timing and regulation of the mechanisms controlling these events may vary at different stages of NMJ growth. As virtually nothing is known at this point about such mechanisms, as a first step, we expressed a *myc*-tagged *cdc2* construct in neurons using the C155 driver and examined the NMJ localization and levels of the tagged protein at two different time points: at 96 hr after egg lay (AEL) during late second instar, when the NMJ is normally still growing; and at 144 hr AEL during the wandering third instar stage when the NMJ normally has stopped growing and boutons are no longer dividing (Schuster et al. 1996). We found that at 96 hr AEL, Cdc2 levels are very low at the NMJ and the protein is localized preferentially in the most proximal boutons (Figure 5A). In contrast, at 144 hr AEL Cdc2 levels at the NMJ are substantially higher and the protein is present throughout the NMJ filling all boutons (Figure 5B). Possibly, Cdc2 levels are low while the NMJ is normally still growing to allow for budding and formation of new boutons. As NMJ growth tapers off during the third instar, Cdc2 levels then might increase to limit further budding or addition of new boutons. This model predicts that we might expect to see less Cdc2 accumulate in NMJs where boutons divide excessively. To test this idea, we expressed *UAS-cdc2.myc* in a $Mob2^{H4\text{-}5}$ mutant background and found that Cdc2 levels were significantly reduced compared with

controls (Figure 5C). These results support the idea that Cdc2 functions to restrict new bouton formation and limit NMJ growth and that the levels of this protein in presynaptic terminals is differentially regulated throughout NMJ development.

Trc localizes to the 'bud neck' in developing NMJs

Regulation of septum formation and completion of cytokinesis by the MEN in yeast during the process of bud formation requires localization of the Dbf2-Mob1 complex to the bud neck (Luca and Winey 1998, Komarnitsky et al. 1998). Because the budding of new boutons from pre-existing boutons during NMJ growth shares some morphological similarity with budding in yeast, it was of interest to ask whether Trc localizes to the analogous 'bud neck' structure of dividing boutons. To investigate this possibility, we used *C155-Gal4* to drive expression of a GFP-tagged Trc construct and examined localization at the same two developmental time points as we did for Cdc2--96 hrs and 144 hrs AEL. As in the case of Cdc2, we observe robust localization of Trc to the NMJ consistent with a role for Trc at synapses distinct from its function in cell cycle regulation (Figure 6). Further, we observe differential localization of Trc within boutons during development. At the later time point (144hrs) when NMJ growth is mostly complete, Trc has a diffuse distribution without any particular localization within boutons. In contrast, at 96 hrs, when NMJs are still growing by addition of new boutons, Trc is not evenly distributed but appears to be clustered predominantly at two locations (Figure 6 A1): at some 'bud necks' or the region between two boutons and at the edge of a terminal bouton, a site where a new bouton is most likely to be added (Figure 6 A1). We also

observe strongly decreased abundance of Trc in a *Mob2*$^{H4-5}$ background although the overall distribution of Trc at the NMJ is maintained (Figure 6). These results suggest that as in cytokinesis, subcellular localization of Trc is important for its function in regulating bouton division and that Mob2 is required for Trc to achieve its proper synaptic localization.

Components of contractile ring negatively regulate bouton division

The results we have presented thus far demonstrate a surprisingly strong link between regulation of budding in yeast and regulation of bouton division at the larval NMJ by components of the MEN. How far does this overlap extend? In yeast, localization of Dbf2 to the bud neck during cytokinesis is required for assembly of a complex of proteins that connect the septum to the actin cytoskeleton in this region. This complex consists of three proteins: Hof1, Cyk3 and Inn1. Like Dbf2, its yeast counterpart, Trc localizes to the 'bud neck' of dividing boutons at least during early NMJ growth. These observations led us to ask whether components of the contractile ring are also required for proper NMJ growth.

Strict orthologs of Hof1, Cyk3 and Inn1 are not present in *Drosophila*. However, Hof1 and Cyk3 share significant sequence similarity with the *Drosophila* proteins, Hilarin (Hil) and Cyclase-Associated Protein (CAP) respectively. Moreover, similar to Hof1, Hil binds to and regulates septin proteins at the contractile ring (Ji et al 2005). Consequently, we examined the NMJ phenotype of a *Hil* mutant to determine whether it

was required for normal synaptic growth. We found that a presumptive hypomorphic P-element insertion allele (*Hil*^{KG}) when homozygous causes an NMJ overgrowth phenotype (Figure 7 F, J-K). Moreover, heterozygosity for *Hil*^{KG} in a *Mob2*$^{H4-5}$/+ background results in significant enhancement of the mutant phenotypes (Figure 7 D-E, J-K). We observed very similar results with mutations of CAP, an actin binding protein involved with actin filament organization (Yamazaki and Nusse 2002, Freeman et al. 1995, Nomura et al. 2012). A P-element insertion allele (*CAP*^{EY}), when homozygous, results in an overgrowth phenotype with increased number of boutons and branch points (Figure 7 I, J-K) and *CAP*^{EY}/+ shows a dominant interaction with with *Mob2*$^{H4-5}$/+ that also results in NMJ overgrowth (Figure 7 G-H, J-K). These results demonstrate that both Hil and CAP negatively regulate NMJ growth and functionally interact with Mob2. Thus, the conservation of MEN components involved in regulation of NMJ growth extends to components of the contractile ring.

Mob2 **alters actin dynamics**

One ultimate effect of the MEN is to promote cytokinesis by regulating the actin cytoskeleton to promote constriction of the contractile ring via adaptor proteins such as Hil and CAP. Having demonstrated that all the central players of the MEN are retained to function in an entirely new context as regulators of synaptic growth, we hypothesized that a key facet of this mechanism would be regulation of actin assembly during bouton growth and division.

To test this hypothesis, we looked for dominant genetic interactions between *Mob2*$^{H4-5}$ and mutations in affecting known acting-binding proteins. One obvious candidate to test in this context was *multiple wing hairs* (*mwh*), which encodes an F-actin binding protein that is involved in cell morphogenesis and polarity in developing hair cells (Yan et al. 2008, Fang and Adler 2010). Previous work has shown that *trc* and *mwh* genetically interact to inhibit wing hair development and that, loss of *trc* function in the wing leads to a decrease in expression of *mwh* (Fang and Adler 2010). However, *mwh* has not previously been implicated in regulation of NMJ growth. Therefore, we examined larvae homozygous for *mwh*^{1}, a null allele and found that they exhibit a significant elevation in number of boutons and branch points (Figure 8). Moreover, as with the known MEN components, *mwh*^{1} interacts dominantly with *Mob2*$^{H4-5}$ to cause a strong NMJ overgrowth phenotype. Thus, *mwh*, which has not previously been implicated in regulating NMJ growth in any capacity, is a negative regulator of NMJ growth supporting the idea that Mob2 (and the MEN in general) regulates actin dynamics during bouton growth and division.

We also examined the effect of mutations in *chickadee* (*chic*), which encodes profilin, a protein that regulates dynamic turnover of actin filaments by catalyzing the exchange of actin-bound ADP for ATP to promote actin polymerization (Cooley et al. 1992, Veheyen and Cooley 1994). A strong hypomorphic allele (*chic*^{01320}) (Veheyen and Cooley 1994). has no effect on NMJ growth when heterozygous or homozygous in an otherwise wild-type background (Figure 8). However, *chic*^{01320}/+ in a *Mob2*$^{H4-5}$/+ background results in

significant NMJ overgrowth with many of the phenotypic hallmarks of a *Mob2*$^{H4-5}$ homozygote (Figure 8).

To examine the effects of Mob2 on presynaptic actin assembly more directly, we expressed UAS-Moesin.GFP using C155-Gal4. Moesin (Moe) is an actin-filament binding protein that can serve as a reporter to indicate the dynamics and abundance of actin filaments (Edwards et al. 1997). Compared with wild-type controls, the abundance of Moe in synaptic terminals is greatly reduced in a *Mob2*$^{H4-5}$ background (Figure 9). However, the resolution was insufficient to discern any obvious differences in the distribution of the Moe that can be detected in *Mob2*$^{H4-5}$ compared with normal controls. Control of actin dynamics in synaptic boutons thus appears to be an important aspect of the mechanism by which Mob2 and other MEN components ultimately regulate bouton proliferation during NMJ growth, however the precise role of actin in this process remains to be elucidated.

MATERIALS AND METHODS

Fly Stocks

Mob2^{H4-5} was generated from an isofemale collected in Madison, WI by Helen Hartman. *ald*^{exc23} was provided by William Gilliland (DePaul University). *C155-Gal4 UAS-Dcr2* was provided by Kate O'Connor-Giles (University of Wisconsin-Madison). *UAS-trc.GFP* was provided by Paul Adler (University of Virginia). *UAS-cdc14-RNAi* was obtained

from the Vienna *Drosophila* RNAi Center. All other stocks were obtained from the Bloomington Stock Center.

Imaging

All larvae were obtained from low density crosses incubated at 25ºC. Wandering third-instar larvae were dissected in ice-cold Ca^{2+}-free saline and fixed for 15 minutes in 4% formaldehyde in PBS. Larvae were incubated in primary antibodies overnight at 4 ºC and in secondary antibodies for 2-3 hours at room temperature. We used the following antibodies: FITC- or Cy3- conjugated anti-HRP at 1:100 and 1:200 respectively (Jackson ImmunoResearch), rabbit anti-GFP at 1:1000 (Invitrogen), mouse anti-myc at 1:100 (Developmental Studies Hybridoma Bank). Secondary antibodies conjugated to Alexa Fluor 488 and Alexa Fluor 568 were used at 1:200 (Invitrogen). NMJs were imaged using a Zeiss 510 confocal microscope. Brightness and contrast were adjusted using Photoshop (Adobe).

Quantification of boutons and branch points was performed at NMJ4 in segments A2-A4 as described in (Coyle et al. 2004). Branch points were determined for each bouton with branch points defined as the number of projections from that bouton minus one (excluding terminal boutons). Branch points for each bouton were then added to determine the total number of branch points per NMJ. Statistical analyses were performed via Student's t tests for pairwise comparisons. Significance levels of <0.05,

<0.01, <0.001 are indicated by one, two and there asterisks respectively. Error bars denote standard error of the mean.

ACKNOWLEDGEMENTS

We would like to thank Helen Hartman collecting the original natural *D. melanogaster* from which *Mob2*$^{H4\text{-}5}$ was generated. We thank Paul Adler and his laboratory as well as William Gilliland and his laboratory for providing stocks. We also thank all memebers of the B.G. laboratory for helpful discussion and critical comments on the manuscript and the Bloomington Stock Center for supplying numerous stocks. This research was supported by the National Institutes of Health through a predoctoral training grant (T32 GM007507) to the Neuroscience Training Program and a research grant (RO1NS015390) (to B.G.).

REFERENCES

Baillat G, Moqrich A, Castets F, Baude A, Bailly Y, Benmerah A and A Monneron. 2001. Molecular cloning and characterization of phocein, a protein found from the Golgi complex to dendritic spines. *Mol Biol Cell 12:663-73.*

Collins CA and A DiAntonio. 2007. Synaptic development: insights from *Drosophila*. *Curr Opin Neurobiol* 17:35-42.

Cooley L, Verheyen E and K Ayers. 1992. chickadee encodes a Profilin Required for Intercellular Cytoplasm Transport during *Drosophila* Oogenesis. *Cell* 69:173-84.

de Bettignies G and LH Johnston. 2003. The Mitotic Exit Network. *Curr Biol* 13:R301.

Dernburg AF, Sedat JW and RS Hawley. 1996. Direct evidence of a role for heterochromatin in meiotic chromosome segregation. *Cell* 86:135-46.

Edwards, KA, Demsky M, Montague RA, Weymouth N and DP Kiehart. 1997. GFP-Moesin Illuminates Actin Cytoskeleton Dynamics in Living Tissue and Demonstrates Cell Shape Changes during Morphogenesis in *Drosophila*. *Dev Biol* 191:103-17.

Freeman NL, Chen Z, Horenstein J, Weber A and J Field. 1995. An actin monomer binding activity localizes to the carboxyl-terminal half of the Saccharomyces cerevisiae cyclase-associated protein. *J Biol Chem* 270:5680-5.

Gregory SL, Shandala T, O'Keefe L, Jones L, Myrray MJ and R Saint. 2007. A *Drosophila* overexpression screen for modifiers of Rho signaling in cytokinesis. *Fly* 1:13-22.

He Y, Emoto K, Fang C, Ren N, Tian X, Jan Y-N and PN Adler. 2005. *Drosophila* Mob Family Proteins Interact with the Related Tricornered (Trc) and Warts (Wts) Kinases. 16:4139-52.

Hiuashi S. 1996. Checkpoint mechanism that maintains diploidy in *Drosophila*: CDC2 inhibits S phase entry in G2 by a kinase independent mechanism. *Cell Struct Funct* 21:694.

Ji Y, Rath U, Girton J, Johansen KM and J Johansen. 2005. D-Hilarin, a novel W180-domain protein, affects cytokinesis through interaction with the spetin family member Pnut. *J Neurobiol* 64:157-69.

Komarnitsky SI, Chiang YC, Luca FC, Chen J, Toyn JH, Winey M, Johnston LH and CL Denis. 1998. DBF2 protein kinase binds to and acts through the cell cycle-regulated MOB1 protein. *Mol Cell Biol.* 18:2100-7.

Lehner CF and PH O'Farrell. 1990. *Drosophila* cdc2 homologs: a functional homolog is coexpressed with a cognate variant. *EMBO J* 9:3573-81.

Leopold P and PH O'Farrell. 1991. An evolutionarily conserved cyclin homolog from *Drosophila* rescues yeast deficient in G1 cyclins. *Cell* 66:1207-16.

Lai ZC, Wei X, Shimizu T, Ramos E, Rohrbaugh M, Nikolaidis N, Ho LL and Y Li. 2005. Control of cell proliferation and apoptosis by mob as tumor suppressor, mats. *Cell* 120:675-85.

Liu L-Y, Lin C-H and S-S Fan. 2009. Function of *Drosophila* mob2 in photoreceptor morphogenesis. *Cell Tissue Res* 338:377-89.

Luca FC and M Winey. 1998. MOB1, an essential yeast gene required for completion of mitosis and maintenance of ploidy. *Mol Biol Cell* 9:29-46.

McMollum D and KL Gould. 2001. Timing is everything: regulation of mitotic exit and cytokinesis by the MEN and SIN. *Trends Cell Biol* 11:89-95.

Meitinger F, Palani S and G Pereira. 2012. The power of MEN in cytokinesis. *Cell Cycle* 11:219-28.

Nelson B, Kurischko C, Horecka J, Mody M, Nair P, Pratt L, Zougman A, McBroom LD, Hughes TR, Boone C and FC Luca. 2003. RAM: a conserved signaling network that regulates Ace2p transcriptional activity and polarized morphogenesis. *Mol Biol Cell* 14:3782-803.

Normura K, Ono K and S Ono. 2012. CAS-1, a C. elegans cyclase-associated protein, is required for sarcomeric actin assembly in striated muscle. *J Cell Sci* in press

O'Tousa J. 1982. Meiotic chromosome behavior influenced by mutation-altered disjunction in *Drosophila* melanogaster females. *Genetics* 102:503-24.

Schulte J, Sepp KJ, Jorquera RA, Wu C, Song Y, Hong P and JT Littleton. 2010. DMob4/Phocein Regulates Synapse Formation, Axonal Transport, and Microtubule Organization. *J Neurosci* 30:5189-203.

Schuster CM, Davis GW, Fetter RD and CS Goodman. 1996. Genetic Dissection of Structural and Functional Componenets of Synaptic Plasticity. I. Fasciclin II Controls Synaptic Stabilization and Growth. *Neuron* 17:641-54.

Shimizu T, Ho LL and ZC Lai. 2008. The mob as tumor suppressor gene is essential for early development and regulates tissue growth in *Drosophila*. *Genetics* 178"957-65.

Sigrist S, Jacobs H, Stratmann R and CF Lehner. 1995. Exit from mitosis is regulated by *Drosophila* frizzy and the sequential destruction of cyclins A, B and B3. *EMBO J* 14:4827-38.

Su TT, Walker J and J Stumpff. 2000. Activating the DNA damage checkpoint in a developmental context. *Curr Biol* 10:119-26.

Trammell MA, Mahoney NM, Agard DA and RD Vale. 2008. Mob4 plays a role in spindle focusing in *Drosophila* S2 cells. *J Cell Sci* 121:1284-92.

Verheyen E and L Cooley. 1994. Profilin mutations disrupt multiple actin-dependent processes during *Drosophila* development. *Development* 120:717-28.

Weiss EL, Kurischko C, Zhang C, Shokat K, Drubin DG and FC Luca. 2002. Saccharomyces cerevisiae Mob2p-Cbk1p kinase complex promotes polarized growth and acts with the mitotic exit network to facilitate daughter cell-specific localization of Ace2 transcription factor. *J Cell Biol* 158:558-900.

Yamazaki H and R Nusse. 2002. Identification of DCAP, a *Drosophila* homolog of a glucose transport regulatory complex. *Mech Dev* 199:115-9.

Zallen JA, Peckol EL, Tobin DM and CI Bargmann. 2000. Neuronal cell shape and neurite initiation are regulated by the Ndr kinase SAX-1, a member of the Orb6/COT-1/warts serine/threonine kinase family. *Mol Biol Cell* 11:3177-90.

Figure 1

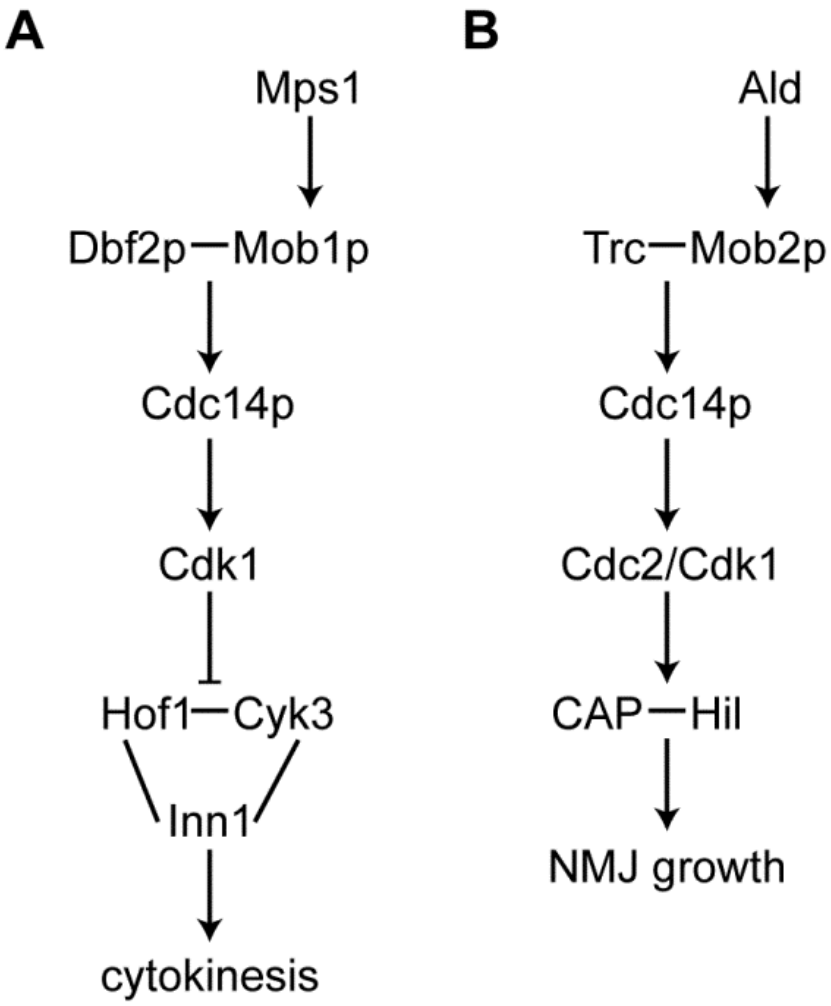
A
Mps1
Dbf2p—Mob1p
Cdc14p
Cdk1
Hof1—Cyk3
Inn1
cytokinesis
B
Ald
Trc—Mob2p
Cdc14p
Cdc2/Cdk1
CAP—Hil
NMJ growth

Figure 1: Components of the Mitotic Exit Network in *Saccharomyces cerevisiae* and their counterparts in *Drosophila*

(A) Many studies in yeast have led to elucidation of the MEN pathway partially diagrammed here. Mps1 is a kinase that phosphorylates Mob1 to activate its binding to Dbf2. When bound to Mob1, the Dbf2 kinase is activated and Cdc14 is then phosphorylated. Cdc14 is a phosphatase and when activated by Dbf2, it dephosphorylates Cdk1 to promote its degradation. Inactivation and breakdown of Cdk1 is required for exit from mitosis. Final steps of this pathway involve assembly of the contractile ring complex, which includes Hof1, Cyk3, and Inn1, at the bud neck followed by septum formation and cytokinesis. (B) A proposed MEN pathway in *Drosophila* based both on previous studies in *Drosophila* that have identified orthologs of some of the yeast components and on studies described here. Aside from the role of this pathway in regulating cell division, we demonstrate an additional role in regulating bouton division during NMJ growth: mutation or RNAi knockdown of each of the components shown in (B) result in NMJ overgrowth phenotypes alone or in combination with mutations of *Mob2*.

Figure 2

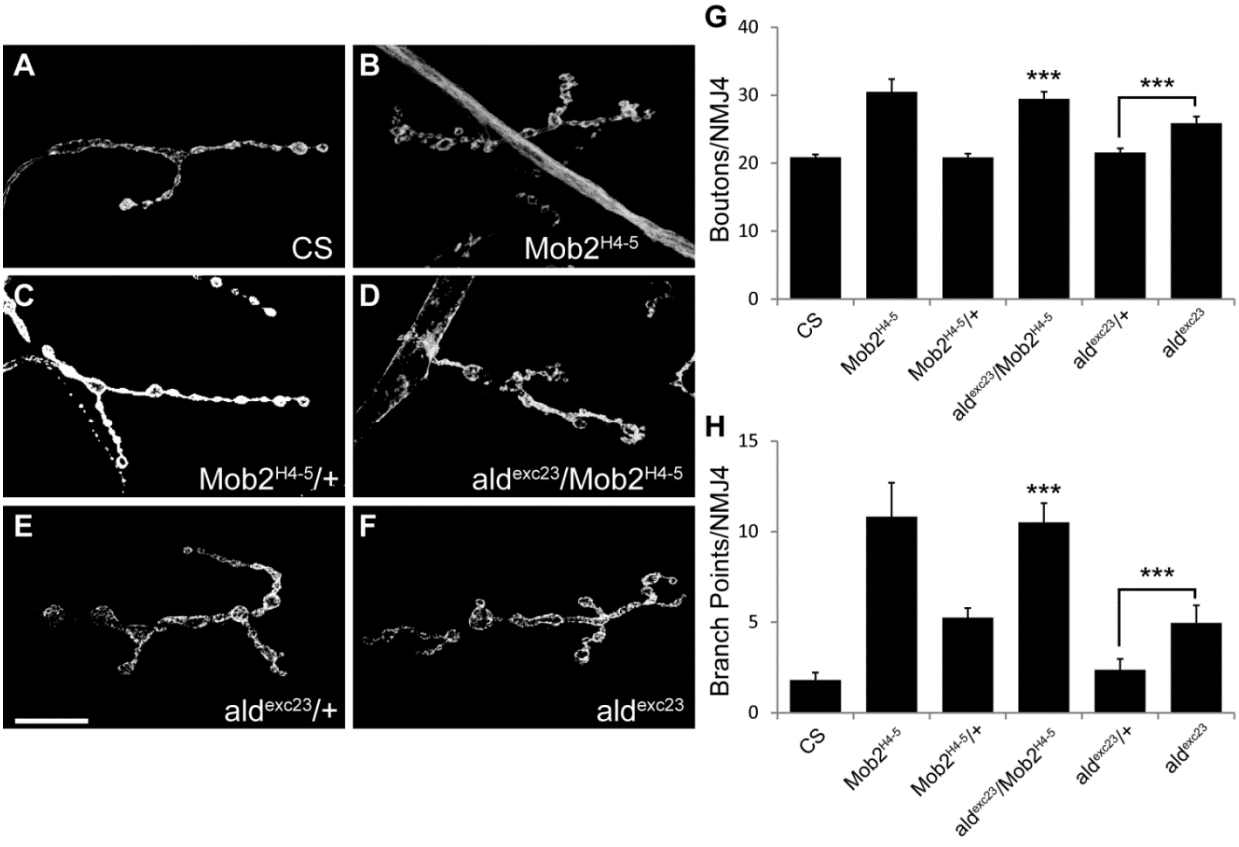
A
CS
B
Mob2H4-5
C
Mob2H4-5/+
D
aldexc23/Mob2H4-5
E
aldexc23/+
F
aldexc23
G
Boutons/NMJ4
40
30
20
10
0
***
***
CS
Mob2H4-5
Mob2H4-5/+
aldexc23/Mob2H4-5
aldexc23/+
aldexc23
H
Branch Points/NMJ4
15
10
5
0
***
***
CS
Mob2H4-5
Mob2H4-5/+
aldexc23/Mob2H4-5
aldexc23/+
aldexc23

Figure 2: *ald* is a negative regulator of NMJ growth and genetically interacts with *Mob2*

(A-F) Confocal images of NMJ4 labeled with FITC-anti-HRP. (A) *Canton-S* (*CS*), laboratory wild-type control. $Mob2^{H4-5}$ homozygotes (B) and ald^{exc23} homozygotes (F) show similar NMJ overgrowth phenotypes. $Mob2^{H4-5}$/+ (C) and ald^{exc23}/+ (E) heterozygotes show very mild NMJ overgrowth phenotypes. In contrast, ald^{exc23}/+;$Mob2^{H4-5}$/+ double heterozygotes (D) exhibit a significantly enhanced NMJ overgrowth phenotype compared with either single heterozygote (C,E). Scale bar, 20µm. Quantification of number of boutons (G) and branch points (H) at NMJ4 in larvae of the genotypes shown. Error bars denote SEM. ***, P<0.001.

Figure 3

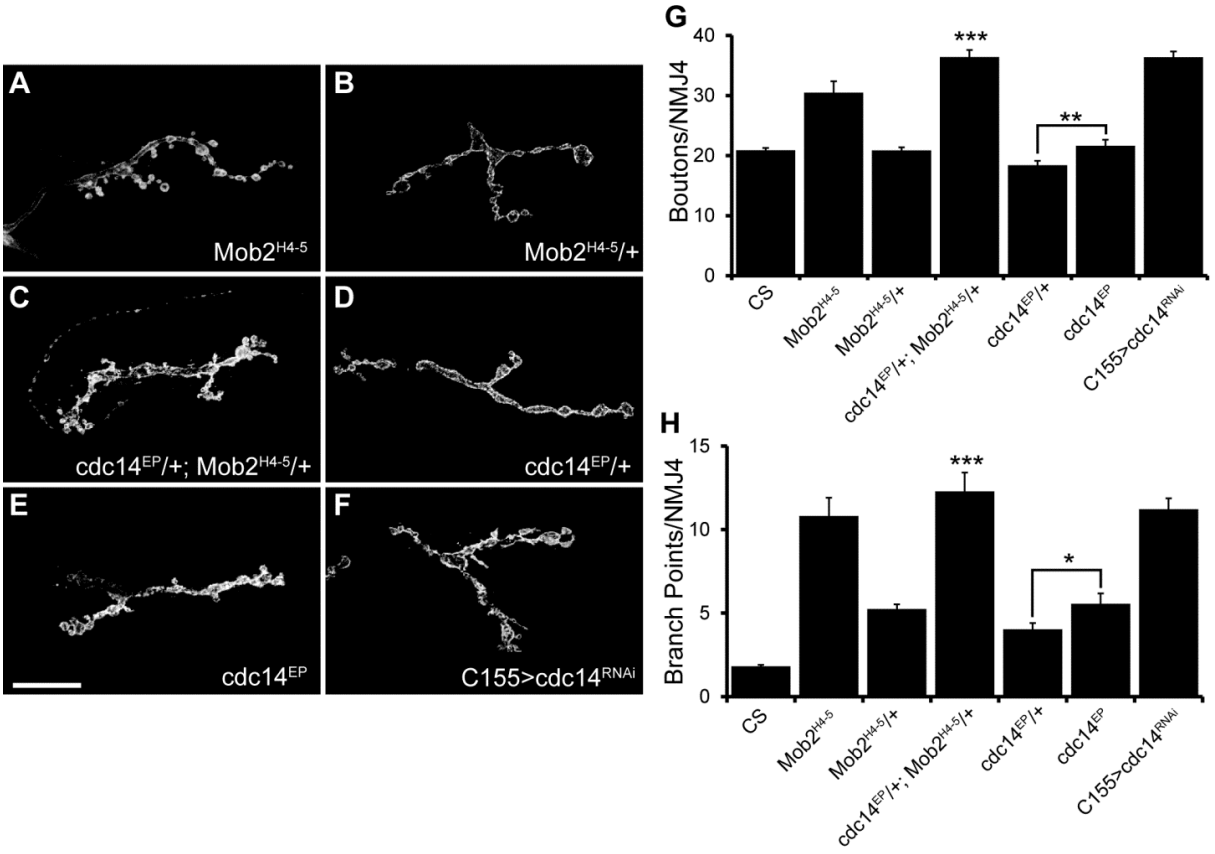
A
Mob2H4-5
B
Mob2H4-5/+
C
cdc14EP/+; Mob2H4-5/+
D
cdc14EP/+
E
cdc14EP
F
C155>cdc14RNAi
G
Boutons/NMJ4
40
30
20
10
0
***
**
CS
Mob2H4-5
Mob2H4-5/+
cdc14EP/+; Mob2H4-5/+
cdc14EP/+
cdc14EP
C155>cdc14RNAi
H
Branch Points/NMJ4
15
10
5
0
***
*
CS
Mob2H4-5
Mob2H4-5/+
cdc14EP/+; Mob2H4-5/+
cdc14EP/+
cdc14EP
C155>cdc14RNAi

Figure 3: *cdc14* is a negative regulator of NMJ growth and genetically interacts with *Mob2*

(A-F) Confocal images of NMJ4 labeled with FITC-anti-HRP. $cdc14^{EP}$ homozygotes (E) have a weak NMJ overgrowth phenotype compared with $Mob2^{H4-5}$ homozygotes (A) However, neuronal RNAi knockdown of *cdc14* using *C155-Gal4* (F) results in a much stronger overgrowth phenotype that resembles $Mob2^{H4-5}$. Heterozygotes for either $Mob2^{H4-5}$ (B) or $cdc14^{EP}$ (D) alone have mild overgrowth phenotypes. In contrast, $cdc14^{EP}$/+;$Mob2^{H4-5}$/+ double heterozygotes (C) exhibit a significantly enhanced overgrowth phenotype. Scale bar, 20µm. Quantification of number of boutons (G) and branch points (H) at NMJ4 in larvae of the genotypes shown. Error bars denote SEM. *, P<0.05; **, P<0.01; ***, P<0.001.

Figure 4

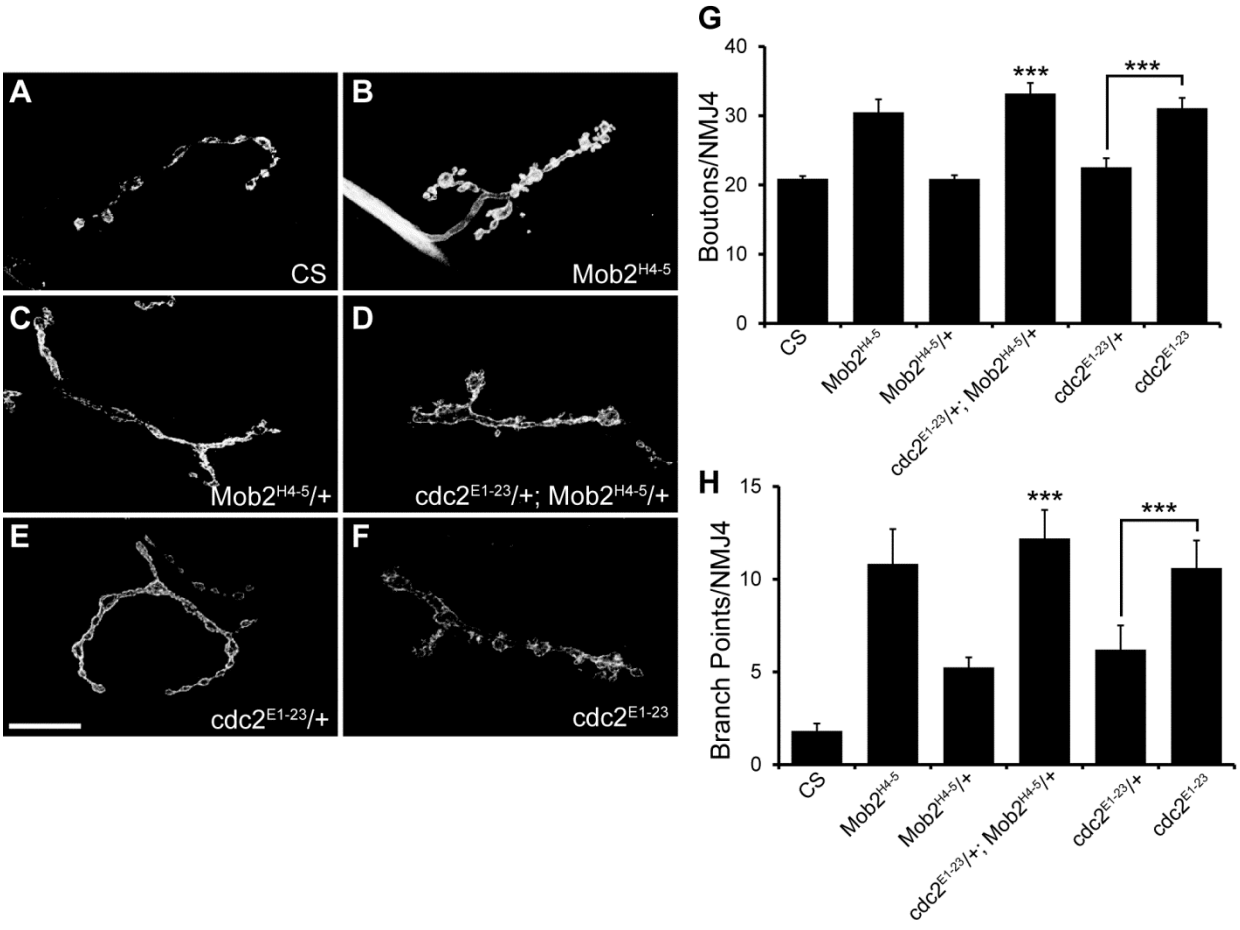
A
CS
B
Mob2H4-5
C
Mob2H4-5/+
D
cdc2E1-23/+; Mob2H4-5/+
E
cdc2E1-23/+
F
cdc2E1-23
G
Boutons/NMJ4
40
30
20
10
0
***
***
CS
Mob2H4-5
Mob2H4-5/+
cdc2E1-23/+; Mob2H4-5/+
cdc2E1-23/+
cdc2E1-23
H
Branch Points/NMJ4
15
10
5
0
***
***
CS
Mob2H4-5
Mob2H4-5/+
cdc2E1-23/+; Mob2H4-5/+
cdc2E1-23/+
cdc2E1-23

Figure 4: *cdc2* is a negative regulator of NMJ growth and genetically interacts with *Mob2*

((A-F) Confocal images of NMJ4 labeled with FITC-anti-HRP. *Mob2*$^{H4-5}$ (B) and *cdc2*$^{E1-23}$ (F) homozygotes have similar NMJ overgrowth phenotypes. Heterozygotes for *Mob2*$^{H4-5}$ (C) or *cdc2*$^{E1-23}$ (E) have very mild overgrowth phenotypes. By comparison, *cdc2*$^{E1-23}$/+;*Mob2*$^{H4-5}$/+ double heterozygotes (D) exhibit a significantly enhanced overgrowth phenotype. Scale bar, 20µm. Quantification of number of boutons (G) and branch points (H) at NMJ4 in larvae of the genotypes shown. Error bars denote SEM. ***, P<0.001.

Figure 5

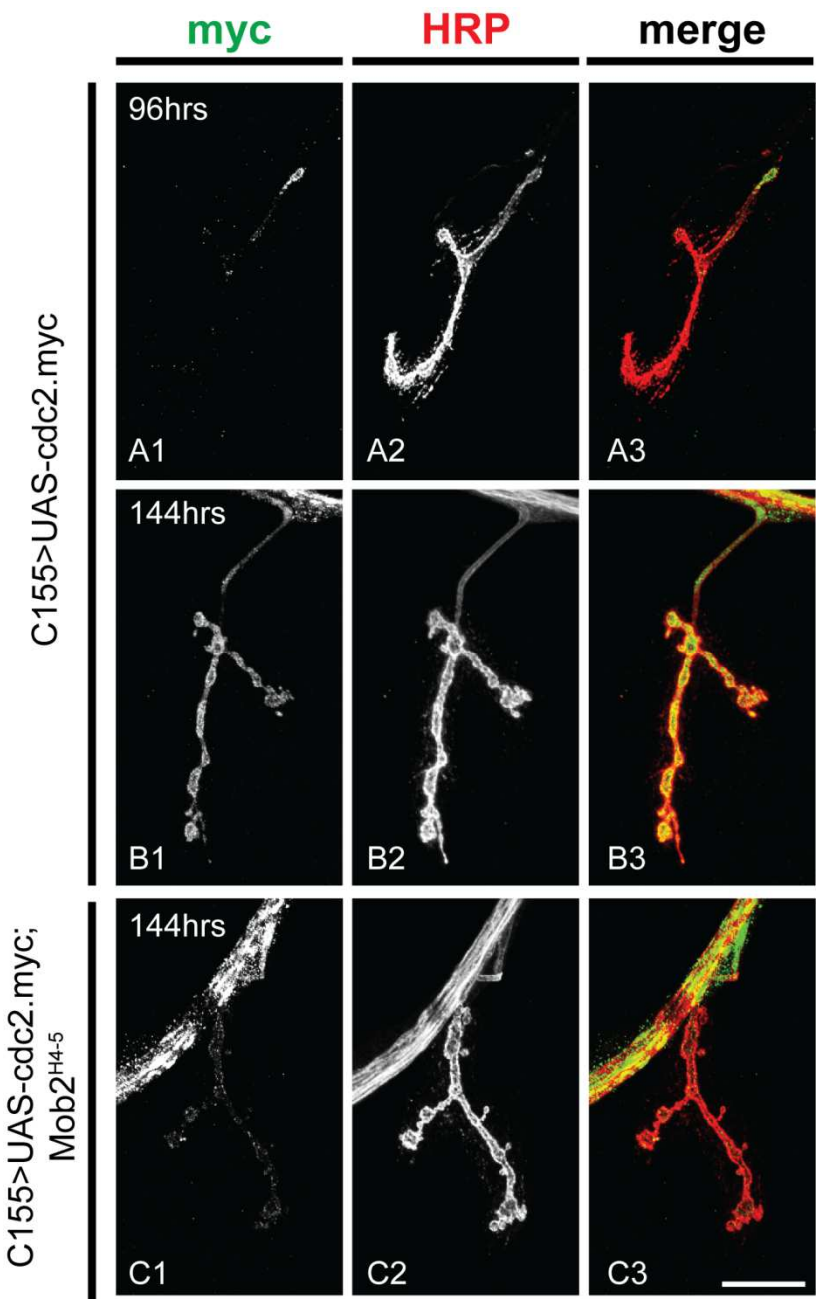
myc
HRP
merge
96hrs
A1
A2
A3
144hrs
B1
B2
B3
C155>UAS-cdc2.myc
144hrs
C1
C2
C3
C155>UAS-cdc2.myc;
Mob2H4-5

Figure 5: Cdc2 localizes to presynaptic terminals and is differentially expressed throughout NMJ development

(A-C) Confocal images of NMJ4. Expression of a myc-tagged version of Cdc2, encoded by *UAS-cdc2.myc*, was driven pan-neuronally by *C155-Gal4*. (A1) In NMJs from late second instar larvae (96 hrs AEL), the level of Cdc2 at presynaptic terminals is very low and the signal is restricted to the most proximal regions of the NMJ. (B1) By contrast, in NMJs from late third instar larvae (144 hrs AEL) Cdc2 is readily detected at high levels throughout the entire presynaptic terminal. (C1) In a $Mob2^{H4-5}$ mutant background at 144 hr AEL Cdc2 can still be detected throughout the presynaptic terminal but at considerably reduced levels compared with a wild-type background (B1). (A2-C2) The same NMJs shown in panels A1-C1 stained with Cy3-anti-HRP. Scale bar, 20µm.

Figure 6

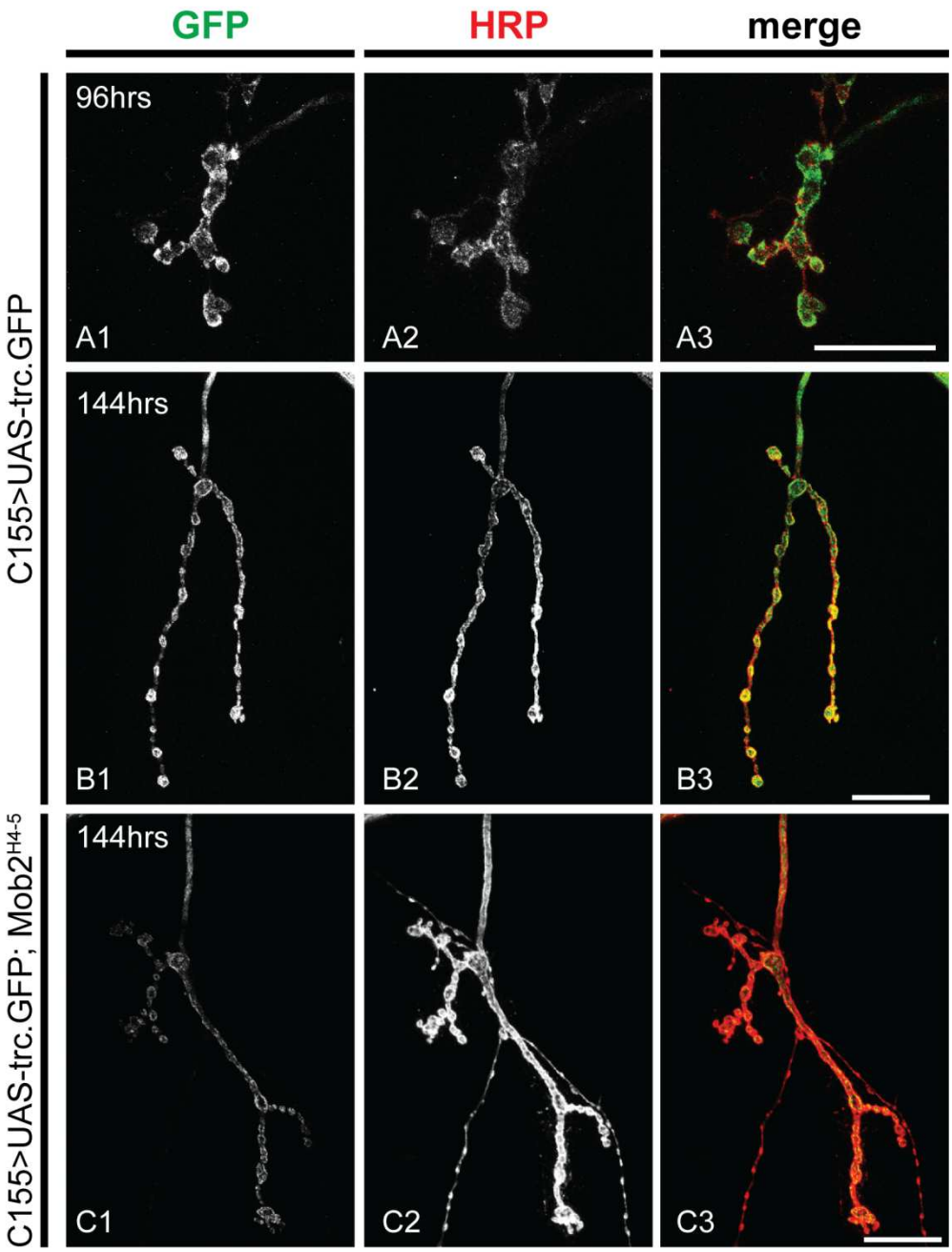
GFP
HRP
merge
96hrs
A1
A2
A3
144hrs
B1
B2
B3
144hrs
C1
C2
C3
C155>UAS-trc.GFP
C155>UAS-trc.GFP; Mob2H4-5

Figure 6: Trc localizes to particular regions of developing boutons

(A-C) Confocal images of NMJ4. Expression of *UAS-trc.GFP* was driven pan-neuronally by *C155-Gal4*. In both late second instar larvae (A1) and late third instar larvae (B1) Trc is prominently localized to NMJ nerve terminals. However, the distribution of Trc within boutons is different at these two stages. (A1) At 96 hr AEL when NMJs are still adding new boutons, Trc appears to localize primarily at "bud necks" where new boutons are emerging from a parent bouton as well as at the leading edge of the terminal bouton, a site where NMJ growth occurs by addition of new boutons. (B1) At 144 hr AEL when NMJ growth is complete, TRC no longer shows sub-localization within boutons but is more diffusely distributed within all boutons. (C1) In a *Mob2H*$^{4-5}$ background at 144 hr AEL, Trc is still distributed throughout presynaptic terminals but at greatly diminished levels. (A2-C2) The same NMJs as shown in panels A1-C1 stained with Cy3-anti-HRP. Scale bar, 20µm.

Figure 7

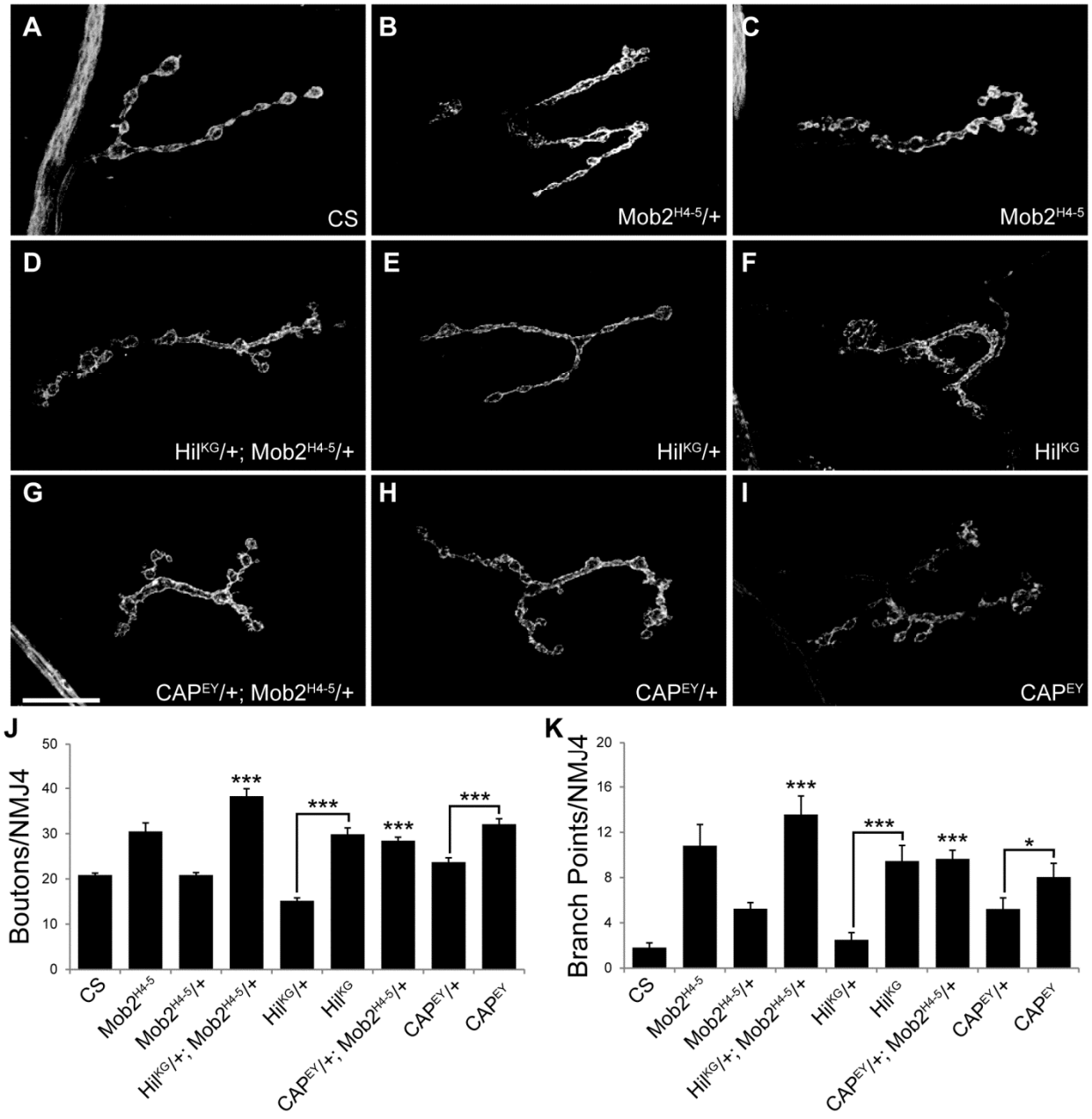
A
CS
B
Mob2H4-5/+
C
Mob2H4-5
D
HilKG/+; Mob2H4-5/+
E
HilKG/+
F
HilKG
G
CAPEY/+; Mob2H4-5/+
H
CAPEY/+
I
CAPEY
J
Boutons/NMJ4
0
10
20
30
40
50
***
***
***
***
CS
Mob2H4-5
Mob2H4-5/+
HilKG/+; Mob2H4-5/+
HilKG/+
HilKG
CAPEY/+; Mob2H4-5/+
CAPEY/+
CAPEY
K
Branch Points/NMJ4
0
4
8
12
16
20
***
***
***
*
CS
Mob2H4-5
Mob2H4-5/+
HilKG/+; Mob2H4-5/+
HilKG/+
HilKG
CAPEY/+; Mob2H4-5/+
CAPEY/+
CAPEY

Figure 7: Hil and *CAP* are negative growth regulators of NMJ growth that genetically interact with *Mob2*

(A-I) Confocal images of NMJ4 labeled with FITC-anti-HRP. $Mob2^{H4-5}$ homozygotes (C), Hil^{KG} homozygotes (F) and CAP^{EY} homozygotes (I) all have NMJ overgrowth with similar phenotypic features. $Mob2^{H4-5}$/+ heterozygotes (B) and Hil^{KG}/+ heterozygotes (E) have mild overgrowth phenotypes CAP^{EY}/+ heterozygotes (H) have a somewhat stronger NMJ overgrowth phenotype compared with the other two heterozygotes. Hil^{KG}/+;$Mob2^{H4-5}$/+ (D) and CAP^{EY}/+; $Mob2^{H4-5}$/+ double heterozygotes (H) exhibit significantly enhanced overgrowth phenotypes compared with the respective single heterozygotes (B, E, H). Scale bar, 20µm. Quantification of number of boutons (J) and branch points (K) at NMJ4 in larvae of the genotypes shown. Error bars denote SEM. *, P<0.05; ***, P<0.001.

Figure 8

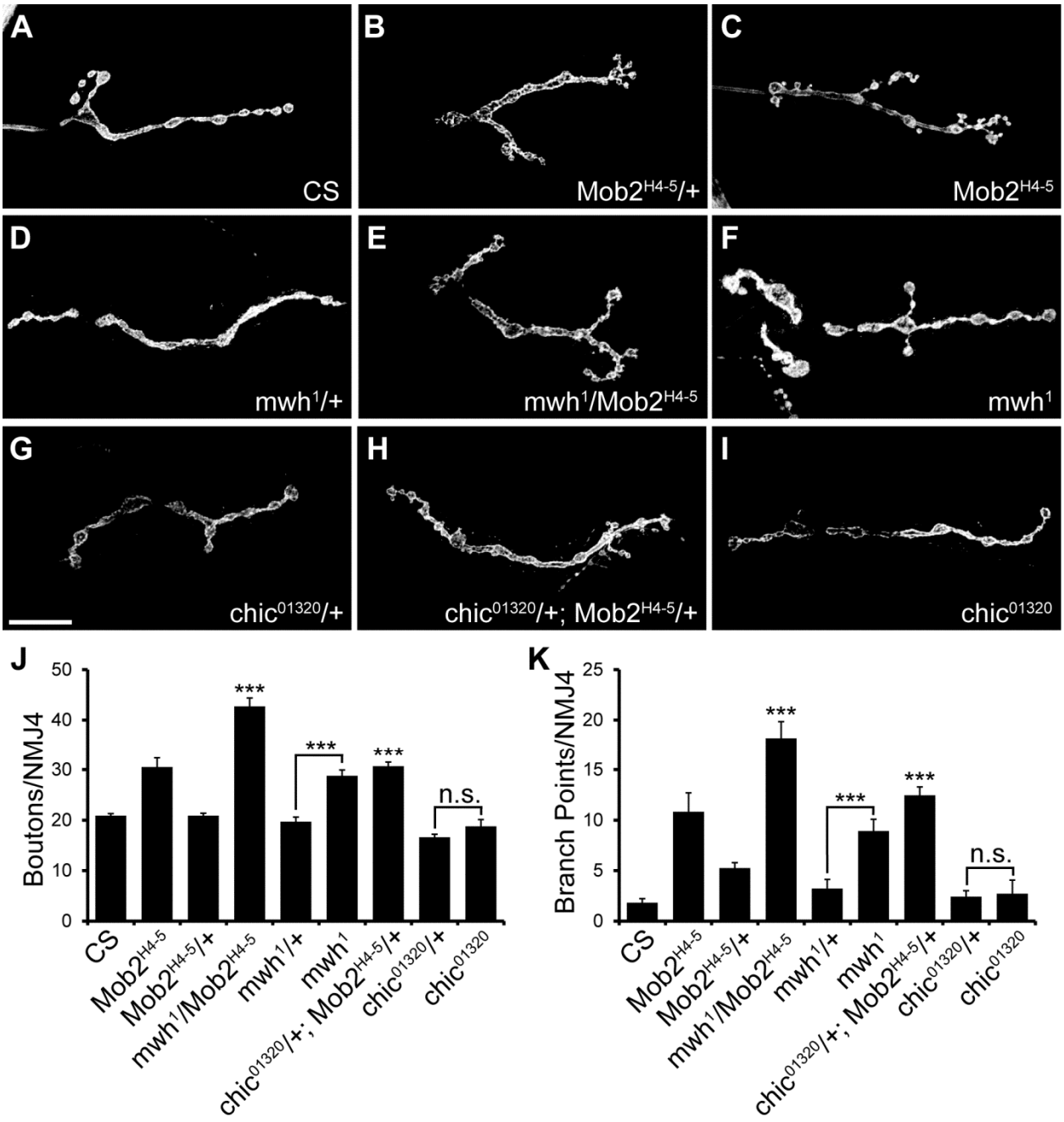
A
CS
B
Mob2H4-5/+
C
Mob2H4-5
D
mwh1/+
E
mwh1/Mob2H4-5
F
mwh1
G
chic01320/+
H
chic01320/+; Mob2H4-5/+
I
chic01320
J
Boutons/NMJ4
50
40
30
20
10
0
***
***
***
n.s.
CS
Mob2H4-5
Mob2H4-5/+
mwh1/Mob2H4-5
mwh1/+
mwh1
chic01320/+; Mob2H4-5/+
chic01320/+
chic01320
K
Branch Points/NMJ4
25
20
15
10
5
0
***
***
***
n.s.
CS
Mob2H4-5
Mob2H4-5/+
mwh1/Mob2H4-5
mwh1/+
mwh1
chic01320/+; Mob2H4-5/+
chic01320/+
chic01320

Figure 8: *mwh* and *chic* are negative regulators of NMJ growth and genetically interact with *Mob2*

(A-I) Confocal images of NMJ4 labeled with FITC-anti-HRP. *mwh*^{1} homozygotes (F) have an NMJ overgrowth phenotype similar to that of *Mob2*$^{H4-5}$ homozygotes (C). *chic*^{01320} homozygotes (I) appear normal. Heterozygotes for *mwh*^{1} (D) or *chic*^{01320} (G) have normal NMJs. *Mob2*$^{H4-5}$ heterozygotes (B) have weakly overgrown NMJs. *mwh1/Mob2*$^{H4-5}$ (E) and *chic*^{01320}/+; *Mob2*$^{H4-5}$/+ double heterozygotes (H) exhibit significantly enhanced NMJ overgrowth phenotypes compared with the corresponding single heterozygotes (B,D, G). Scale bar, 20µm. Quantification of number of boutons (G) and branch points (H) at NMJ4 in larvae of the genotypes shown. Error bars denote SEM. n.s., not significant (P>0.05); ***, P<0.001.

Figure 9

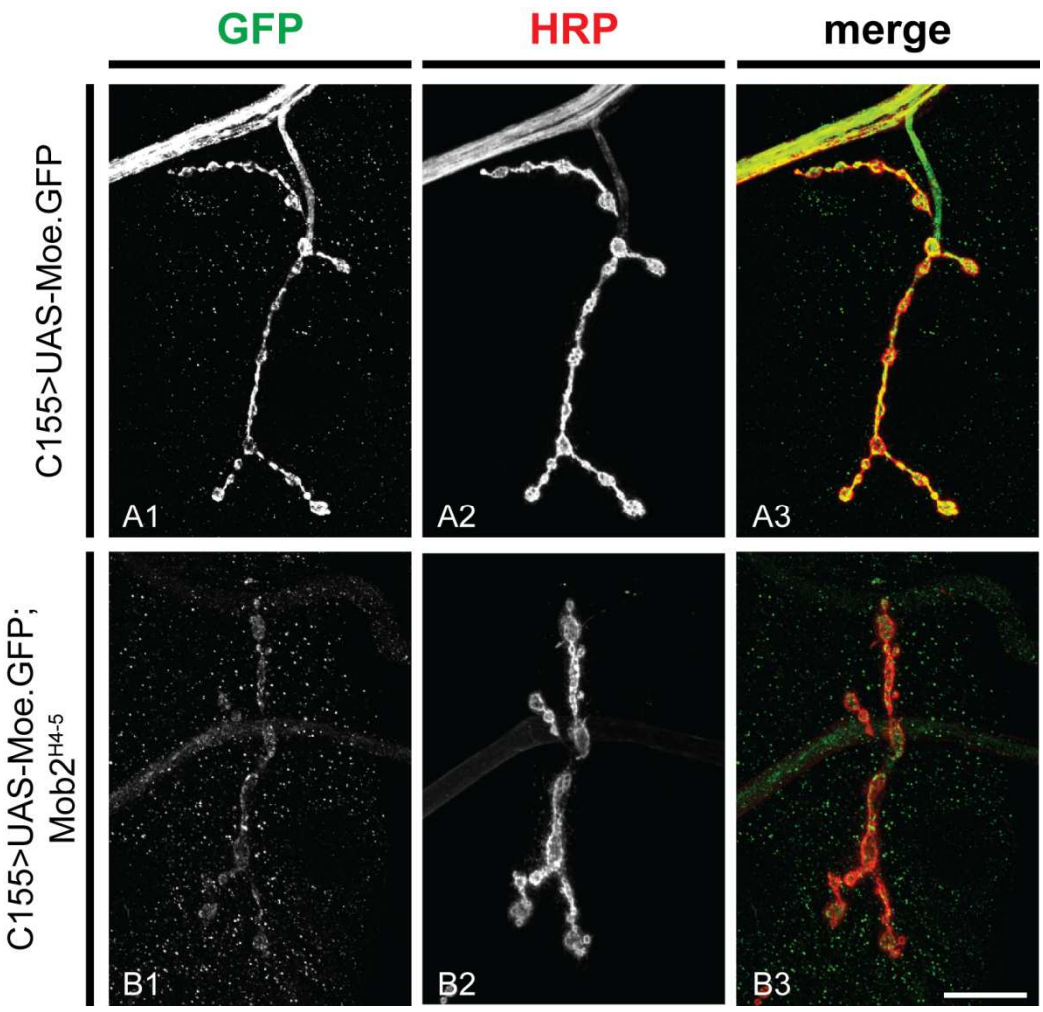
GFP
HRP
merge
C155>UAS-Moe.GFP
C155>UAS-Moe.GFP;
Mob2H4-5
A1
A2
A3
B1
B2
B3

Figure 9: Moesin expression is decreased in a Mob2 background

(A-B) Confocal images of NMJ4. Expression of *UAS-Moe.GFP* was driven pan-neuronally with *C155-Gal4* in wild-type (A) and $Mob2^{H4-5}$ (B) backgrounds. Moe signal is substantially reduced in Mob2H4-5 NMJs (B1) compared with wild-type (A1) indicating that assembly of actin filaments is aberrant in $Mob2^{H4-5}$. (A2, B2) The same NMJs stained with Cy3-anti-HRP. Scale bar, 20µm.

CHAPTER 5

Discussion and Future Directions

In this dissertation, I used two approaches to investigate the evolution of the morphological trait of larval neuromuscular junction (NMJ) morphology. In Chapter 2, I demonstrated that NMJ morphology is a rapidly evolving trait that varies extensively among different *Drosophila* species. I further demonstrated that genetic drift alone cannot explain the variation observed and therefore natural selection is contributing to the divergence of NMJ morphology. Despite this variability in synaptic form, I do not observe any difference in gross physiology. Therefore, it is still unclear what selection is acting upon to generate the diversity. In Chapter 3, I examined the NMJ morphologies of natural populations of *D. melanogaster*. While NMJ morphology is largely conserved among populations of *D. melanogaster*, some mild variability was observed. Through further characterization by isolating single chromosomes of one of these variant lines, H4, we determined that mutations in multiple genes encoding both positive and negative regulators of NMJ morphology are segregating within this line. Focusing on one subisolate with NMJ overgrwoth, I mapped the polymorphism to *Mob2*, which functions presynaptically through an interaction with the kinase *tricornered* (*trc)*. This study identified a novel regulator of synaptic growth, while also providing insights into the evolution of a neural trait. In Chapter 4, I investigate pathway in which Mob2 acts to regulate NMJ growth. Each of the core members of the Mitotic Exit Network (the yeast Mob1 pathway) have been co-opted from their role in cytokinesis to regulate bouton budding. Ultimately, aberrant actin dynamics contribute to the NMJ phenotype observed in *Mob2* mutants. In this chapter, I will describe future experiments and expand my discussion of these results.

The role of *Mob2* in cytoskeletal dynamics during NMJ development

In Chapter 4, I show that aberrant actin dynamics ultimately contributes to the overgrown NMJ phenotype observed in *Mob2* mutants. While Moesin localization has suggested a decrease in actin localization at the presynaptic NMJ, this technique does not allow for high enough resolution to clearly observe localization within a bouton. Unfortunately, antibody staining for actin (for example phalliodin staining) is not useful because there are high levels of actin in the muscle which obscures resolution in the presynaptic portion of the NMJ. To address whether actin is specifically mislocalized in *Mob2* mutant neuron, I plan to express *UAS-LifeAct* using a neuron specific Gal4 driver. LifeAct is a Tomato tagged 17-amino acid peptide that incorporates into actin filaments without disrupting actin dynamics (Riedl et al. 2008, construct courtesy of Jill Wildonger). Localization of Lifeact in a wild-type background mimics the general pattern of Moesin localization (Figure 1); therefore I expect to also see a decrease in Lifeact expression in a *Mob2* mutant background as well. The Lifeact construct could also be used for live imaging to monitor actin filament formation during the growth phase of NMJ development. By labeling actin more directly and with higher resolution we can address such questions as: Does actin create a contractile ring-like structure in dividing boutons? Does actin co-localize to 'bud necks' with Trc? These experiments could provide insights into the mechanism by which actin dynamics regulate bouton division and synapse formation.

There is a close relationship between actin and microtubule dynamics during neural development. Since actin is misregulated in Mob2 mutants, are microtubules also

aberrant? Additionally, *Mob4* mutants, that exhibit an NMJ overgrowth phenotype that is characteristically very similar to that of *Mob2*, display aberrant microtubule structures (Schute et al. 2010). Therefore, are both actin and microtubule dynamics regulated by Mob2 and the Mitotic Exit Network? To begin to address this question, I examined Futsch localization through antibody staining at larval NMJs. Futsch is the *Drosophila* homolog of Microtubule-associated protein 1B (MAP1B) and is expressed specifically in neurons (Hummel et al. 2000). In a wild-type genetic background, Futsch antibodies normally label a thin, discrete structure throughout the NMJ. Occasionally, in terminal boutons looped structures are observed (Figure 2). These loops are thought to be stabilizing to microtubule ends (Roos et al. 2000). However, in a *Mob2* mutant background Futsch staining is variable, but consistently aberrant. In some NMJs I observe excess loops present in non-terminal boutons. Other NMJs exhibit Futsch staining that fills the proximal boutons entirely, but more distal boutons lack all Futsch staining (Figure 2). Normal Futsch localization is never observed in a *Mob2* mutant background suggesting that microtubule dynamics are disrupted. To further investigate this aberration, I looked directly at tubulin structures by staining for both tyrosinated-tubulin (try-tub) and acetylated-tubulin (ace-tub). When tubulin is translated, the final amino acid is a tyrosine (tyr-tub). This pool of tubulin is considered highly dynamic. Stabilization can occur through one of two post-translational modifications. Both methods begin by cleaving the tyrosine residue. Then either the subsequent residue is cleaved (glu-tub) or tubulin can be acetylated (ace-tub) (Garnham and Roll-Mecak 2012). Therefore, try-tub labeling should indicate nascent tubulin that is highly dynamic, while ace-tub labeling indicates stabilized tubulin structures. Compared to a wild-type

genetic background, *Mob2* mutants showed higher levels of try-tub and lower levels of ace-tub in neurons (Figure 2). These results suggest that tubulin structures are failing to stabilize in *Mob2* mutants. This is a bit confounding because mutants that disrupt microtubule stability generally have undergrown rather than overgrown NMJs (Roos et al. 2000, Bettencourt da Cruz et al. 2005, Pawson et al. 2008, Koch et al. 2008, Godena et al. 2011). The mechanism by which microtubule dynamics are contributing to NMJ growth and how actin and microtubule dynamics interact at the NMJ are still unclear. One approach to begin to address these questions would be to monitor microtubule dynamics using live imaging at the NMJ through expression of a GFP tagged End binding protein 1 (EB1::GFP) specifically in neurons (construct courtesy of Jill Wildonger). EB1 is a plus-end-tracking protein that can be utilized to monitor the dynamic addition and subtraction of tubulin (Zheng et al. 2008). Tracking the GFP 'comets' during development of the NMJ may lead to a better understanding of the function of microtubules during bouton proliferation.

A role for septins during NMJ development

In Chapter 4, I discussed how Hillarin (Hil) and cyclase-associated protein (CAP) mediate the connection between septin proteins and actin filaments during cytokinesis. Because both genes are negative regulators of NMJ growth and function in a common pathway with Mob2, are Hil and CAP also physically interacting with septin proteins in the NMJ? This leads to more basic questions such as: Are septin proteins expressed in post mitotic motor neurons? Do any septins specifically localize to the NMJ? Do they genetically interact with *Mob2* or other members of the Mitotic Exit Network to regulate

NMJ growth? In *Drosophila*, there are 5 septin proteins. One of those proteins, Pnut has been well studied for its role in cytokinesis and genetically and physically interacts with Hil during cytokinesis (Ji et al. 2005). I began to investigate the role of septins by looking at larval NMJs of pnut mutants as well as testing for a dominant genetic interaction between *pnut* and *Mob2*. *pnut* null mutants are embryonic lethal, therefore I could not examine pnut null NMJs. However, a null mutation heterozygous with a putative hypomorphic insertion allele ($pnut^{XP}/pnut^{DG}$) yielded undergrown NMJs. This suggests that Pnut is a positive regulator of NMJ growth. $pnut^{XP}$/+ larval NMJs have a very mild undergrowth phenotype, however in combination with $Mob2^{H4-5}$/+ NMJs were significantly undergrown with very simple NMJ structures that are comparable to $pnut^{XP}/pnut^{DG}$ NMJs (Figure 3). These results suggest that Pnut is acting downstream of Mob2 to regulate NMJ growth. To further investigate the role of Pnut at the NMJ, I looked at localization of Pnut using an antibody. Pnut is expressed in post-mitotic neurons and localizes specifically to NMJs. Compared with a wild-type genetic background which showed very little Pnut localization, I observed a significant increase in Pnut localization in $Mob2^{H4-5}$ NMJs (Figure 3). It is possible that the increase in Pnut localization in a *Mob2* mutant background contributes to the excess growth observed, however additional experiments are needed to confirm the mechanistic interaction between *pnut* and *Mob2*. For example, does overexpression of Pnut in a wild-type background cause NMJ overgrowth? Does Pnut localization vary during NMJ growth? Additionally, Pnut is one of five septins, therefore are other septin proteins also important for NMJ development? Is there functional redundancy among the septin proteins?

Expanding the Mob2 pathway

In Chapter 4, I described numerous dominant genetic interactions between *Mob2* and members of the Mitotic Exit Network, actin binding proteins, etc. From this work, it seems that the $Mob2^{H4\text{-}5}$ heterozygous background is highly sensitive for identifying dominant dose-dependent genetic interactions. While the candidate approach has proved highly productive, our description of Mob2's mechanism to regulate NMJ growth is still incomplete. To gain a better understanding of Mob2 function, I propose conducting a forward genetic screen utilizing the *Drosophila* deficiency collection to look for dominant enhancement of the $Mob2^{H4\text{-}5}$/+ NMJ phenotype. Using this method we can systematically screen the entire genome for loss-of-function interactions. Preliminary results from the screen conducted by undergraduate student Lalanti Venkat are encouraging (Figure 4). Among 52 deficiencies of various sizes screened from the 2nd and 3rd chromosomes 13 have been identified that show dominant enhancement of the $Mob2^{H4\text{-}5}$/+ NMJ phenotype. Two of the deficiency regions uncovered genes already known to dominantly enhance the *Mob2* mutant phenotype: *chickadee* and *CAP*, thus providing proof of concept. From these results I expect that additional new members of the Mob2 pathway responsible for regulating NMJ growth will be identified.

Natural populations of *D. melanogaster* as a resource to identify novel regulators of NMJ growth

Chapter 3 describes the identification of a polymorphism regulating *Mob2* expression from a natural isolate of *D. melanogaster*. Natural populations provide a wealth of polymorphisms that regulate morphological traits, such as NMJ formation. While

artificial mutagenesis has been invaluable for discovering NMJ growth regulators, nature mutates organisms through different mechanisms. For example, polymorphisms in natural populations often affect cis-regulatory elements only altering level, timing or pattern of expression of the gene. Therefore, by screening through collections of natural isolates we may be able to identify genes and pathways that were missed with artificial mutagenesis. Two collections of natural isolates of *D. melanogaster* exhibit some exciting novel phenotypes (Figure 5). One collection was generated by Trudy MacKay (North Carolina State University). These lines were collected in Raleigh, NC and have subsequently undergone numerous rounds of single-pair matings to isogenize the lines and full genome sequences are currently being generated (Mackay et al. 2012). Additionally, a multi-lab database is being created to tabulate morphological and behavioral variation among the lines as a way to more systematically identify correlations between varying phenotypes (Harbison et al. 2009, Morozova et al. 2009, Edwards et al. 2009, Clowers et al. 2010). The second collection is continually being generated by John Pool (University of Wisconsin). He has compiled isofemale lines from different regions of Africa. These lines are more genetically variable because they have been kept by mass matings, not limiting the number of segregating chromosomes. However, full genome sequence data from haploid embryos has been collected from many of the lines (Pool and Aquadro 2007, Langley et al. 2012). Both collections provide interesting opportunities to identify novel regulators of NMJ growth while also having the potential to also investigate this regulation with population genetics. What is the prevalence of a certain polymorphism among populations? How often do independent polymorphisms of a gene arise in distinct populations? Taken together,

studying the *Drosophila* larval NMJ among natural populations helps to gain a better understanding of the genes and pathways upon which evolution is acting to evolve synapses and possibly nervous systems more generally.

References

Bettencourt da Cruz A, Schwarzel M, Schulze S, Niyyati M, Heisenberg M and D Kretzschmar. 2005. Disruption of the MAP1B-related protein FUTSCH leads to changes in the neuronal cytoskeleton, axonal transport defects, and progressive neurodegeneration in *Drosophila*. *Mol Biol Cell* 16:2433-42.

Clowers KL, Lyman RF, Mackay TF and TJ Morgan. 2010. Genetic variation in senescence marker protein-30 is associated with natural variation in cold tolerance in *Drosophila*. *Genet Res* 92:103-13.

Edwards AC, Ayroles JF, Stone EA, Carbone MA, Lyman RF and TF Mackay. 2009. A transcriptional network associated with natural variation in *Drosophila* aggressive behavior. *Genome Biol* 10:R76.

Garnham CP and A Roll-Mecak. 2012. The chemical complexity of cellular microtubules: Tubulin post-translational modification enzymes and their roles in tuning microtubule functions. *Cytoskeleton* 69:442-63.

Godena VK, Romano G, Romano M, Appocher C, Klima R, Buratti E, Baralle FE and F Feiguin. 2011. TDP-43 regulates *Drosophila* neuromuscular junctions growth by modulating Futsch/MAP1B levels and synaptic microtubules organization. *PLoS One* 6:e17808.

Harbinson ST, Carbone MA, Ayroles JF, Stone EA, Lyman RF and TF Mackay. 2009. Co-regulated transcriptional networks contribute to natural genetic variation in *Drosophila* sleep. *Nat Genet* 41:371-5.

Hummel T, Krukkert K, Roos J, Davis G and C Klambt. 2000. *Drosophila* Futsch/22C10 is a MAP1B-like protein required for dendritic and axonal development. *Neuron* 26:357-70.

Ji Y, Rath U, Girton J, Johansen KM and J Johansen. 2005. D-Hillarin, a novel W180-domain protein, affects cytokinesis through interaction with the septin family member Pnut. *J Neurobiol* 64:157-69.

Koch I, Schwarz H, Beuchle D, Goellner B, Langegger M and H Aberle. 2008. *Drosophila* ankyrin 2 is required for synaptic stability. *Neuron* 58:210-22.

Langley CH, Stevens K, Cardeno C, Lee YC, Schrider DR, et al. 2012. Genomic Variation in Natural Populations of *Drosophila* melanogaster. *Genetics* in press

Mackay TF, Richards S, Stone E, Barbadilla A, Ayroles JF, et al. 2012. The *Drosophila* melanogaster Genetic Reference Panel. *Nature* 482:173-8.

Morozoca TV, Ayroles JF, Jordan KW, Duncan LH, Carbone MA, Lyman RF, Stone EA, Govindaraju DR, Ellison RC, Mackay TF and RR Anholt. 2009. Alcohol sensitivity in *Drosophila*: translational potential of systems genetics. *Genetics* 183:733-45.

Pawson C, Eaton BA and GW Davis. 2008. Formin-dependent synaptic growth: evidence that Dlar signals via Diaphanous to modulate synaptic actin and dynamic pioneer microtubules. *J Neurosci* 28:11111-28.

Pool JE and CF Aquadro. 2007. The genetic basis of adaptive pigmentation variation in *Drosophila* melanogaster. *Mol Ecol* 16:2844-51.

Riedl J, Crevenna, AH, Kessenbrock K, Yu JH, Neukirchen D, Bista M, Bradke F, Jenne D, Holak TA, Werb Z, Sixt M and R Wedlick-Soldner. 2008. Lifeact: a versatile marker to visualize F-actin. *Nat Meth* 5:605-7.

Roos J, Hummel T, Ng N, Klambt C and GW Davis. 2000. *Drosophila* Futsch regulates synaptic microtubule organization and is necessary for synaptic growth. *Neuron* 26:371-82.

Schulte J, Sepp K, Jorquera RA, Wu C, Song Y, Hong P and JT Littleton. 2010. DMob4/Phocein regulates synapse formation, axonal transport and microtubule organization. *J Neurosci* 30:5189-203.

Zheng Y, Wildonger J, Ye B, Zhang Y, Kita A, Younger SH, Zimmerman S, Jan LY and YN Jan. 2008. Dynein is required for polarized dendritic transport and uniform microtubule orientation in axons. *Nat Cell Biol* 10:1172-80.

Figure 1

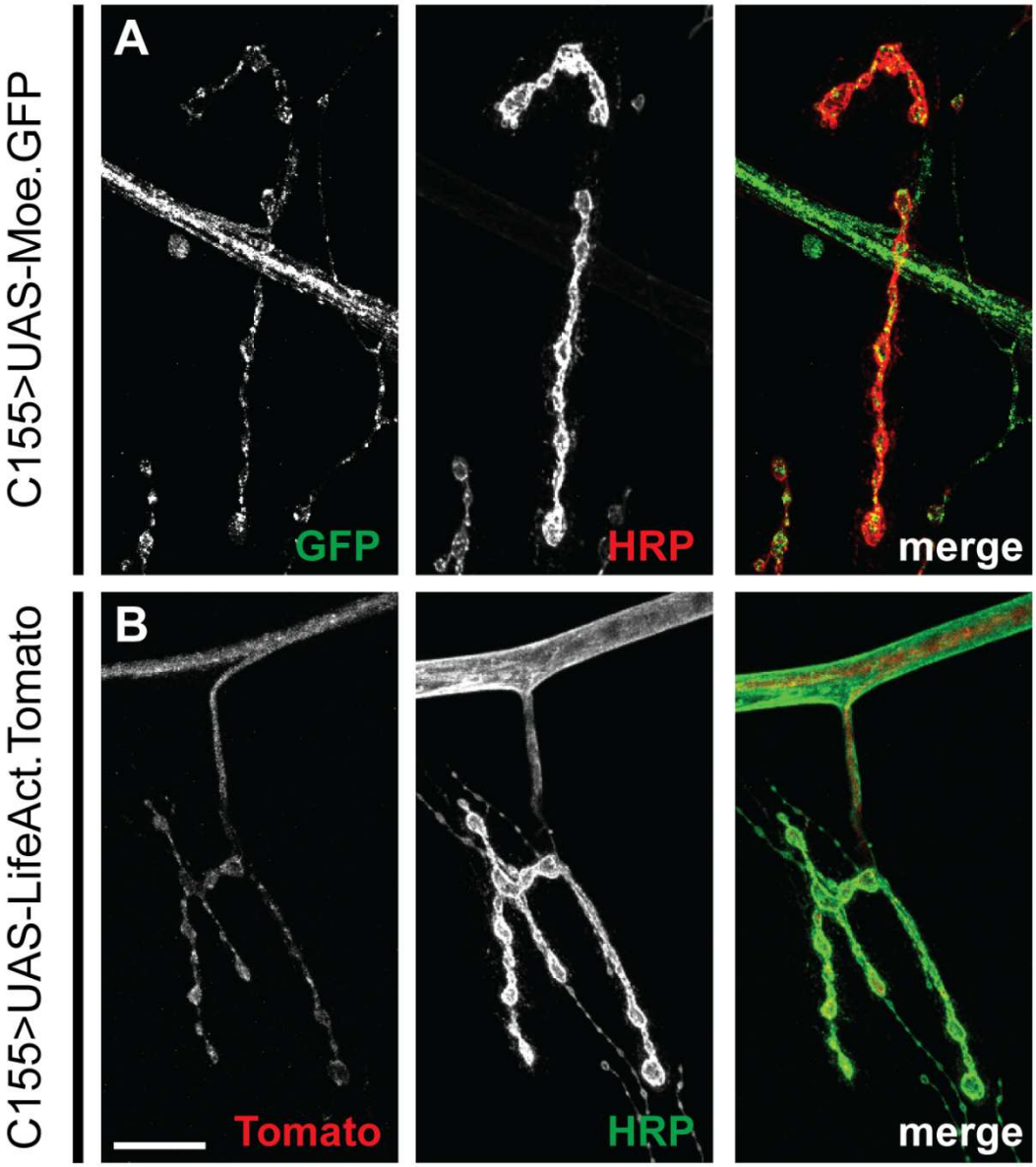
C155>UAS-Moe.GFP
A
GFP
HRP
merge
C155>UAS-LifeAct.Tomato
B
Tomato
HRP
merge

Figure 1: Moesin and LifeAct expression at the NMJ

(A-B) Confocal images of NMJ4. Expression of UAS-Moe.GFP (A) or UAS-LifeAct.Tomato (B) was driven pan-neuronally with *C155-Gal4*. Similar expression patterns are observed with both constructs; however the LifeAct expression provides higher resolution. The same NMJs are stained with anti-HRP (Cy3 with Moe.GFP and FITC with LifeAct.Tomato). Scale bar, 20µm.

Figure 2

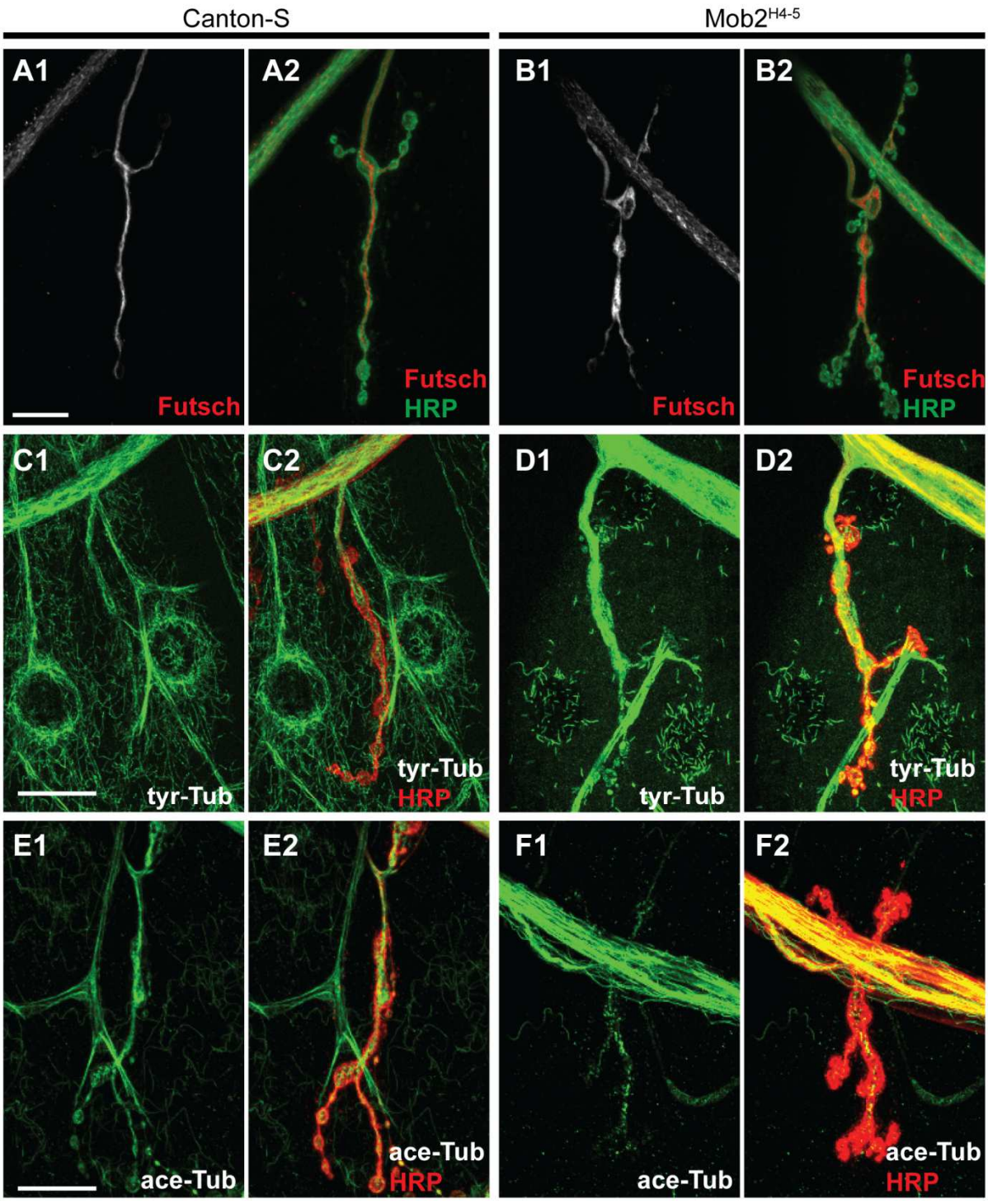
Canton-S
Mob2H4-5
A1
Futsch
A2
Futsch
HRP
B1
Futsch
B2
Futsch
HRP
C1
tyr-Tub
C2
tyr-Tub
HRP
D1
tyr-Tub
D2
tyr-Tub
HRP
E1
ace-Tub
E2
ace-Tub
HRP
F1
ace-Tub
F2
ace-Tub
HRP

Figure 2: Aberrant expression of Futsch, tryosinated-Tubulin and acetylated-Tubulin in a Mob2 background

(A-F) Confocal images of NMJ4. (A-B) NMJs stained for Futsch. Compared to CS where Futsch antibody stains a thin trace throughout the NMJ with a loop in the terminal bouton (A), *Mob2*$^{H4-5}$ NMJs have increased number of microtubule loops that are not in terminal boutons and Futsch staining fills some of the proximal boutons, while some distal boutons lack Futsch staining (B). Each NMJ is stained with FITC-anti-GFP (A2,B2). (C-D) NMJs stained for tyrosinated-Tubulin (tyr-Tub), a marker for nacent Tubulin. Expression of tyr-Tub is greatly increased in *Mob2*$^{H4-5}$ neurons (D) compared with wild-type (C). (E-F) NMJs stained for acetylated-Tubulin (ace-Tub), a marker for stabalized Tubulin. Expression of ace-Tub is decreased in *Mob2*$^{H4-5}$ neurons (E) compared with wild-type (F). Each NMJ is stained with Cy3-anti-GFP (C2,D2, E2, F2). Scale bar, 20µm.

Figure 3

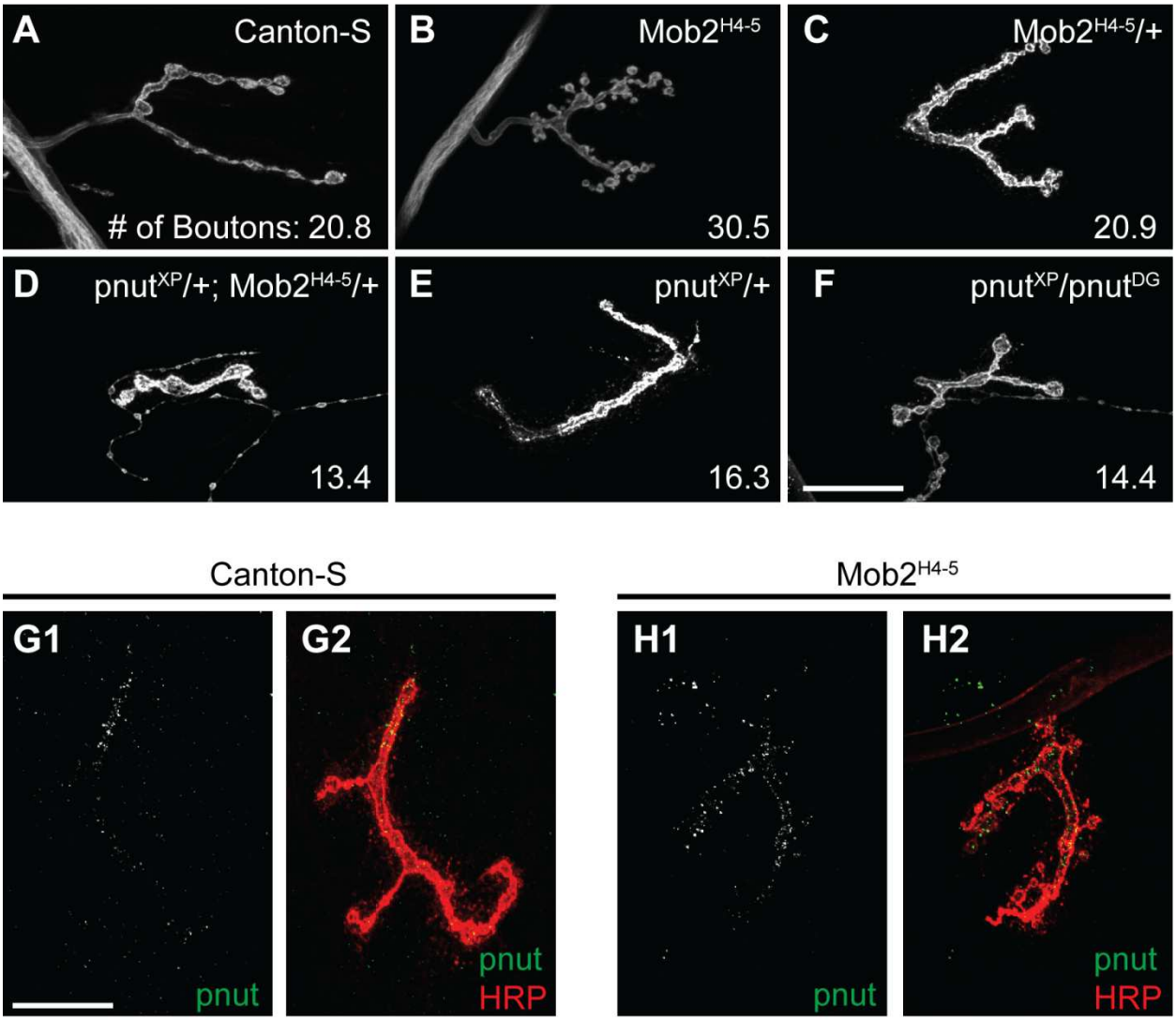
A
Canton-S
# of Boutons: 20.8
B
Mob2H4-5
30.5
C
Mob2H4-5/+
20.9
D
pnutXP/+; Mob2H4-5/+
13.4
E
pnutXP/+
16.3
F
pnutXP/pnutDG
14.4
Canton-S
Mob2H4-5
G1
pnut
G2
pnut
HRP
H1
pnut
H2
pnut
HRP

Figure 3: *pnut* is a positive regulator of NMJ growth that interacts with *Mob2*

(A-F) Confocal images of NMJ4 labeled with FITC-anti-HRP. *Mob2*$^{H4-5}$ homozygotes (B) have overgrown phenotypes, while *pnut*^{XP}/*pnut*^{DG} larvae (F) have undergrown NMJs. Heterozygotes for *Mob2*$^{H4-5}$ (C) or *pnut*^{XP} (E) have very mild overgrowth and undergrowth phenotypes respectively. By comparison, the *pnut*^{XP}/+; *Mob2*$^{H4-5}$/+ double heterozygotes (D) are significantly undergrown with a phenotype comparable to the *pnut*^{XP}/*pnut*^{DG} larvae. Quantifications of the average number of boutons per NMJ4 are written on each corresponding image. (G-H) Confocal images co-stained with anti-Pnut and Cy3-anti-HRP. Pnut expression is greatly increased in *Mob2* mutant (H) compared to wild-type (G). Scale bar, 20µm.

Figure 4

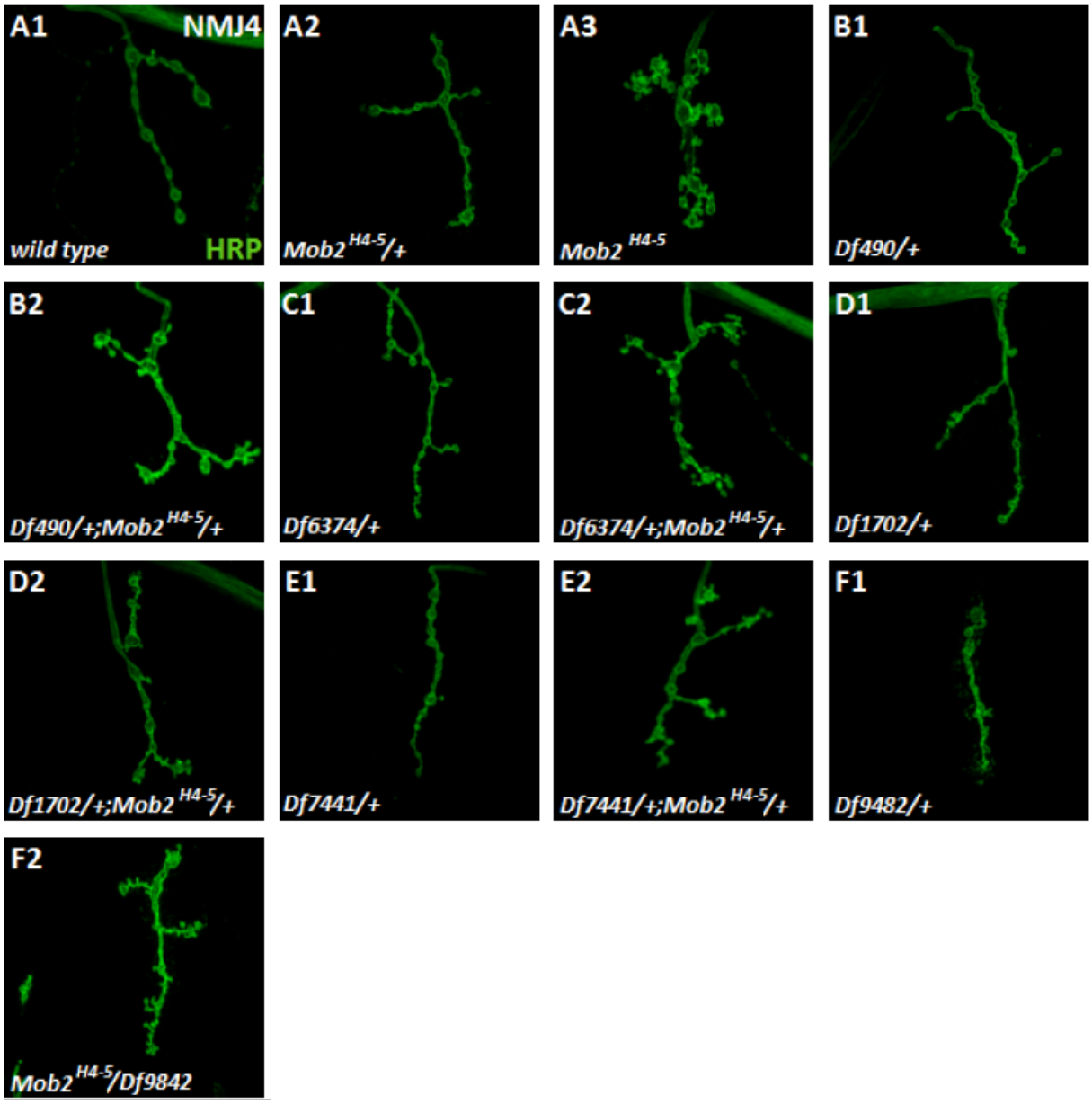
A1
NMJ4
wild type
HRP
A2
Mob2 H4-5/+
A3
Mob2 H4-5
B1
Df490/+
B2
Df490/+;Mob2 H4-5/+
C1
Df6374/+
C2
Df6374/+;Mob2 H4-5/+
D1
Df1702/+
D2
Df1702/+;Mob2 H4-5/+
E1
Df7441/+
E2
Df7441/+;Mob2 H4-5/+
F1
Df9482/+
F2
Mob2 H4-5/Df9842

Figure 4: Deficiency screen for dominant enhancement of Mob2^{H4-5}/+ NMJ phenotype

(A-F) Confocal images of NMJ4 stained with FITC-anti-HRP. Five examples of dominant enhancement of *Mob2*$^{H4-5}$/+ NMJ phenotype with a Df (B2, C2, D2, E2, F2) compared with single heterozygote controls. Strong enhancement with increases in both number of boutons and branch points are observed. Figure courtesy of Lalanti Venkat.

Figure 5

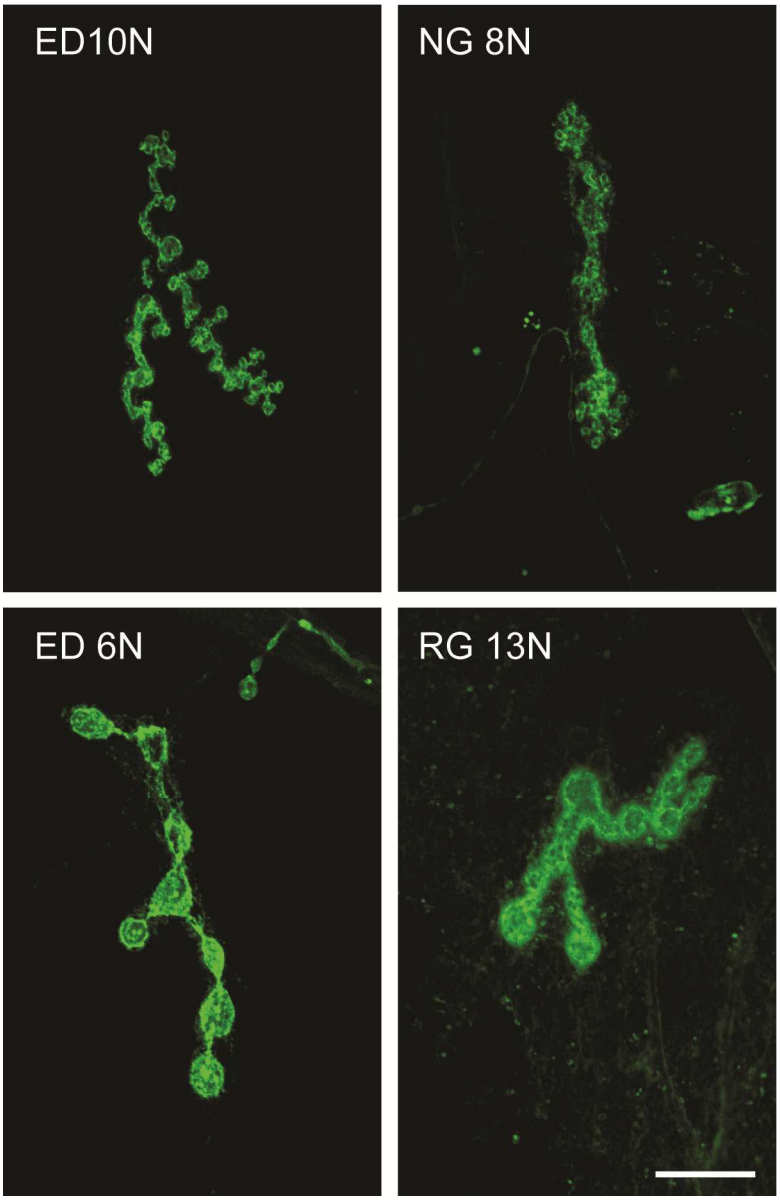

Figure 5: Aberrant NMJ morphologies in African natural populations of *D. melanogaster*

Confocal images of NMJ4 stained with FITC-anti-HRP. ED10N and NG8N are examples of overgrown NMJs observed. ED10N also exhibits a zig-zag pattern of growth that has not been observed with mutation analysis. NG8N has a more standard overgrowth phenotype with strongly hyperbudded terminal boutons. ED6N and RG13N are two examples of NMJ undergrowth observed. In addition to the undergrowth phenotype, RG13N also exhibits aberrant HRP staining with fuzzy staining surrounding the boutons. These examples suggest that additional novel growth regulators could be identified by mapping the causative polymorphisms in these populations.